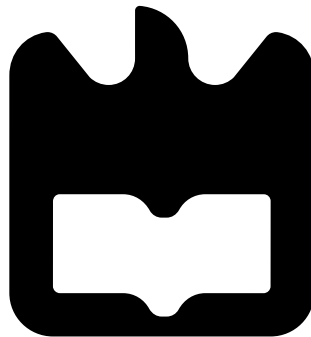




**Filipe Miguel
Esturrenho Barradas**

**Amplificadores Paramétricos de RF
RF Parametric Amplifiers**





**Filipe Miguel
Esturrenho Barradas**

Amplificadores Paramétricos de RF

RF Parametric Amplifiers

Dissertação apresentada à Universidade de Aveiro para cumprimento dos requisitos necessários à obtenção do grau de Mestre em Engenharia Electrónica e de Telecomunicações, realizada sob a orientação científica de José Carlos Esteves Duarte Pedro e de Pedro Miguel da Silva Cabral, Professores do Departamento de Electrónica, Telecomunicações e Informática da Universidade de Aveiro

Dissertation presented to the University of Aveiro for the fulfilment of the requisites necessary to obtain the degree of Master In Electronics and Telecommunication Engineering, developed under the scientific guidance of José Carlos Esteves Duarte Pedro and Pedro Miguel da Silva Cabral, Professors in the Department of Electronics, Telecommunications and Informatics of the University of Aveiro

O Júri / The Jury

Presidente / President

Prof. Doutor Dinis Gomes de Magalhães dos Santos
Professor Catedrático, Universidade de Aveiro

Arguente Principal / Main
Examiner

Prof. Doutor Jose Angel Garcia
Professor Titular, Universidad de Cantábria, Espanha

Orientador / Advisor

Prof. Doutor José Carlos Esteves Duarte Pedro
Professor Catedrático, Universidade de Aveiro

Co-Orientador / Co-Advisor

Doutor Pedro Miguel da Silva Cabral
Professor Auxiliar Convidado, Universidade de Aveiro

Agradecimentos / Acknowledgements

Gostaria de agradecer ao pessoal da sala 317 por me darem abrigo todos os dias da semana enquanto progredia incessantemente o trabalho aqui realizado. Um brinde a trabalhar entre amigos!

À minha namorada por inabalável suporte e eterna compreensão.

À família por me acolherem nos fins-de-semana, pelo suporte financeiro e amor de tantos anos.

A ambos os orientadores José Carlos Esteves Duarte Pedro e Pedro Miguel da Silva Cabral pela ajuda fornecida e pelo tempo disponibilizado.

Em especial a José Carlos Esteves Duarte Pedro pelas horas de discussões interessantes.

Agradeço à Universidade de Aveiro pela aprendizagem que me permitiu ao longo destes cinco anos e por proporcionar todas as oportunidades que me foram apresentadas.

Não poderia também deixar de reservar um espaço para agradecer ao Instituto de Telecomunicações por me ter acolhido desde há três anos em vários projectos de bolsa que contribuíram em muito para o meu desenvolvimento.

Finalmente, agradeço à Fundação para a Ciência e Tecnologia (FCT) por ter financiado alguns dos projectos com o meu envolvimento e pelo seu contínuo trabalho para o desenvolvimento da investigação científica em Portugal.

Palavras-Chave

Amplificação Paramétrica, Amplificadores de RF, Aplicações de Varactores, Sistemas Não-Lineares

Resumo

Recentemente tem-se feito um esforço no sentido de aumentar a eficiência em amplificadores de RF, no entanto, o transistor é um dispositivo intrinsecamente ineficiente. Utilizando amplificadores paramétricos pode-se teoricamente chegar a 100% de eficiência mesmo operando em modo linear.

A razão desta elevada eficiência é o dispositivo activo utilizado, já que os amplificadores paramétricos utilizam uma reactância controlada, que não consome potência. Esta mudança de elemento activo modifica completamente o princípio de funcionamento dos amplificadores.

Neste trabalho este tipo de amplificação é estudado, relações e transformações conhecidas são examinadas primeiro para obter propriedades limite gerais. Depois é feita análise de pequeno sinal para se obterem outras características importantes. Finalmente, um novo modelo de grande sinal é derivado e apresentado. Este modelo é capaz de prever algumas características do amplificador, tal como o AM/AM.

Utilizando o modelo de grande sinal apresentado projecta-se um amplificador, sendo este posteriormente simulado.

Keywords

Non-Linear Systems, Parametric Amplification, RF Amplifier, Varactor Applications

Abstract

In recent years a significant effort has been made towards efficiency increase in RF amplifiers. The transistor is, however, an intrinsically inefficient device. Parametric amplification can theoretically be 100% efficient even operating in linear mode.

The reason behind this efficiency is the active device. These amplifiers forget the transistor to use a controlled reactance, which cannot consume power. This switch in active element changes the whole principle of operation of the amplifiers.

In this work this type of amplification is studied. Known relations and transformations are first examined to obtain general limit properties of the used elements. Then small-signal analysis is performed to obtain other important characteristics. Finally, a novel large signal model is developed and presented. This model is capable of accurately predicting the non-linear responses of the amplifier, such as the AM/AM.

Using the presented large-signal model, an amplifier is designed and simulated.

Table of Contents

Table of Contents	i
List of Figures	v
List of Tables	ix
List of Acronyms	xi
1 Introduction	1
1.1 Motivation and Context	1
1.2 Objectives	3
1.3 Structure	4
2 Notes on Amplification	5
2.1 Definition	5
2.2 Linearity	6
2.2.1 Definition	6
2.2.2 Restrictions	7
2.2.3 Measuring Non-Linearity	8
2.3 System Modeling	10
2.4 Efficiency	10
2.5 Transistor Based Amplifier	11
2.5.1 Overview	11
2.5.2 Class A	15
2.5.3 Class B	17
2.5.4 Class AB	19
2.5.5 Class C	21
2.5.6 Wrap Up	22
2.5.7 Class D	23
2.5.8 Class E	24
2.5.9 Class F	25
2.5.10 Wrap Up	26
2.5.11 Efficient Architectures	26

2.5.12	Conclusions	31
3	Properties of Non-Linear Elements	33
3.1	Representation of Non-Linearity	33
3.1.1	Series	33
3.1.2	Frequency Based	36
3.2	Manley-Rowe Relations	39
3.2.1	Uses and Limitations	40
4	Parametric Amplifier	43
4.1	Definition	43
4.2	Energy Considerations	44
4.3	Searching for the Active Element	49
4.3.1	The Diode	50
4.3.2	The 3-Terminal MOSVar	52
4.4	Small-Signal Analysis	54
4.4.1	General Considerations	55
4.4.2	Inverting ParAmp	57
4.4.3	Non-inverting ParAmp	58
4.4.4	Extracting the Parameters	65
4.4.5	Limitations	66
4.5	Large-Signal Analysis	66
4.5.1	General Considerations	66
4.5.2	Voltage Pumped Capacitance	67
4.5.3	Current Pumped Elastance	74
5	Designing a Parametric Amplifier	77
5.1	Specifications	77
5.2	Pumping Type	77
5.3	Topology	77
5.3.1	Ring Topology	78
5.4	Non-Linearity and Tuning	79
5.5	Simulations	80
5.6	Practical Implementation	85
6	Conclusions and Future Work	87
6.1	General Aspects	87
6.2	Comparison to Previous Work	88
6.3	Future Work	89
6.4	Final Remarks	89
	Bibliography	91

A Mathematics	93
A.1 Parametric First Order Linear Differential Equation	93
A.1.1 Solution	93
A.1.2 Linearity Proof	95
B Circuits	97
B.1 Parasitics Test	97
B.2 Doubly Balanced Voltage Pumped ParAmp	99

List of Figures

1.1	Influence of the PAPR on the Efficiency	2
1.2	Effect of Power Supply Modulation In the Transistor Load Line	2
1.3	Effect of Load Modulation in the Transistor Load Line	3
2.1	The Several Blocks Comprising an Amplifier	5
2.2	Frequency Interference in a Linear System - Sampling Example	7
2.3	Reference System	7
2.4	1dB Compression Point	8
2.5	Two Tone Output Spectrum from Non-Linear System	9
2.6	Continuous Output Spectrum from Non-Linear System	10
2.7	Equivalent Transistor Amplifier Output Circuit for Calculating the Efficiency	12
2.8	Idealized Equivalent Transistor Amplifier Output Circuit for Calculating the Efficiency	12
2.9	A transistor with coupled load	14
2.10	Current-Mode Transistor Amplifier Equivalent	15
2.11	Transistor Output Current Vs Input Voltage	16
2.12	Transistor Output Current Vs Output Voltage	16
2.13	Class A Behaviour	17
2.14	Transistor Output Current Vs Input Voltage	17
2.15	Transistor Output Current Vs Output Voltage	18
2.16	Class B Behaviour	18
2.17	Transistor Output Current Vs Input Voltage	20
2.18	Class AB Behaviour	20
2.19	Transistor Output Current Vs Input Voltage	21
2.20	Class C Behaviour	22
2.21	Amplifier Classes Vs Conduction Angle	22
2.22	Efficiency and Current Gain Vs Conduction Angle	23
2.23	Transistor in Class D	24
2.24	Transistor in Class E	24
2.25	Transistor in Class F	25
2.26	Class F Ideal Waveforms	26
2.27	PA Efficiency Vs Relative Output Voltage	27
2.28	ET Block Diagram	28

2.29	ET Efficiency in Class B	28
2.30	EER Block Diagram	29
2.31	DHT Block Diagram	30
2.32	Doherty Example Efficiency Curve	30
3.1	Power Series Equivalent System	34
3.2	Volterra Series Equivalent System	35
3.3	Non-Linearity Spectrum	37
3.4	Conversion Output Spectrum	37
4.1	Conceptual Parametric Amplifier	44
4.2	Trigonometric Circle of Energy	45
4.3	Variation of the Diode Capacitance with the Applied Voltage	50
4.4	Variation of the Diode Elastance with the Stored Charge (Normalized)	52
4.5	Diode Varactor Model	52
4.6	The 3-Terminal MOSVar	53
4.7	MOSVar Behaviour, adapted from [13]	54
4.8	Small Signal Input and Output Frequencies	54
4.9	Non-Linear Capacitance Concept ParAmp	55
4.10	Equivalent Small-Signal Circuit, Inverting ParAmp	58
4.11	Equivalent Small-Signal Circuit, Non-Inverting ParAmp	59
4.12	Equivalent Small-Signal Circuit, with Admittance Terminations	59
4.13	Gain Variation with the Output's Frequency	63
4.14	Gain Variation with the Capacitance	63
4.15	Sensitivity of the Gain to the Non-Linearity	65
4.16	Dependence and Transformations in the Non-Linear System	67
4.17	Voltage Pumped, Voltage Controlled Capacitance	68
4.18	Test Circuit, Circuit Level Simulation	72
4.19	Simulation and Model Results for the Test Circuit	73
4.20	Current Pumped, Charge Controlled Elastance	75
5.1	Ring Topology Example, Evidencing the Inherent System Symmetry	78
5.2	Part of the Amplifier to be Designed	79
5.3	Simulation Results Vs Model Results with (left) and without (right) the Parasitic Components	82
5.4	Simulation Results Vs Model Results for the ParAmp to be Implemented	83
5.5	Capacitance Curve and Used Approximation	83
5.6	Simulation and Model Bandwidth for the Designed ParAmp Using Diodes (left) and Using Linearly Varying Capacitances	84
5.7	Simulation and Model Pump Influence over the Gain for the Designed ParAmp Using Diodes (left) and Using Linearly Varying Capacitances	84
5.8	ParAmp Practical Implementation	85
B.1	The used Active Component Including the Parasitics	98

B.2 Test Circuit for the Influence of the Parasitic Components in the Model . .	98
B.3 Doubly Balanced Voltage Pumped ParAmp	100

List of Tables

2.1	Nomenclature	11
2.2	Waveforms at the Transistor and Output Terminals and the Instantaneous Dissipated Power	14
4.1	Test Circuit, Simulation Parameters	71

List of Acronyms

ACPR Adjacent-Channel Power Ratio

ADS Advanced Design System

BJT Bipolar Junction Transistor

BLA Best Linear Approximation

BMA Best Mixer Approximation

DC Direct Current

DCC Direct Current Choke

DHT Doherty

EER Envelope Elimination and Restoration

ESR Equivalent Series Resistor

ET Envelope Tracking

FET Field Effect Transistor

FoM Figure of Merit

GaAs Galium Arsenide

IMD Intermodulation Distortion

IMR Intermodulation Ratio

LSB Lower Side Band

MatLab Matrix Laboratory

MOSFET Metal-Oxide-Semiconductor Field-Effect Transistor

MOSVar Metal-Oxide-Semiconductor Varactor

NMOS N-channel Metal-Oxide-Semiconductor

NMSE Normalized Mean Square Error

PA Power Amplifier

PAE Power Added Efficiency

PAPR Peak-to-Average Power Ratio

ParAmp Parametric Amplifier

PCB Printed Circuit Board

PDF Probability Distribution Function

RF Radio Frequency

RFC Radio Frequency Choke

Chapter 1

Introduction

1.1 Motivation and Context

In recent years, a significant effort has been made towards improving efficiency in electronic devices. The study of, so called, "Green Technology" has been increasing and the continued search for better energy usage is everlasting.

In communications, the need for a rise in efficiency has also been felt, not only for mobile devices (which are dependent on a restrictive amount of energy), but also for base stations (due to the high energy cost). Raising the efficiency in signal amplification is, therefore, very important, as it is at this stage that the highest powers are handled.

Current-mode topologies of Radio Frequency (RF) Power Amplifiers (PAs) have inherently low efficiencies for small signal inputs. However, modern communication systems use modulation techniques which possess a high Peak-to-Average Power Ratio (PAPR), as defined in equation 1.1. If the amplifier is intended to be linear, it will operate mainly in the back-off region, which means reduced efficiency.

$$PAPR = \frac{\max_{0 < t < +\infty} |x(t)|^2}{\lim_{T \rightarrow +\infty} \frac{1}{T} \int_0^T |x(t)|^2 dt} \quad (1.1)$$

To better understand the efficiency dependence with the PAPR, please examine figure 1.1. The figure shows typical efficiency dependence on the input amplitude. The envelope's amplitude Probability Distribution Functions (PDFs) of a signal with a high PAPR and a signal with a low PAPR are also represented. Both signals have been adjusted to drive the PA at maximum efficiency without saturating it. The signal whose PDF peak is closer to maximum amplifier drive will obtain a better average efficiency.

To raise the efficiency, but keep linearity, modern topologies make use of efficiency boosting techniques, such as load modulation or power supply modulation. These techniques allow the PA to operate at higher efficiency for lower inputs and include: Envelope Tracking (ET) and Envelope Elimination and Restoration (EER), for the power supply modulation, and the Doherty (DHT), for the load modulation.

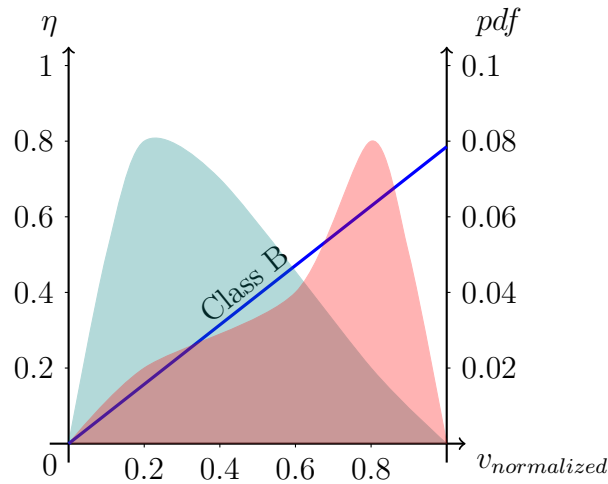


Figure 1.1: Influence of the PAPR on the Efficiency

The techniques based on power supply modulation operate by reducing Direct Current (DC) power consumption. This can be done by separating the phase and amplitude information that is contained in the input signal. The amplitude information is used to modulate the power supply, while the phase information is maintained in the input wave. This is exemplified in figure 1.2 where the characteristic curves of a transistor are plotted for a varying power supply.

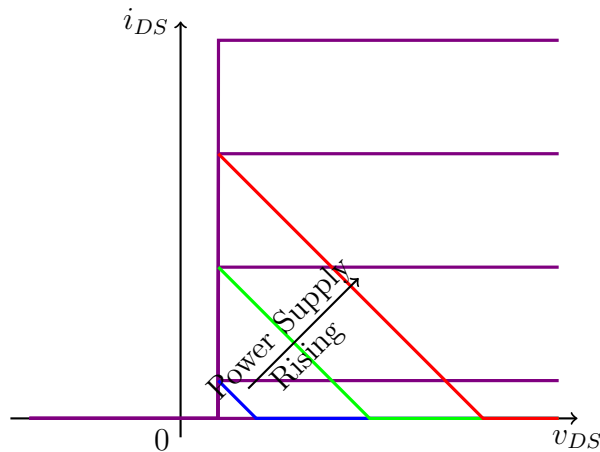


Figure 1.2: Effect of Power Supply Modulation In the Transistor Load Line

The techniques based on load modulation operate by designing the amplifier for a higher load resistance (which means it will saturate for lower input powers). Then some technique is used to reduce the load (another amplifier, in the DHT architecture) when the input power drives the PA too much into saturation. This is exemplified in figure 1.3 where the characteristic curves of a transistor are plotted for a varying load.

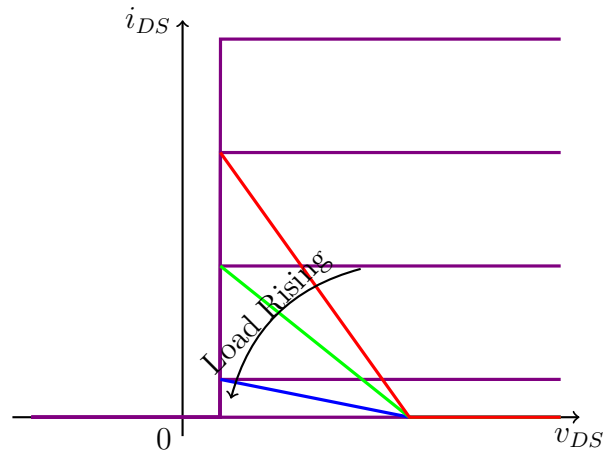


Figure 1.3: Effect of Load Modulation in the Transistor Load Line

There is, however, another option to raise the efficiency. While the traditional PAs are based on the transistor, which is a controlled conductance, there is the possibility to create a PA based on a controlled reactance. Reactances cannot dissipate energy and so the efficiency should be much higher than the transistor based PAs. This type of amplification is already known and called parametric amplification. This name was given because it is based on the variation of a parameter of the system. Parametric amplification using non-linear reactances has already been investigated and the cornerstones that make possible the practical implementation of this type of amplifiers have been researched. Unfortunately, most of them have been tried in the high-frequency low-noise field up to the 1970's or 1980's where high gain low-noise Gallium Arsenide (GaAs) Field Effect Transistor (FET) transistors almost completely replaced this technology. However, very recently, parametric amplification received a renewed attention due to its potential high efficiency. This Thesis aims to further research this type of amplification, clarifying the behaviour of the circuits and the physical operation of the systems. In fact, and throughout this Thesis, the identifier "Parametric Amplification" will signify "Efficient, Power, Parametric Amplification".

1.2 Objectives

The main objective of this Thesis is to study the possibility of implementing reactance based RF PAs. To evaluate this possibility, a number of secondary objectives should be accomplished. First, the basic working methodology of these type of amplifiers should be well understood. Second, methods to extract the system characteristics must be studied and understood, or developed, if needed. Finally, a proof of concept amplifier should be developed, this way proving a test of feasibility.

These objectives should be accomplished sequentially since each one is mounted on the back of the previous.

- **Understand basic behaviour**

The mechanisms by which power is transferred to the output must be well understood. This applies to the most basic governing relations as well. This first step provides the proof of possibility, providing an answer to the question: "*Is it possible?*".

- **Extract system characteristics**

This part consists of system modelling and the extraction of characteristics through the models. This objective provides proof of usability, which means that, it answers the question: "*Is it useful?*".

- **System implementation**

This last objective should fill the gap between theory and practice, serving as a proof of concept. The objective gives the proof of practicality, providing an answer to the question: "*Can it be done in practice?*".

1.3 Structure

In the first chapter (chapter 1), the motivation and the context of this Thesis is made clear and the objectives are presented. Furthermore, the structure of this work is also explained. This first chapter serves as a broad overview over the work developed further on.

The work starts with some notes on amplification (chapter 2). This serves the purpose of explaining, exploring and broadening some concepts such as linearity and modelling. After this, an overview and a closer look at transistor based amplifiers is given to point out limitations in current amplification techniques and state the motivation for this Thesis.

Then, a closer look at non-linearities and their modelling techniques is given (chapter 3). This is needed because the type of amplification suggested in the Thesis requires non-linear components. This chapter is, therefore, the mathematical cornerstone of this Thesis.

The work continues on to a chapter on parametric amplification (chapter 4) where the amplification technique is explained and the used components are modelled. After this, small-signal circuit analysis is applied to the system to extract some characteristics and develop small-signal design rules. Finally, large signal analysis is performed under more restrictive conditions to optimize the proposed design methods and extract large signal behaviour.

The next chapter is dedicated to the parametric amplifier development (chapter 5), it includes simulations using both the developed models and a circuit level simulator.

The final chapter of this Thesis is dedicated to the drawn conclusions (chapter 6) and some final remarks.

Chapter 2

Notes on Amplification

2.1 Definition

Amplification is a technique through which energy from a source is modulated to produce a signal possessing some wanted characteristics dependent on some other signal. However, it is intended that this modulator provides more power at the output than that provided at its input, thus amplifying the signal driving it.

Usually, modulation, mixing and amplification can be achieved separately, and so, amplifiers are wanted to be linear and also time invariant. Even if the same device achieves amplification, mixing and modulation, the processes which generate each effect can usually be separated. From a system point of view, what we would have are several blocks that comprise the final device, as shown in figure 2.1, where the graphics represent the spectrum of the signal at each point.

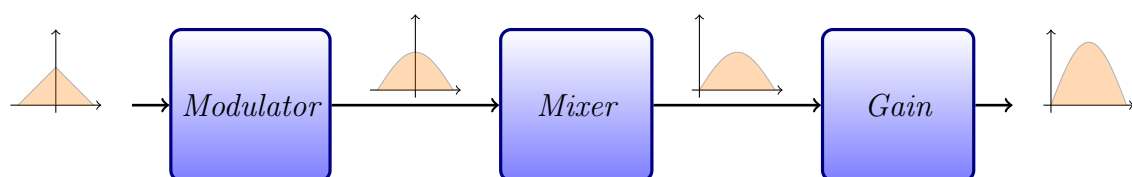


Figure 2.1: The Several Blocks Comprising an Amplifier

The modulator takes the input information and changes it into some other form, the mixer changes the frequency and finally the gain changes the power. Usually it is not wanted that the amplification process changes the modulation, linear amplifier. If the amplifier does not change the frequency then it is also time-invariant.

2.2 Linearity

2.2.1 Definition

An amplifier that modulates a power source into a copy of the original signal is linear. If this copy occurs at the same frequency, than it is also time-invariant. This aspect of amplification defines one of the most important characteristics of system analysis.

This work will focus on linear amplification. Note that this does not mean that the used components are linear, or even that the output will be a linear copy of the input, it only means that linearity will be a characteristic under observation, more details are given in section 2.2.2.

For further purposes the definition of linearity is described in equation (2.1), and explained in the next paragraph.

$$F[\alpha x + \beta y] = \alpha F[x] + \beta F[y] \quad F \text{ is a mathematical operator} \quad (2.1)$$

Notice how F is described as a mathematical operator (further on, functions are represented with low case letters) and not a function in itself. This is done so that implicit definitions of systems, such as the differential equation, can be used to prove linearity. Also, note how the output is not necessarily the input multiplied by some constant, defining the gain of the system, but is indeed a transformation through some operator. For instance, the sampling operation is linear, as shown in equation 2.2.

$$F[x(t)] = x(t) \sum_{n=0}^{+\infty} \delta(t - nT_s)$$

$$F[\alpha y(t) + \beta z(t)] = [\alpha y(t) + \beta z(t)] \sum_{n=0}^{+\infty} \delta(t - nT_s) \quad (2.2)$$

$$F[\alpha y(t) + \beta z(t)] = \alpha F[y(t)] + \beta F[z(t)]$$

Parametric differential equations, such as equation 2.3 are also linear, in the case of equation 2.3 the proof is included in appendix A.1.

$$F[x(t)] \rightarrow f(t)y(t) + g(t) \frac{dy(t)}{dt} = x(t) \quad (2.3)$$

Linearity is thus very broad and should be approached carefully. A good example is the sampling, even though a sampling system is linear, as proved before, this does not mean that the original signal can be recovered from the output. In fact, interference between the frequencies generated by each input frequency can make the process irreversible, this is what happens when the Nyquist condition is violated, as shown in figure 2.2.

Usually, linear systems are also considered to be time-invariant, this is the condition for not generating new frequencies at the output. There is a simple proof that can be considered as evidence to this: for a system to be time-invariant none of the characteristics

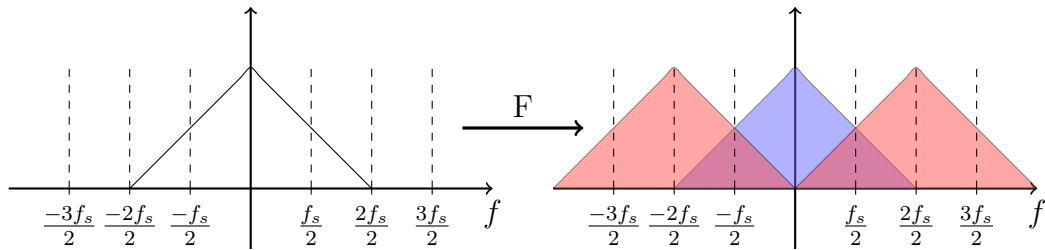


Figure 2.2: Frequency Interference in a Linear System - Sampling Example

defining the system can vary in time. However, for a system to produce new frequencies at the output, either the system varies in time or there is some non-linear mechanism. This means that a system both linear and time-invariant cannot generate new frequencies [1].

2.2.2 Restrictions

As shown in the previous section the concept of linearity is very broad and, unless it is paired with time-invariance, can produce output frequencies that are not of interest. It follows that some restrictions to linearity should be applied so that it only includes the researched systems.

In this work it is intended that the output of the amplifier is a copy of the input, that can occur at a different middle frequency. Therefore, the system's linearity will be a comparison against the response of the system shown in figure 2.3 which has the response described by equation 2.4.

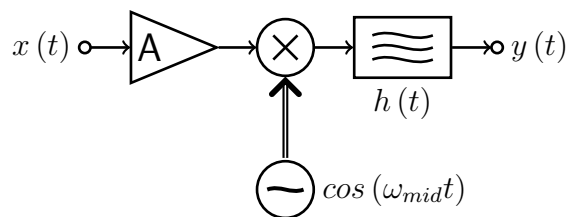


Figure 2.3: Reference System

$$y(t) = A [x(t) \cos(\omega_{mid}t)] * h(t) \quad (2.4)$$

In the system from figure 2.3 A is a gain, and $h(t)$ is a normalized, linear, time-invariant, filter, the only frequency generation mechanism is the mixer. With this type of system the output can only be a filtered copy of the input at a different frequency, as it is intended in the devices developed in this work.

2.2.3 Measuring Non-Linearity

Every system in existence ends up being intrinsically non-linear when operated under general conditions. A resistor will end up burning for high powers, the gain of an amplifier will end up compressing for lack of an infinite power source. Linearity is, therefore, a luxury that exists only for a restricted set of conditions, the quality of the observations amongst them.

Since the systems are inherently non-linear there must be some methods to quantify non-linearity. This is so because, while linearity is very well defined, non-linearity is defined only as its inverse which will forcibly be vast.

In this section some methods for quantifying non-linearity in amplification are explained.

1dB Compression Point

The 1dB compression point is a measure of the non-linearity based on the gain of the amplifier. As it was said before, due to the limitations on available power, the gain of an amplifier will compress for higher input powers. When the gain compresses 1dB the output power at that point is said to be the 1dB compression point.

The 1dB compression point can be regarded as the transition zone between small-signal operation and large-signal operation. In figure 2.4 the concept is illustrated.

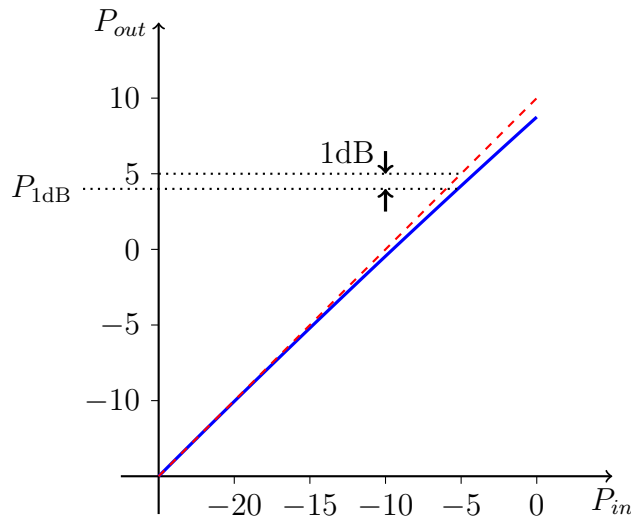


Figure 2.4: 1dB Compression Point

Intermodulation

The inter-modulation is usually measured in terms of Intermodulation Ratio (IMR). The IMR is the ratio between the power at the fundamental and the Intermodulation Distortion (IMD), the IMD are the mixing products that fall inside the band of the amplified

signal. If we imagine a two tone signal, these components would be of the type $2\omega_1 - \omega_2$ and $2\omega_2 - \omega_1$. To avoid confusion the IMR is usually taken with the worst IMD component.

$$IMR = \frac{P_{fundamental}}{P_{IMD}} \quad (2.5)$$

To better understand the concept, figure 2.5 shows a typical output spectrum of a non-linear system excited by two input sine waves of different frequencies.

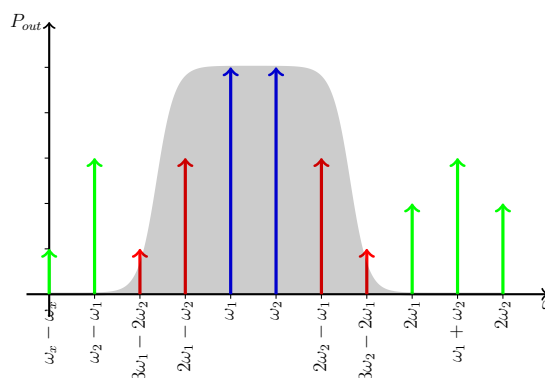


Figure 2.5: Two Tone Output Spectrum from Non-Linear System

The IMD generates in- and out-of-band frequency components. The out-of-band components are easily filtered out, the in-band components will pass through to the output endangering linearity. The IMR is calculated with an IMD component in-band, typically the third modulation product as it usually has the most power.

Adjacent Channel

The Adjacent-Channel Power Ratio (ACPR) is the equivalent of the IMR for continuous signals in the frequency domain. When this is the case, and there is no clear frequency marker to measure IMR, the ACPR must be used. The ACPR integrates the power along all of the adjacent channel and ratios it in relation to the main channel power. As in the IMR, the adjacent channel may be considered anywhere, usually the worst case is taken. In some cases, the ACPR may be measured for more than one adjacent channel. The bandwidth of the adjacent channel may not be the same as the main channel. Figure 2.6 illustrates the concept.

The ACPR can be calculated by integrating the adjacent channels to infinity or in a limited bandwidth, or even subdividing the adjacent channels and calculating an ACPR for each. A general formula to calculate the ACPR is shown in equation 2.6

$$ACPR = \frac{\int_{B_w} S_{adjacent} d\omega}{\int_{\omega_{low}}^{\omega_{high}} S_{main} d\omega} \quad (2.6)$$

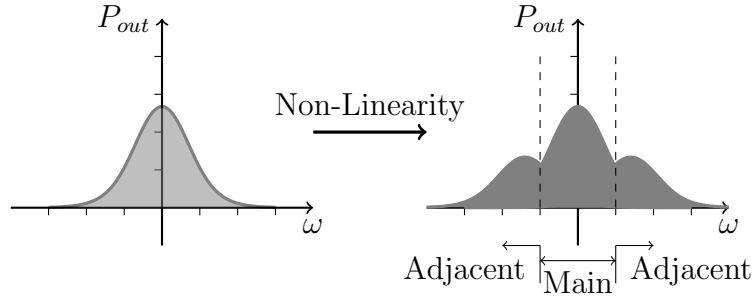


Figure 2.6: Continuous Output Spectrum from Non-Linear System

Error to Linear Equivalent

So far, the presented techniques to measure non-linearity with signal data have been frequency based. The error can be used to measure the difference between the expected output of the system, if it were linear, and the true output of the system, thus providing a measure of non-linearity. To obtain a single quantity the error is usually integrated and normalized. Furthermore, to avoid cancelling positive errors with negative, the error is usually squared. This is known as the Normalized Mean Square Error (NMSE). The NMSE is calculated using equations 2.7.

$$NMSE = \frac{\int_{-\infty}^{+\infty} |y(t) - \hat{y}(t)|^2 dt}{\int_{-\infty}^{+\infty} |y(t)|^2 dt} \quad (2.7)$$

The approximation of y , \hat{y} , can be anything, if it is the Best Linear Approximation (BLA) then the NMSE provides a measure of linearity.

2.3 System Modeling

The devices in this work are modelled from a linear, time-invariant point of view, using the BLA. The BLA is calculated by shifting the input to the output's ω_{mid} in the frequency domain, in accordance to the reference system. This is actually called the Best Mixer Approximation (BMA) [2]. The BMA gives the frequency response of the output filter $h(t)$ and also the system gain A shown in figure 2.3. Note that the BMA is extracted for the upper side band and lower side band, independently.

2.4 Efficiency

For PAs, the efficiency is usually measured in two different ways, one is the classical efficiency, denoted by η throughout this Thesis, that is calculated in this work according to equation 2.8.

$$\eta = \frac{[P_{out}]_{RF}}{[P_{in}]_{PS} + [P_{in}]_{RF}} \quad (2.8)$$

The other, is the Power Added Efficiency (PAE) which is defined in equation 2.9.

$$PAE = \frac{[P_{out}]_{RF} - [P_{in}]_{RF}}{[P_{in}]_{PS}} \quad (2.9)$$

These measurements represent efficiency in two different ways. While η represents the global efficiency of the system, meaning, how much power it let's out versus how much power goes in. The PAE measures the efficiency in relation to the power that is added to the input, meaning, how much power is added versus how much power the supply gets in.

The PAE is usually regarded as a better Figure of Merit (FoM) than η .

2.5 Transistor Based Amplifier

2.5.1 Overview

Modern amplifiers are all ultimately based in the transistor. The transistor is, however, intrinsically inefficient as it is a controlled resistance, be it in current (Bipolar Junction Transistor (BJT)) or in voltage (FET). The implications of this is that it is impossible to take an ideal transistor amplifier to 100% efficiency unless it is operated in a switching mode. This can be proved for single ended amplifiers with the help of figures 2.7, 2.8 and equations 2.10, 2.11. In this case, the voltage is taken as the input and output of the system. In the equations, the usual nomenclature is followed, small letters with capital letter subscripts symbolize the signal plus the bias, capital letters with capital letter subscripts symbolize the bias and small letters with small letter subscripts symbolize the signal as seen in table 2.1.

Style	Meaning
M_x	Signal+Bias
M_X	Bias
m_x	Signal

Table 2.1: Nomenclature

A transistor amplifier can be represented as seen in figure 2.7. In this figure, the controlled current source is the transistor core, Z_T is the lumped equivalent of the transistor's parasitic elements, Z_D is the lumped equivalent of the elements connecting to the power source, and Z_L is the load.

The power flowing into each component can be described as seen in equation 2.10 where $Y_x = \frac{1}{Z_x}$.

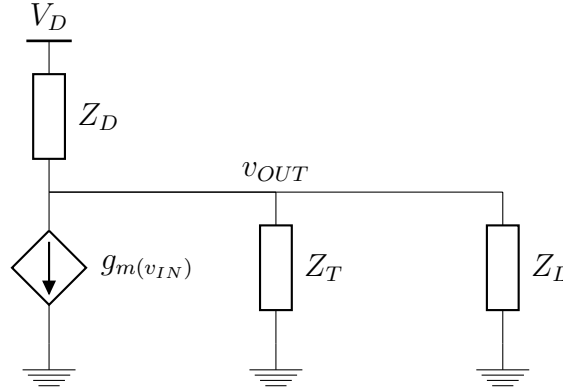


Figure 2.7: Equivalent Transistor Amplifier Output Circuit for Calculating the Efficiency

$$\begin{aligned}
 P_L &\propto \int \text{real}(Y_L) |V_{out}|^2 d\omega \\
 P_T &\propto \int v_{OUT} g_m(v_{IN}) dt + \int \text{real}(Y_T) |V_{out}|^2 d\omega \\
 P_D &\propto \int \text{real}(Y_D) |V_D - V_{out}|^2 d\omega \\
 \eta &= \frac{P_L}{P_D + P_T}
 \end{aligned} \tag{2.10}$$

Looking at equation 2.10 we can maximize the output power and minimize all the other powers. To do this, let's consider the following ideal case: Z_D is an infinite impedance at every frequency except DC, Z_T is infinite at every frequency and Z_L is an infinite impedance at DC and purely resistive at all other frequencies, also, $g_m(v_{IN}) = g_m v_{IN}$ to ensure linearity. This case is described in figure 2.8.

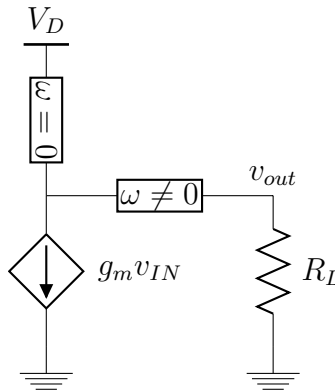


Figure 2.8: Idealized Equivalent Transistor Amplifier Output Circuit for Calculating the Efficiency

The efficiency depends heavily on the input signal, as shown in equation 2.11, but it can never be 100% with the exception of a square wave input signal, even considering this idealized scenario.

$$\begin{cases}
 P_T = \lim_{T \rightarrow \infty} \frac{1}{T} \int_0^T (V_D + v_{out}) g_m v_{IN} dt \\
 P_L = \lim_{T \rightarrow \infty} \frac{1}{T} \int_0^T -v_{out} g_m v_{in} dt
 \end{cases}$$

$$\begin{cases}
 P_T = \lim_{T \rightarrow \infty} \frac{1}{T} \int_0^T V_D g_m V_{IN} dt + \lim_{T \rightarrow \infty} \frac{1}{T} \int_0^T v_{out} g_m v_{in} dt \\
 P_L = \lim_{T \rightarrow \infty} \frac{1}{T} \int_0^T -v_{out} g_m v_{in} dt
 \end{cases} \quad (2.11)$$

$$\eta = \frac{\lim_{T \rightarrow \infty} \frac{1}{T} \int_0^T v_{in}^2 dt}{V_{IN} v_{in_{max}}}$$

Using this formula, one can calculate the efficiency for some waveforms. A full swing sine wave reaches 50% efficiency, a full swing triangular wave reaches 33% efficiency and a full swing square wave reaches 100% efficiency. It is easier to understand these numbers by looking at the waveforms shown in figure 2.2.

Note that, with this setup, the voltages can go above the output voltage source. The filters can be interpreted as an infinite inductance (to filter the signal) and an infinite capacitor (to filter the bias), the capacitor can, therefore, double the voltage after it is fully charged. A way to implement something similar to this is to use a transistor coupled load as shown in figure 2.9.

The limitations to the efficiency happen because the amplifier works as a transconductance (FET) or a current gain (BJT). One cannot help but wonder if there is the possibility to obtain the same results by controlling a reactance, either inductive or capacitive. If this could be done with a pure reactance, the restrictions to efficiency would not apply, as the reactance cannot dissipate power. This Thesis aims at investigating this possibility.

There are many known techniques to reduce the power dissipation in the transistor and thus augment the efficiency. A common technique is to reduce the conduction angle of the transistor, generally compromising a bit of linearity.

Another technique is reducing the DC voltage at the output dynamically when it is not needed, this has been done both continuously and in steps.

A brief study of each amplification class is included hereafter. This serves to better understand the limitations of the transistor technology, as these are what make the work done in this Thesis appealing. First, the classes based on the reduction of the conduction angle are examined from an ideal point of view, then, some classes that use switching are examined.

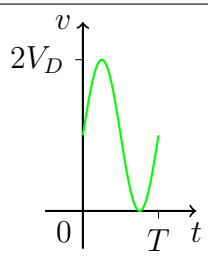
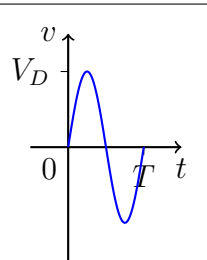
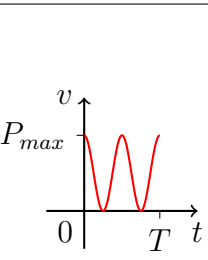
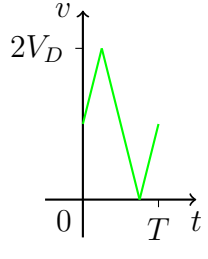
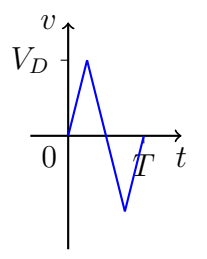
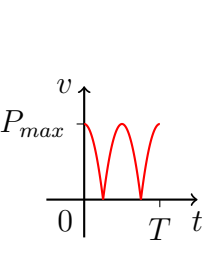
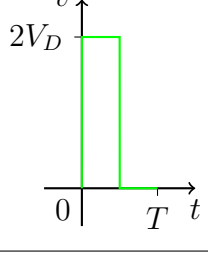
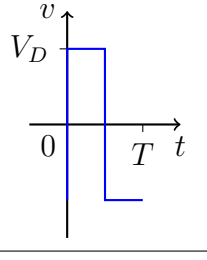
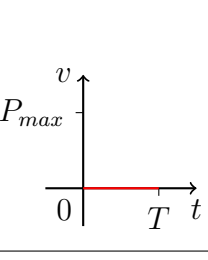
Transistor Voltage	Output Voltage	Dissipated Power
		
		
		

Table 2.2: Waveforms at the Transistor and Output Terminals and the Instantaneous Dissipated Power

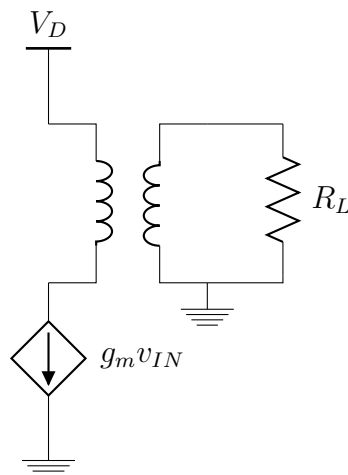


Figure 2.9: A transistor with coupled load

2.5.2 Class A

This class is the least efficient. The transistor is biased in conduction, which means that it is consuming power even when no signal is being amplified. The maximum efficiency for a sinusoidal signal is 50%, which is rather low. The power considerations for this class of operation have been developed in the overview, however, here the analysis is deepened to better understand the class A operation.

A class A amplifier would have the equivalent circuit shown in figure 2.10. The coil and capacitor harmonically tune the load, they create a tank circuit resonant at the carrier frequency.

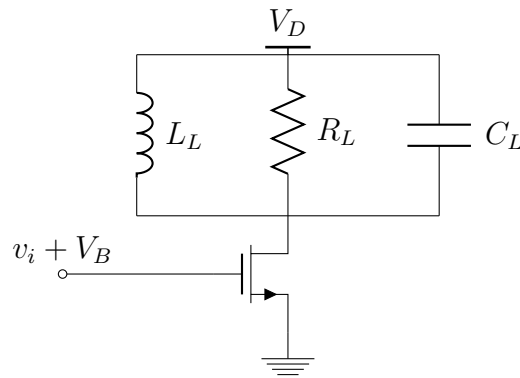


Figure 2.10: Current-Mode Transistor Amplifier Equivalent

To analyse this class more simply, let's assume a linear transconductance FET transistor with an abrupt cut-off, of course, such a transistor cannot exist because it would imply abrupt changes in the derivatives of the transconductance. Nonetheless, this greatly simplifies analysis and, as such, this model will be used. Figure 2.11 shows the current output as a function of the voltage at the transistor's gate as well as a typical class A quiescent current point.

If we take this ideal transistor and expand the concept to the output we would have the characteristics shown in figure 2.12.

With the use of these figures the perturbations can be propagated from the gate to the drain graphically to understand the work of the class A transistor. This is shown in figure 2.13.

If we analyse the graphics carefully, the strengths and weaknesses of the class A configuration come to light. First, notice how the amplifier is very linear when in this configuration, the transistor is always in conduction in a zone where the transconductance is linear and, therefore, the output is a scaled replica of the input. Because the transistor is always in conduction, there is always some power dissipating through it, as seen in the overview. For a full-swing sinusoid, the power consumed in the transistor is the same as the output power, which means that, if there is no other other dissipation source, the maximum efficiency is 50%. This can be extracted from the graphics using equation 2.12.

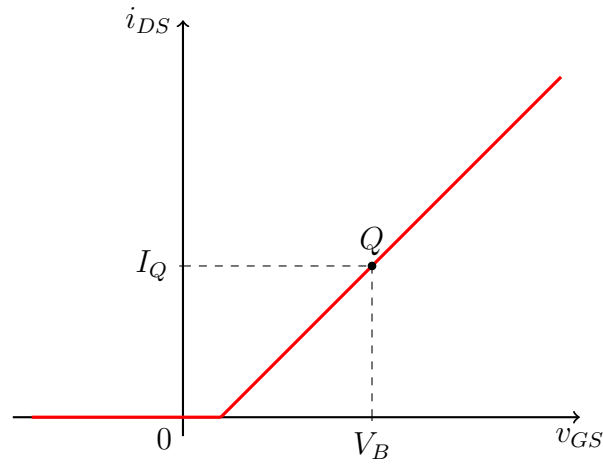


Figure 2.11: Transistor Output Current Vs Input Voltage

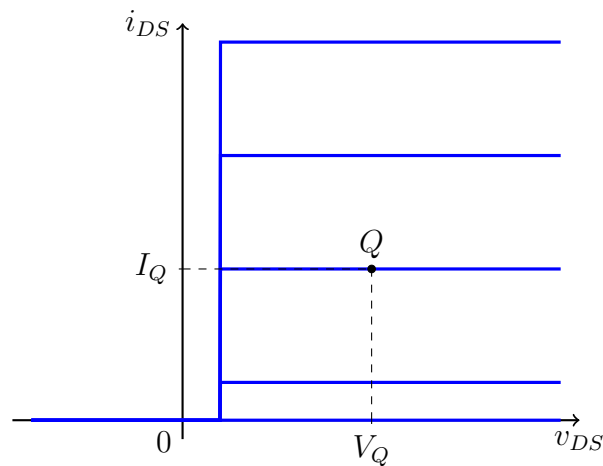


Figure 2.12: Transistor Output Current Vs Output Voltage

$$\left\{ \begin{array}{l} P_T = \frac{v_{DS_{max}} i_{DS_{max}}}{2} = V_Q I_Q - \frac{V_Q I_Q}{2} \\ P_L = \frac{v_{ds_{max}} i_{ds_{max}}}{2} = \frac{V_Q I_Q}{2} \\ \eta = \frac{P_L}{P_L + P_T} = 50\% \end{array} \right. \quad (2.12)$$

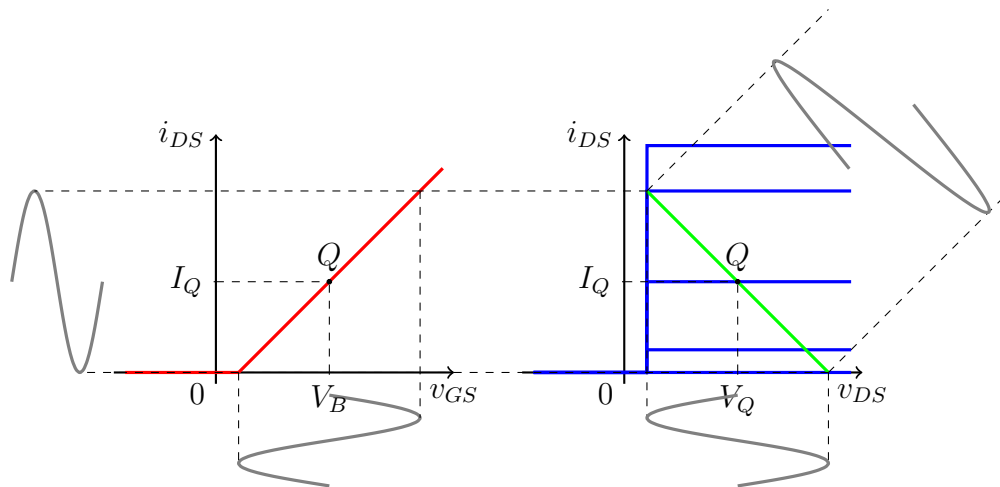


Figure 2.13: Class A Behaviour

2.5.3 Class B

The only difference from a class A to a class B amplifier is the input bias. This means that the circuit in figure 2.10 shown before, also applies to the class B case.

The class B amplifier is biased just before conduction starts, this means that the transistor is cut-off if there is no input signal but starts conduction as soon as there is some positive signal variation. The transistor is therefore working in a non-linear way: in cut-off for every negative signal excitation and in conduction for positive signal excitations. The figure 2.14 shows the bias point for a class B amplifier.

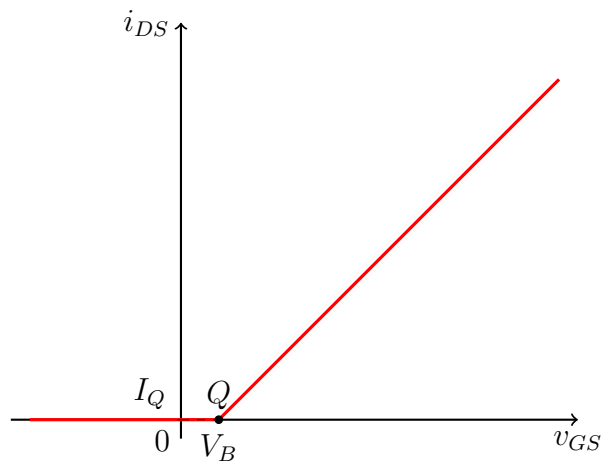


Figure 2.14: Transistor Output Current Vs Input Voltage

We can use the same methodology as before to obtain the approximate behaviour of the class B amplifier. To do this, first we need figure 2.15 to relate the transistor current with the output voltage.

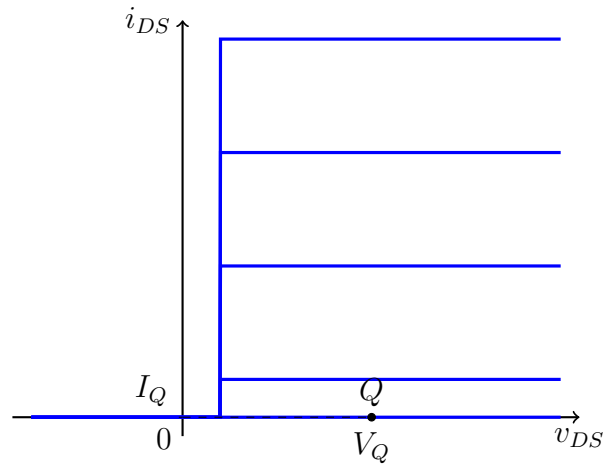


Figure 2.15: Transistor Output Current Vs Output Voltage

Then we can simply project input variations onto the output to obtain the behaviour, as shown in figure 2.16.

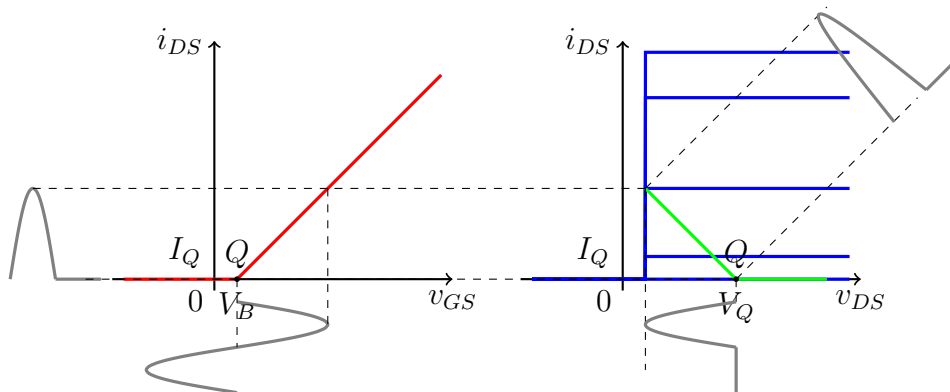


Figure 2.16: Class B Behaviour

Notice how the output is not a copy of the input. However, because the harmonic distortion is even, this is of little matter in RF, since the load is harmonically tuned and the only surviving component would be the original excitation signal's frequency, there is, however, consequences to the gain.

If we calculate the Fourier series of the class B output it is possible to calculate the gain loss in relation to the class A, this is done in equation 2.13. Notice how the fundamental only has one half of the total current swing. This means that, in relation to the class A amplifier, the class B has half the current gain.

Looking at the Fourier series in equation 2.13, we also confirm that there exists no odd harmonics at the output which confirms that the distortion is even and thus should be easily filtered out in RF frequencies.

$$\left\{ \begin{array}{l} i_{ds(t)} = \begin{cases} 0, (2k-1)T < t < (2k+1)\frac{T}{2} \\ I \sin(\omega_p t), (2k+1)\frac{T}{2} < t < (2k+1)T \end{cases} \\ I_{ds(\omega)} = \frac{1}{T_p} \int_0^{\frac{T_p}{2}} I \sin(\omega_p t) e^{jk\omega_p t} dt = \begin{cases} \frac{I}{4j}, k = -1 \\ -\frac{I}{4j}, k = 1 \\ \frac{I}{\pi} \frac{1}{1-k^2}, k = 2n, n \in Z \\ 0, \text{others} \end{cases} \end{array} \right. \quad (2.13)$$

Class B amplifiers can also be used in push-pull configurations to solve the linearity and gain problem. In this case, two transistors are used, one conducts from 0 to 180 degrees and the other from 180 to 360 degrees. This means that the output will be a copy of the input if both transistors have the same gain. This type of configuration can suffer from some distortion problems if the transistors do not start conduction at the expected angles or if they possess different gains.

The efficiency of a class B amplifier can also be calculated using the Fourier series but applying it to the current. The efficiency can be calculated using equation 2.14.

$$\left\{ \begin{array}{l} P_{DC} = \frac{I_{max}}{\pi} V_D \\ P_L = \frac{1}{2} \frac{I_{max}}{2} V_D \\ \eta = \frac{P_L}{P_{DC}} = \frac{\pi}{4} \approx 78.5\% \end{array} \right. \quad (2.14)$$

2.5.4 Class AB

In practice, transistor based power amplifiers end up being operated either in class AB or class C. True Class B amplifiers are impossible to create, because there is no such point at which the transistor can be biased from which it would start conducting at some minimal disturbance. Class A amplifiers can be created but are too inefficient to use in power amplification. What we end up with is an amplifier that conducts with no input signal but not from 0 to 360 degrees.

If we make use of the previous figures, the polarization point would be somewhere after class B and before class A, as shown in figure 2.17 and the behaviour is shown in figure 2.18.

In the case of the class AB, the amplifier will have more gain and less efficiency than the class B, depending on the conduction angle, and vice-versa for the class A. Again, a push-pull type of operation can be arranged to make the amplifier more linear. Both transistors will be conducting in a small region of the signal. The efficiency of this class can be calculated in terms of the conduction angle and considering that only the fundamental

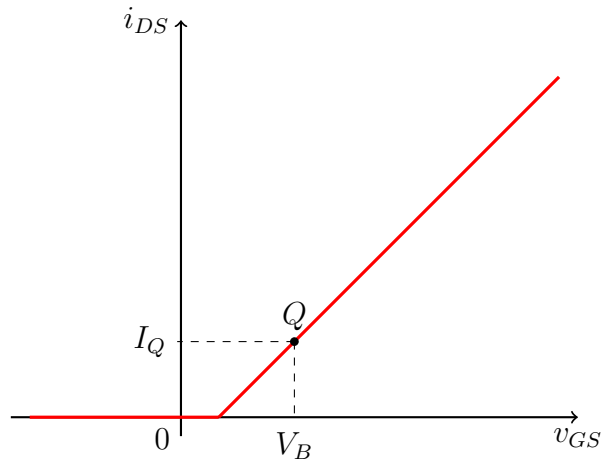


Figure 2.17: Transistor Output Current Vs Input Voltage

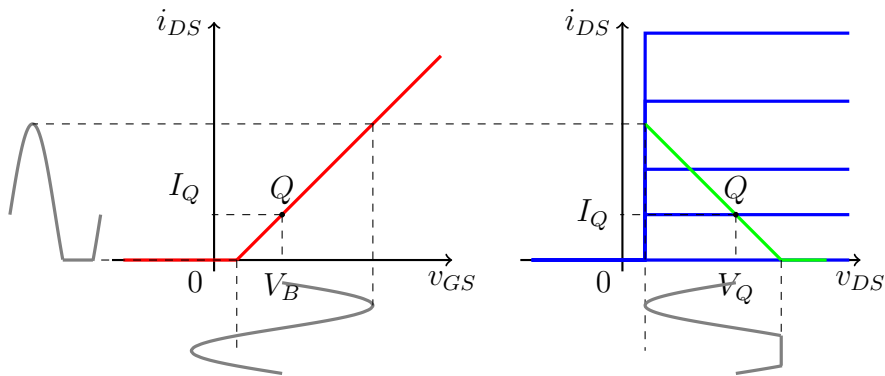


Figure 2.18: Class AB Behaviour

delivers power to the load. This is done in equation 2.15. For a class AB θ_{min} can be calculated as $-\theta_{max}$ for $\theta_{max} \in [\frac{\pi}{2}, \pi]$, the first limit being a class B and the last a class A. The conduction angle is rearranged to ease the calculation of the Fourier series coefficients. I_{max} is the maximum current minus the bias.

$$\left\{ \begin{array}{l} |F[i_{DS}]| = \begin{cases} \frac{I_{max}(\sin(\theta_{max}) - \sin(\theta_{min}) - \theta_{max}\cos(\theta_{max}) + \theta_{min}\cos(\theta_{min}))}{2\pi}, f = 0 \\ -I_{max} \frac{\sin(2\theta_{max}) - 2\theta_{max}}{2\pi}, f = \text{fundamental} \end{cases} \\ P_{DC} = V_D I_{max} \frac{\sin(\theta_{max}) - \theta_{max}\cos(\theta_{max})}{\pi} \\ P_L = -\frac{1}{2} V_D I_{max} \frac{\sin(2\theta_{max}) - 2\theta_{max}}{2\pi} \\ \eta = \frac{1}{4} \frac{2\theta_{max} - \sin(2\theta_{max})}{\sin(\theta_{max}) - \theta_{max}\cos(\theta_{max})} = \frac{1}{4} \frac{\theta_{cond} - \sin(\theta_{cond})}{\sin(\frac{\theta_{cond}}{2}) - \frac{\theta_{cond}}{2}\cos(\frac{\theta_{cond}}{2})} \end{array} \right. \quad (2.15)$$

2.5.5 Class C

To finalize the study of this group of amplifiers, in which the operation mode is controlled by a change in the bias (thus varying the conduction angle), the class C amplifier is the only missing link. The same methodology as before can be used to extract the crude behaviour of the amplifier and some characteristics, figures 2.19 and 2.20 can help. The amplifier distorts the output yet again, but if we consider that only the fundamental frequency remains at the load, the same equation as in the class AB can be applied to obtain the efficiency.

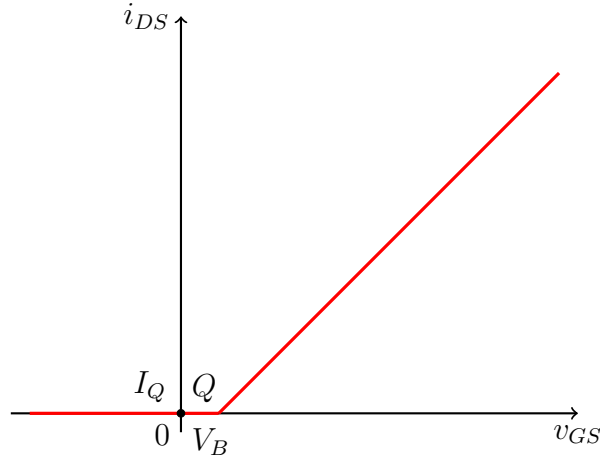


Figure 2.19: Transistor Output Current Vs Input Voltage

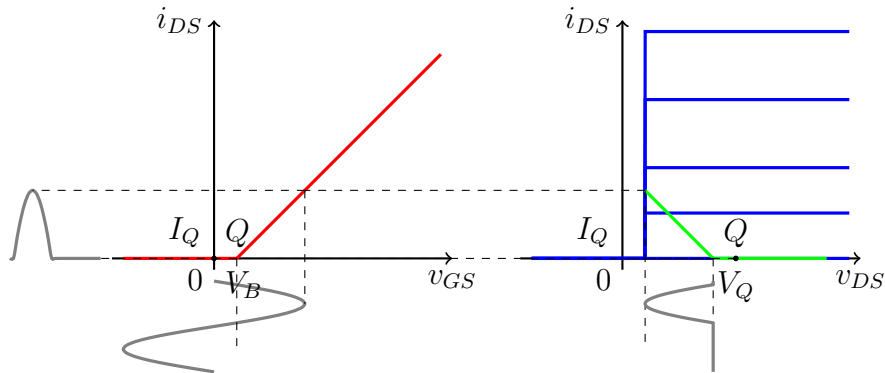


Figure 2.20: Class C Behaviour

2.5.6 Wrap Up

We can use to unit circle to show the classes of operation for several conduction angles, this is shown in figure 2.21. Notice how class A and class B are only points in the circle but class C and class AB are zones.

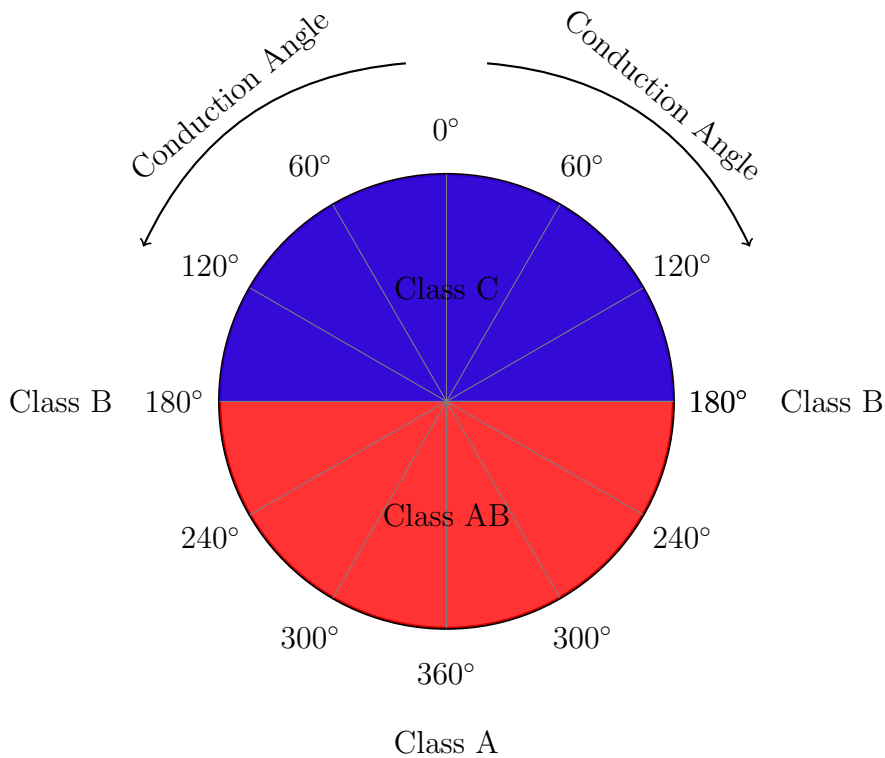


Figure 2.21: Amplifier Classes Vs Conduction Angle

The efficiency for any conduction angle in these classes of amplification can be shown to be the one described in equation 2.16. Here, θ_{max} is half the conduction angle, this is

the same equation as in the class AB case, which can be used for any conduction angle.

$$\left\{ \begin{array}{l} |F[i_{DS}]| = \begin{cases} \frac{I_{max}(\sin(\theta_{max}) - \sin(\theta_{min}) - \theta_{max}\cos(\theta_{max}) + \theta_{min}\cos(\theta_{max}))}{2\pi}, & f = 0 \\ -I_{max} \frac{\sin(2\theta_{max}) - \theta_{max} + \theta_{min}}{2\pi}, & f = \text{fundamental} \end{cases} \\ P_{DC} = V_D I_{max} \frac{\sin(\theta_{max}) - \theta_{max}\cos(\theta_{max})}{\pi} \\ P_L = -\frac{1}{2} V_D I_{max} \frac{\sin(2\theta_{max}) - 2\theta_{max}}{2\pi} \\ \eta = \frac{1}{4} \frac{2\theta_{max} - \sin(2\theta_{max})}{\sin(\theta_{max}) - \theta_{max}\cos(\theta_{max})} = \frac{1}{4} \frac{\theta_{cond} - \sin(\theta_{cond})}{\sin(\frac{\theta_{cond}}{2}) - \frac{\theta_{cond}}{2}\cos(\frac{\theta_{cond}}{2})} \end{array} \right. \quad (2.16)$$

It is evident that there is a close relation between the gain, efficiency and linearity in the transistors operated in this mode. Some of these aspects can be brought to light with the simple study that was executed in this section. In figure 2.22, the maximum efficiency and the gain have been plotted versus the conduction angle.

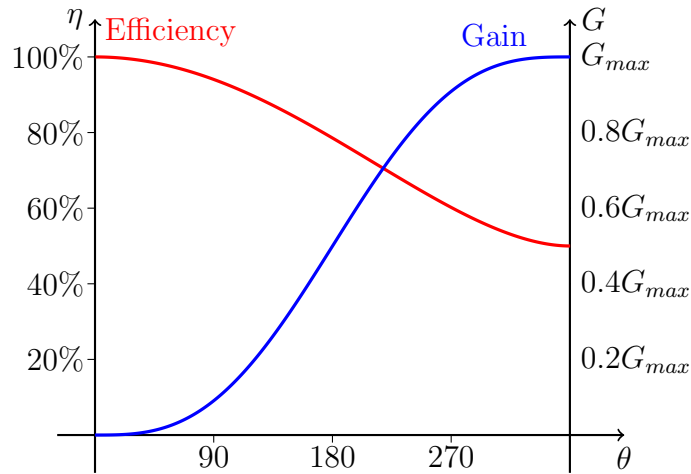


Figure 2.22: Efficiency and Current Gain Vs Conduction Angle

It can be extracted from figure 2.22 that, as said before, the transistor is an inherently resistive device and cannot operate at high efficiency in typical configurations. Some techniques make use of the efficiency peak by operating with switching, these are briefly studied hereafter.

2.5.7 Class D

The class D amplifier works with a square wave at its input. The output is then filtered through an harmonically tuned filter. The concept amplifier is shown in figure 2.23 where

a push-pull configuration was used.

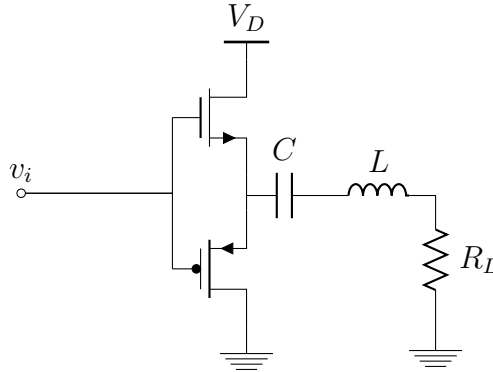


Figure 2.23: Transistor in Class D

The voltage accumulated in the parasitic capacitance of the transistor will hold the output voltage in the transistor transition forcing power dissipation, much like a logic CMOS gate. This is the main problem with the class D amplifier and the reason it cannot reach the theoretic 100% efficiency, the problem aggravates for higher frequencies [3].

2.5.8 Class E

The class E amplifier solves the problem of the class D amplifier. The amplifier uses only one switch, initially the switch is turned on and charges a coil serving as a Radio Frequency Choke (RFC) maintaining zero output voltage, then the transistor is switched off and a pulse of current is applied to the output filter, this filter then determines how the system will behave. The amplifier is shown in figure 2.24. This class of operation was first presented in [4].

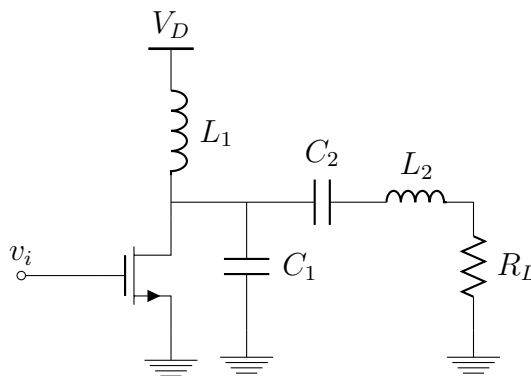


Figure 2.24: Transistor in Class E

In a class E amplifier the filter must obey two conditions. The first is that the voltage must be zero when the switch is turned on again, the second is that its derivative must also be zero.

The conditions in the class E amplifier minimize the efficiency loss making this amplifier type very efficient. The parasitics of the transistor are absorbed into the output filter which eliminates the problem of the class D. The main problem with the class E amplifier is the high non-linearity and the design of the output filter.

2.5.9 Class F

The class F is not really a switching amplifier, however it was included here due to the desired square wave in the output, either in voltage or in current. The class F uses harmonic control techniques to make different types of terminations for each harmonic, the load is only seen at the fundamental, odd and even harmonics see either a short and open circuit or an open and short circuit, respectively. This means that a square wave in voltage or current is generated at the transistor output. This class was first presented in [5].

Typically a voltage square wave is chosen for ease of implementation, this means short circuits for the even harmonics and open circuits for the odd harmonics (the parasitic impedances of the transistor end up in parallel with short-circuits, making them negligible). An example of a circuit tuned this way is shown in figure 2.25.

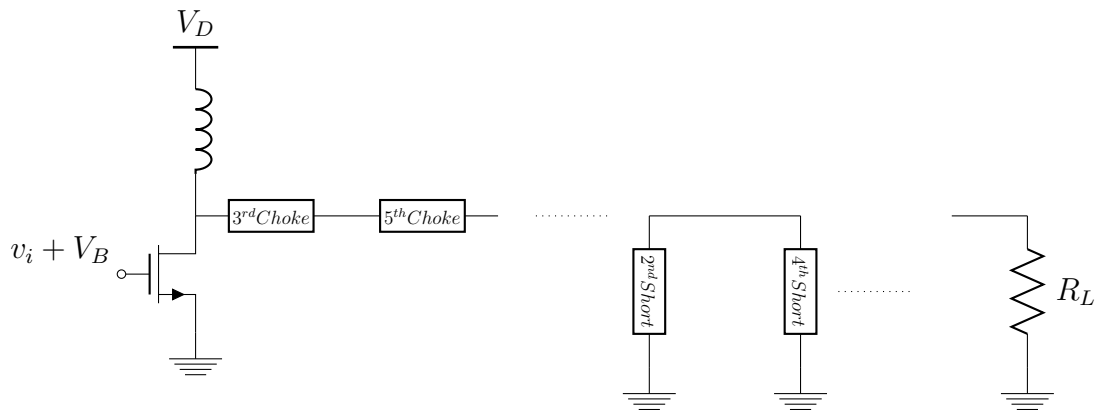


Figure 2.25: Transistor in Class F

The problem with the class F is that the circuit behaviour at the higher harmonics is not always as expected. This leads to waveforms that are not exactly squared and, therefore, dissipation. Also it is impossible to develop the infinite number of filters that are necessary to obtain a square wave. Still, this technique allows for a high gain in efficiency. The desired waveforms at the transistor output are shown in figure 2.26.

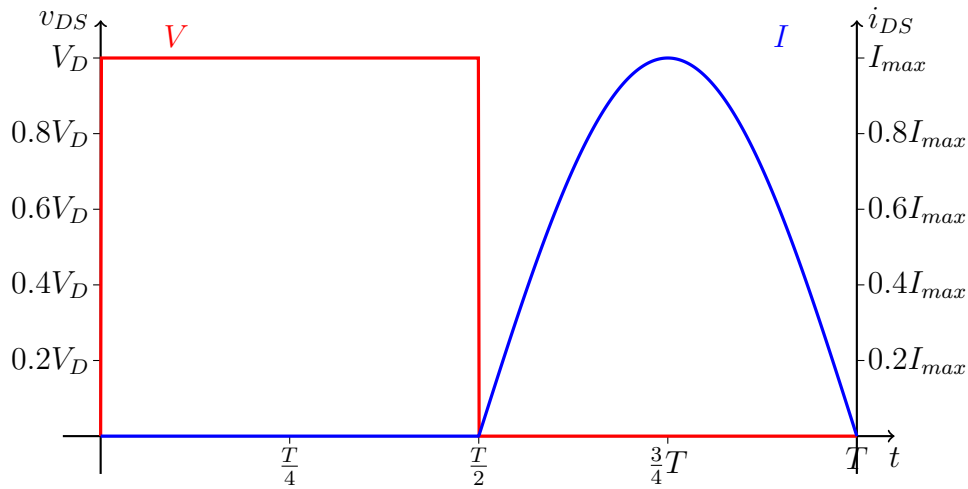


Figure 2.26: Class F Ideal Waveforms

2.5.10 Wrap Up

Switching mode power amplifiers can achieve higher efficiencies than classical topologies. They require however a more complex design, analysis and modelling of the transistor.

2.5.11 Efficient Architectures

To further raise the efficiency the amplifier may make use of several architectures which use more transistors that cooperate to obtain the output signal. These techniques work by reducing the DC power consumption, as explained in the introduction. Some of these architectures are explained lightly here.

Previously, when the efficiency was calculated, optimum operating points were always considered. For instance, if we look at the conduction angle based amplifiers more closely, it's possible to see that the efficiency also varies with output's envelope. If we recalculate the general efficiency equation taking into account that the amplifier may not be working at full capacity we get equation 2.17. In the equation α is the value of the envelope in relation to the maximum and θ_{alpha} is the conduction angle allowed by the value of the envelope.

$$\left\{ \begin{array}{l} |F [i_{DS}]| = \begin{cases} I_{max} \frac{\alpha \sin(\theta_\alpha) - \theta_\alpha \cos(\theta_{max})}{\pi}, f = 0 \\ I_{max} \frac{2\alpha\theta_\alpha + \alpha \sin(2\theta_\alpha) - 4\cos(\theta_{max})\sin(\theta_\alpha)}{2\pi}, f = \text{fundamental} \end{cases} \\ P_{DC} = V_D I_{max} \frac{\alpha \sin(\theta_\alpha) - \theta_\alpha \cos(\theta_{max})}{\pi} \\ P_L = \frac{1}{2} \alpha V_D I_{max} \frac{2\alpha\theta_\alpha + \alpha \sin(2\theta_\alpha) - 4\cos(\theta_{max})\sin(\theta_\alpha)}{2\pi} \\ \eta = \frac{1}{4} \alpha \frac{(2\alpha\theta_\alpha + \alpha \sin(2\theta_\alpha) - 4\cos(\theta_{max})\sin(\theta_\alpha))}{\alpha \sin(\theta_\alpha) - \theta_\alpha \cos(\theta_{max})} \end{array} \right. \quad (2.17)$$

The conduction angle allowed by the envelope can be expressed as a function of α and θ_{max} , the efficiency can then be plotted as a function of α and θ_{max} . To determine this function note that there are three possible states, the transistor is always in conduction, the transistor is never in conduction or the transistor conducts partially. The first case happens when $-\alpha - \cos(\theta_{max}) > 0$, the second when $\alpha - \cos(\theta_{max}) < 0$ and the third when $\alpha \cos(\theta_\alpha) - \cos(\theta_{max}) < 0$ has a solution. In figure 2.27 the ideal efficiency curve for two amplifier classes is shown.

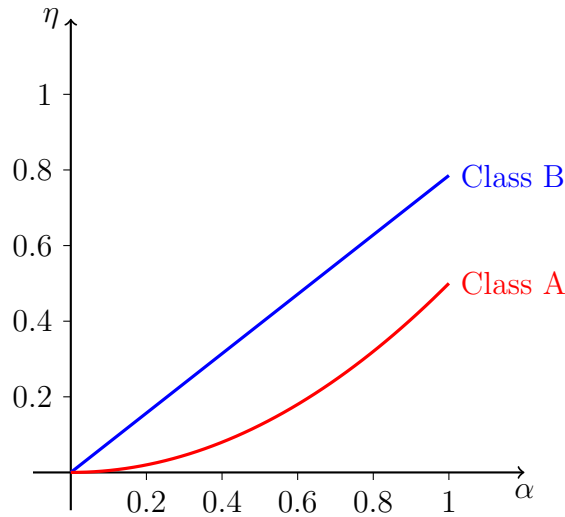


Figure 2.27: PA Efficiency Vs Relative Output Voltage

Envelope Tracking

The ET architecture modules the amplifier's power supply so that it can always operate at maximum efficiency, [6]. The transistor is used in a linear mode, such as class B, but has

an overall higher efficiency. Figure 2.28 shows the block diagram of the ET architecture. An interesting explanation of this architecture can be consulted in [7].

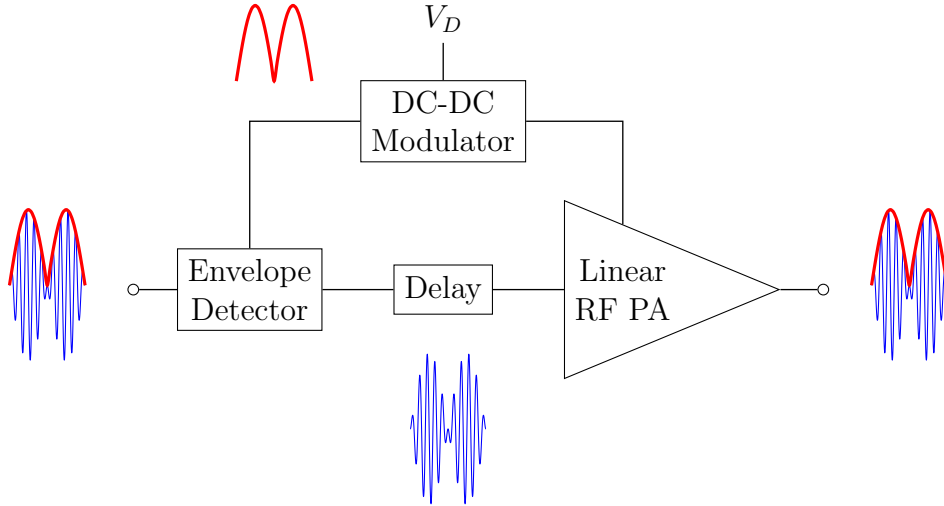


Figure 2.28: ET Block Diagram

If we take the previous equations, this modulation of the power supply would mean that the power at DC would be additionally multiplied by α which would mean that a class B amplifier would have a constant efficiency of $\frac{\pi}{4}$. In fact, the power supply always has a small voltage drop across the modulator which would mean that the multiplication factor would be $\frac{\alpha+\beta}{1+\beta}$. This β factor is a function of the minimum DC voltage attainable $\beta = \frac{V_{D_{min}}}{V_D - V_{D_{min}}}$. The closer the β factor is to zero the more quickly the efficiency rises. Figure 2.29 shows the efficiency for several β factors for a class B amplifier.

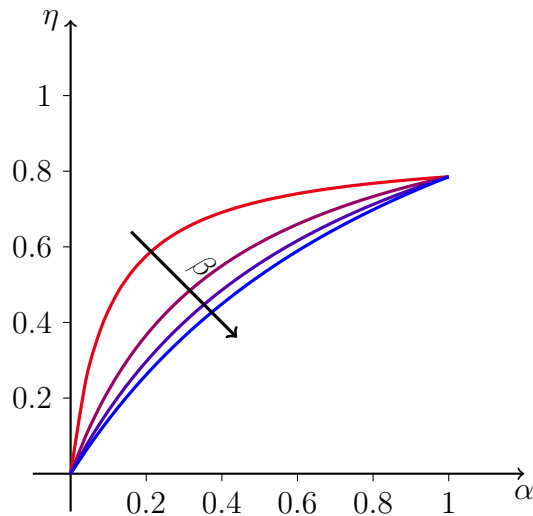


Figure 2.29: ET Efficiency in Class B

Envelope Elimination and Restoration

The EER architecture is similar to ET but a switching mode amplifier is used, such as a class D amplifier, [8]. Figure 2.30 shows the block diagram of the EER architecture.

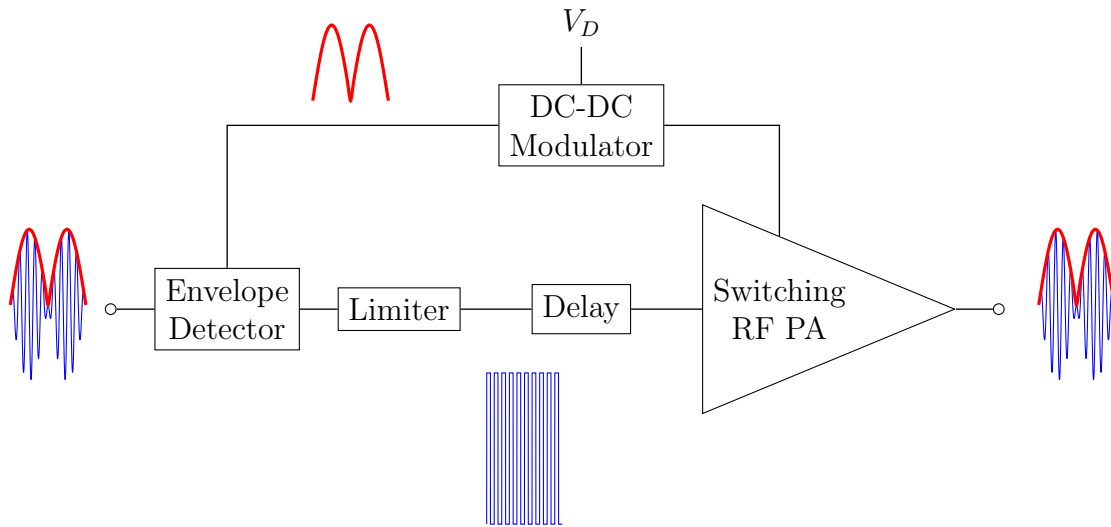


Figure 2.30: EER Block Diagram

A switching mode PA does not have the same problems at lower input powers that the linear PA does since it is always operated with a square input wave. Instead, the losses of switching PAs are connected to the switching times of the voltage and current, these losses are proportional to the energy stored in the parasitic capacitance across the transistors when switching occurs, in turn this energy is proportional to the square of the power supply voltage, to which the output power is also proportional. This means that the drop in efficiency for lower inputs does not happen, instead we would have the same efficiency across the whole input power variation.

Doherty

The DHT amplifier was presented in [9]. The DHT architecture differs greatly from the other two. In this case, instead of modulating the power supply, the load is modulated. To do this, another amplifier is used to boost the current when the input power rises above a certain limit. Because of this, the main amplifier is applying only some of the current that the load is consuming, effectively seeing it as a smaller load. Figure 2.31 shows the DHT block diagram.

This type of architecture is more efficient because the carrier amplifier can be designed for a smaller load, meaning it will reach optimum efficiency quicker. In an evenly split two-way Doherty, the optimum efficiency of the carrier is reached at half power, then the peaking amplifier will start conduction and drop the efficiency a little to recover it for higher powers. Nonetheless, a high improvement in the overall efficiency is achieved. This

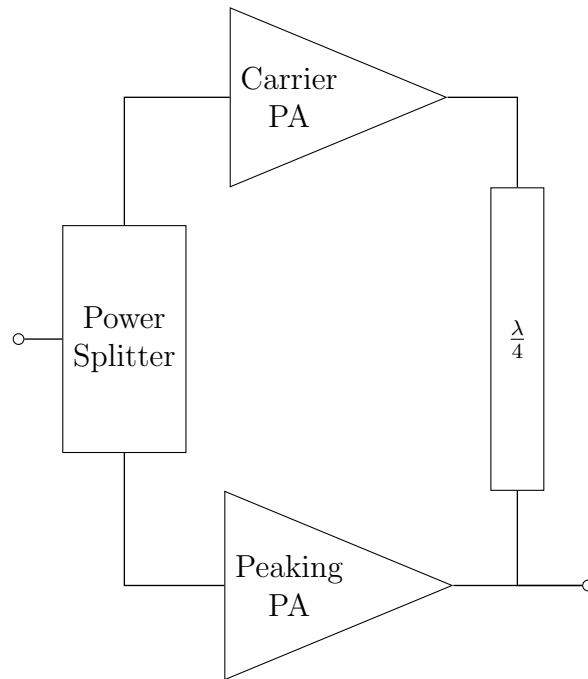


Figure 2.31: DHT Block Diagram

efficiency can be calculated using the following method, consider both amplifier in class B, take the previous formulas and make $\alpha_1 = 2\alpha$ and $\alpha_2 = 2\alpha - 1$ and in both cases restrict α to the interval $[0, 1]$, figure 2.32 shows a characteristic efficiency curve.

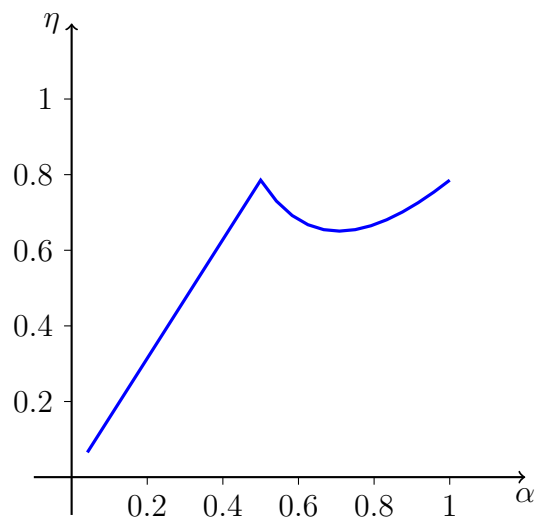


Figure 2.32: Doherty Example Efficiency Curve

2.5.12 Conclusions

The transistor is an intrinsically inefficient device because it is a controlled conductance and thus consumes power except in zero or infinite state. Because of this, the transistor may be regarded as a bad choice for highly efficient applications.

To raise the efficiency we are forced to use techniques that put the transistor working as closely to a switching mode as possible. This requires more advanced modelling and design techniques. Raising the efficiency is also accomplished using efficient architectures that make use of power supply modulation or load modulation.

The use of parametric amplification with the help of controlled reactances may be a possible solution to raise the efficiency and work with easier topologies and design techniques. The allure of this technique is that the basic device is in itself efficient, contrary to the transistor.

Chapter 3

Properties of Non-Linear Elements

3.1 Representation of Non-Linearity

To be able to analyse the system correctly, the non-linearities must be described in some way. This section is given to describe and explain several methods of non-linearity representation. The methods are more thoroughly explained in [1].

Before presenting the methods it is convenient to divide the non-linearities into categories, usually the non-linearities are said either *strong* or *weak*. A *weak* non-linearity can be described using a series, either a power series (such as the Taylor approximation) or a convolutive series (such as the Volterra series). A *strong* non-linearity cannot be accurately described using the series method, usually harmonic-balance and time-domain methods are used to analyse such circuits.

The non-linearities can also be divided in *two-terminal* and *transfer*. A *two-terminal* non-linearity is a capacitance, inductance or resistance, a *transfer* non-linearity would be, for instance, a non-linear FET transconductance.

In this Thesis two main techniques are used to represent the non-linearity. As a first step a polynomial approximation of the non-linearity is used for both small-signal and large-signal analysis. Then, frequency techniques are used to develop models for both analysis. In the small-signal case the conversion matrix is used, for the large-signal a technique similar to harmonic balance is used. The Volterra series are also presented here for the purpose of completeness.

This section lays the basis for the analysis performed onward.

3.1.1 Series

Series are a common form of non-linearity representation. Series are used when non-linearities are *weak* and do not cause great impact on the system's linear response. Nevertheless, they cause sufficient impact to be worth the study. Series are not usually used for *strong* non-linearities because the number of necessary coefficients would be so high the resulting relations, even if accurate, would provide little information on the behaviour of the system.

Power Series

The power series forces the restriction that no non-linearity possesses memory. When using this type of representation it is assumed that the memory can be represented as a linear filter and the non-linearity as a static polynomial. This is very comfortable because the system can then be divided in two blocks, the linear filter and the non-linearity, figure 3.1.

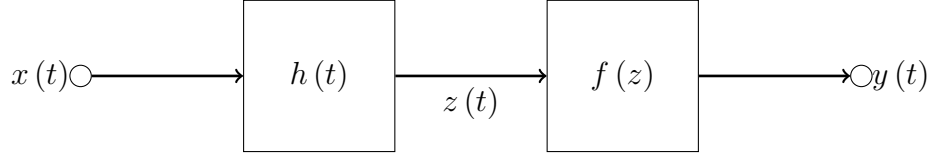


Figure 3.1: Power Series Equivalent System

Equation 3.1 shows the non-linear power series general formula. The ways in which the coefficients can be extracted are numerous. If there is empirical data a method for minimizing the NMSE can be used to obtain the best power series approximation. If there is an analytical description of the circuit another process is to use known mathematical constructs such as the Taylor series.

$$f(z(t)) = \sum_{n=1}^N k_n z(t)^n \quad (3.1)$$

The method to approximate the non-linearity is dependent on the excitation. The Taylor series is the best punctual approximation, the NMSE minimization provides the best approximation giving all points the same weight. Between these two extremes there are other weighting functions that can be used to obtain the coefficients for the polynomial.

The use of polynomials is helpful because there is a direct translation to the frequency domain. This is very useful because the frequency domain analysis is usually favoured over a time domain analysis. Equation 3.2 shows the translation of the power series into frequency when the input is a multi-tone excitation.

$$\begin{aligned}
 z(t) &= \sum_{m=-M}^M Z_m e^{j\omega_m t} \\
 k_n z(t)^n &= k_n \left[\sum_{m=-M}^M Z_m e^{j\omega_m t} \right]^n = \\
 &= k_n \sum_{m_1=-M}^M \sum_{m_2=-M}^M \dots \sum_{m_n=-M}^M Z_{m_1} Z_{m_2} \dots Z_{m_n} e^{j\omega_{m_1} t} e^{j\omega_{m_2} t} \dots e^{j\omega_{m_n} t}
 \end{aligned} \quad (3.2)$$

If the number of coefficients is small, this kind of analysis can give precious insight into the system. If the number of coefficients is high, the effort and the mixing of effects makes

this kind of analysis too laborious and complex to provide useful information.

If we take equation 3.2 and put it as a function of x , the filter $h(t)$ will reveal its influence on the output, this is shown in equation 3.3.

$$\begin{aligned}
 k_n z^n(t) &= k_n \left[\sum_{m=-M}^M Z_m e^{j\omega_m t} \right]^n = \\
 &= k_n \sum_{m_1=-M}^M \dots \sum_{m_n=-M}^M H(\omega_{m_1}) \dots H(\omega_{m_n}) X_{m_1} \dots X_{m_n} e^{j\omega_{m_1} t} \dots e^{j\omega_{m_n} t}
 \end{aligned} \tag{3.3}$$

This form is important as an introduction to the Volterra series.

Volterra Series

The Volterra series eliminates the restriction of separating the memory from the non-linearities, maintaining only the basic problem of the series representation: it is useful only for describing *weak* non-linearities. In the Volterra series the non-linearity is considered a black box that can be described by this series, figure 3.2.

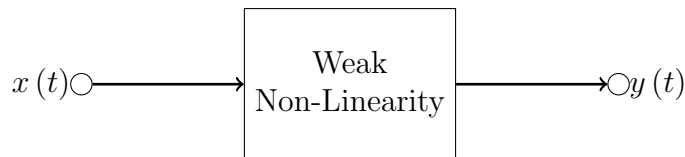


Figure 3.2: Volterra Series Equivalent System

In the time domain the Volterra series takes on the appearance of a series of convolutions to describe the non-linear memory. This representation is of little practical use for analogue systems analysis, a frequency domain representation is of much higher value. In the frequency domain the series can be described by a group of non-linear transfer functions called the Volterra kernels.

If we look at the form of equation 3.3 we can identify the kernels of the power series, in this case they have the form:

$$k_n H(\omega_{m_1}) \dots H(\omega_{m_n}) \tag{3.4}$$

Because the non-linearity was considered memoryless, the kernel is simply the multiplication of the linear transfer function for each frequency. If we generalize the problem and want to include memory in the non-linearities, then the kernels need to be generalized to become any function of the frequencies. The Volterra series can therefore be described as the summation of the general terms shown in equation 3.5, where $H(\omega_{m_1}, \dots, \omega_{m_n})$ are the Volterra kernels.

$$\sum_{m_1=-M}^M \dots \sum_{m_n=-M}^M H(\omega_{m_1}, \dots, \omega_{m_n}) X_{m_1} \dots X_{m_n} e^{j\omega_{m_1} t} \dots e^{j\omega_{m_n} t} \quad (3.5)$$

Again, this analysis is only beneficial for a small number of kernels, otherwise it provides little information on the working of the system.

3.1.2 Frequency Based

There are several frequency based methods to analyse non-linear systems, amongst these, the conversion matrix using large signal/small signal analysis is focused here. This analysis provides valuable information on the circuits analysed henceforth.

Conversion Matrix

Conversion matrix is a method by which it is possible to calculate the behaviour of a system to a small signal and a large signal excitation. The large signal is considered the driver of the system and establishes an operating point. The small signal does not drive the non-linearities and will simply operate in a linear mode with frequency conversion.

To understand this effect consider a function of a large signal X and an incremental small signal x . This function can be expanded around the operating point forced by the large signal as a Taylor series:

$$F(X + x) = F(X) + \frac{dF(X)}{dX}x + \frac{1}{2} \frac{d^2F(X)}{dX^2}x^2 + \dots \quad (3.6)$$

The response of the system to the small-signal should be found by removing the system's response to the large signal ($f(X)$). Additionally, if the small signal is small enough the polynomial terms beside the first order are negligible. The remaining term is simply a linear transformation of the small-signal through the driven non-linearity:

$$f(x) \approx \frac{dF(X)}{dX}x \quad (3.7)$$

This is much the same as is done when analysing the small-signal response of the transistor with the large signal acting as the bias. The big difference of this large signal is that it varies over time, this means that it will produce non-linear distortion when driving the non-linearity and new frequency components are generated. The small signal is mixed with all the frequencies and generates new components at the sum and difference of each one.

To analyse this effect, consider that both the large and small signals are sinusoids of incommensurate frequencies, such that $x = A\cos(\omega_0 t)$ and $X = B\cos(\omega_p t)$, incommensurate quantities z_k can be defined as seen in equation 3.8.

$$\sum_{k=0}^K n_k z_k = 0, \forall n_k \in Z \quad (3.8)$$

Assume as well that the function $F(u)$ is a non-linearity being driven by the large signal. As seen before the response of the system to the small signal will be equation 3.7. The spectrum of the function $\frac{dF(X)}{dX}$ is similar to the spectrum shown in figure 3.3.

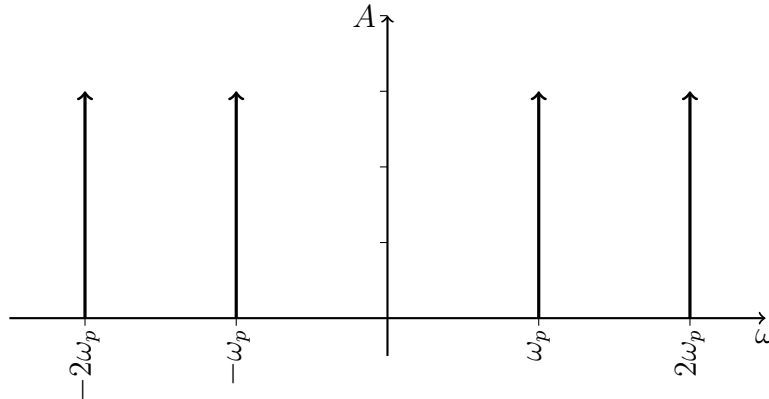


Figure 3.3: Non-Linearity Spectrum

When a small-signal is added to the system, the spectrum of the output will take the form of the one shown in figure 3.4.

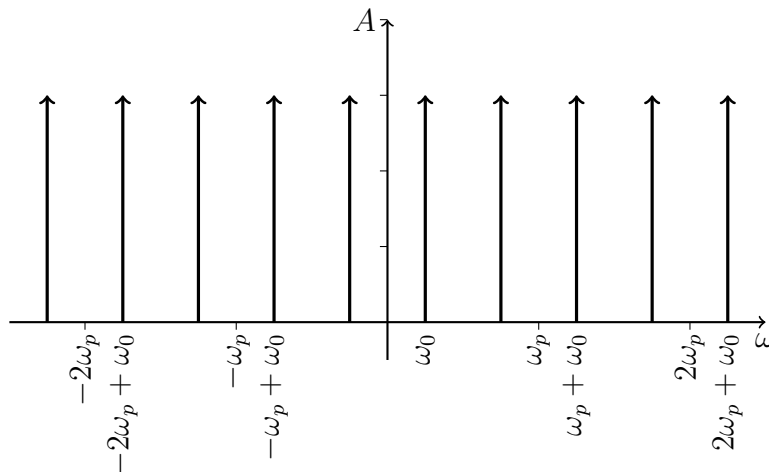


Figure 3.4: Conversion Output Spectrum

Because the small signal is purely real, this response can be fully reconstructed using only one of the terms around each multiple of ω_p . Using this fact we can express the equation of the conversion in the form of a double series as shown in equation 3.9.

$$f(x) \approx \frac{dF(X)}{dX}x = \sum_{n=-\infty}^{+\infty} F_n e^{jn\omega_p t} \sum_{m=-\infty}^{+\infty} x_m e^{j\omega_0 t} = \sum_{n=-\infty}^{+\infty} \sum_{m=-\infty}^{+\infty} F_n x_m e^{j\omega_{m+n} t} \quad (3.9)$$

Finally, this series can also be expressed in the matrix form (when truncated) which effectively describes the circuit as an N-port network at each frequency, as seen in equation 3.10.

$$\begin{bmatrix} f_{-N}^* \\ f_{-N+1}^* \\ \dots \\ f_0 \\ f_1 \\ \dots \\ f_{N-1} \\ f_N \end{bmatrix} = \begin{bmatrix} F_0 & F_{-1} & \dots & F_{-2N} \\ F_1 & F_{-1} & \dots & F_{-2N+1} \\ \dots & \dots & \dots & \dots \\ F_N & F_{N-1} & \dots & F_{-N} \\ F_{N+1} & F_N & \dots & F_{-N+1} \\ \dots & \dots & \dots & \dots \\ F_{2N-1} & F_{2N-2} & \dots & F_{-1} \\ F_{2N} & F_{2N-1} & \dots & F_0 \end{bmatrix} \begin{bmatrix} x_{-N}^* \\ x_{-N+1}^* \\ \dots \\ x_0 \\ x_1 \\ \dots \\ x_{N-1} \\ x_N \end{bmatrix} \quad (3.10)$$

Note that the negative frequency components have been shown as conjugates, this happens to avoid the negative frequency. It is a simple change in definition, the components are defined as phasors that represent the negative frequency. This can be done because the signal is real and therefore the equation $x_{-n}^* = x_n$ is true.

The conversion matrix is very helpful because it allows the use of the frequency domain properties with non-linear components. The conversion matrix works as an N-dimensional component across the several frequencies guiding the frequency translations of the input components to the output. As an example let's apply the conversion matrix to a non-linear capacitor.

Imagine a non-linear capacitor such that its capacitance is described by the function $C(v)$, where v is the voltage across its terminals. If this is the case, then we can write the following equations:

$$\frac{dq(v)}{dv} = C(v) \quad (3.11)$$

$$q(v_{ss}) = C(V_{ls})v_{ss}$$

where V_{ls} is the large signal operation point and v_{ss} is the small signal increment. Here, $C(V_{ls})$ is $\frac{dF(X)}{dX}$, to determine the coefficients needed for the conversion matrix the capacitance function would need to be specified, instead C_n will be used to mark the capacitance coefficients.

If we build the matrix with the C_n coefficients the result is:

$$\begin{bmatrix} Q_{-N}^* \\ Q_{-N+1}^* \\ \dots \\ Q_0 \\ Q_1 \\ \dots \\ Q_{N-1} \\ Q_N \end{bmatrix} = \begin{bmatrix} C_0 & C_{-1} & \dots & C_{-2N} \\ C_1 & C_{-1} & \dots & C_{-2N+1} \\ \dots & \dots & \dots & \dots \\ C_N & C_{N-1} & \dots & C_{-N} \\ C_{N+1} & C_N & \dots & C_{-N+1} \\ \dots & \dots & \dots & \dots \\ C_{2N-1} & C_{2N-2} & \dots & C_{-1} \\ C_{2N} & C_{2N-1} & \dots & C_0 \end{bmatrix} \begin{bmatrix} V_{-N}^* \\ V_{-N+1}^* \\ \dots \\ V_0 \\ V_1 \\ \dots \\ V_{N-1} \\ V_N \end{bmatrix} \quad (3.12)$$

Where V_n are the small signal voltage coefficients, C_n the capacitance large signal coefficients and Q_n the charge coefficients.

To obtain the current we need to differentiate the charge, since we are in the frequency domain a simple multiplication by $j\omega$ would suffice. In the case of the matrix with each row belonging to one frequency this multiplication is also done in the matrix form, using:

$$j \begin{bmatrix} \omega_{-N} & 0 & \dots & 0 \\ 0 & \omega_{-N+1} & \dots & 0 \\ \dots & \dots & \dots & \dots \\ 0 & 0 & \dots & \omega_N \end{bmatrix} \quad (3.13)$$

The final result is the well known form $I = j\Omega CV$ in the matrix form. The conversion matrix is therefore a very helpful construct to analyse small signal behaviour in a large signal driven non-linearity.

3.2 Manley-Rowe Relations

Manley and Rowe described some properties of the interaction of signals applied to non-linear components [10]. These properties were extracted with very broad conditions, the only assumption was that the characteristic of the non-linear device is unitary and, if not, that the hysteresis loop be only double valued. In their work it is described that energy can be extracted from sources interacting in a non-linear reactance and given to a signal generated in the non-linearity, with the power loss equal to the area of the hysteresis loop. In the remainder of this work the devices are considered to have no hysteresis to simplify the relations.

The relations can be extracted in a simpler, more understandable way through simple transformation of the power balance equations, this procedure is shown in equations 3.14, 3.15, 3.16 and 3.17, it as been extracted from [11, p. 804 - p. 807].

In a non-linear capacitance excited by two periodic signals the power conservation can be expressed, in the frequency domain, as:

$$\sum_{n=-\infty}^{+\infty} \sum_{m=-\infty}^{+\infty} P_{n,m} = 0 \quad (3.14)$$

If we multiply and divide $P_{n,m}$ by $n\omega_1 + m\omega_2$ where ω_1 and ω_2 are the fundamental frequencies of the excitation signals we can write:

$$\omega_1 \sum_{n=-\infty}^{+\infty} \sum_{m=-\infty}^{+\infty} n \frac{P_{n,m}}{n\omega_1 + m\omega_2} + \omega_2 \sum_{n=-\infty}^{+\infty} \sum_{m=-\infty}^{+\infty} m \frac{P_{n,m}}{n\omega_1 + m\omega_2} = 0 \quad (3.15)$$

Taking into account that $P_{n,m} = V_{n,m} I_{n,m}^*$ and $Q_{n,m} = -j \frac{I_{n,m}}{n\omega_1 + m\omega_2}$ we can conclude that the series do not depend on the frequency, but only on the voltage and the capacitance. If this is true, then, for arbitrary ω_1 and ω_2 , each of the series must vanish independently and we can write:

$$\begin{aligned}
\sum_{n=-\infty}^{+\infty} \sum_{m=-\infty}^{+\infty} n \frac{P_{n,m}}{n\omega_1 + m\omega_2} &= 0 \\
\sum_{n=-\infty}^{+\infty} \sum_{m=-\infty}^{+\infty} m \frac{P_{n,m}}{n\omega_1 + m\omega_2} &= 0
\end{aligned} \tag{3.16}$$

Finally, knowing that $P_{n,m} = P_{-n,-m}$ the series can be simplified to the common Manley-Rowe power relations.

$$\begin{aligned}
\sum_{n=0}^{+\infty} \sum_{m=-\infty}^{+\infty} n \frac{P_{n,m}}{n\omega_1 + m\omega_2} &= 0 \\
\sum_{n=-\infty}^{+\infty} \sum_{m=0}^{+\infty} m \frac{P_{n,m}}{n\omega_1 + m\omega_2} &= 0
\end{aligned} \tag{3.17}$$

The relations can also be extracted for a non-linear inductance by observing that $\Phi_{n,m} = -j \frac{V_{n,m}}{n\omega_1 + m\omega_2}$, which is completely controlled by the current and the inductance, leaving us in the same conditions as before.

3.2.1 Uses and Limitations

The Manley-Rowe power relations can be used to easily estimate the power gain of a parametric amplifier based on non-linear capacitances or inductances. The power gain is, however, a very restrictive FoM to evaluate a PA, in fact, the PA can have a good power gain but be near useless if it cannot take any power input.

An example of how to extract the power gain from the Manley-Rowe relations is the following, imagine that there exists such a circuit in which only the fundamental frequencies of the excitation ω_1 and ω_2 can survive, as well as their sum. If this is the case, then the relations can be reduced greatly, as shown in equation 3.18.

$$\begin{aligned}
\frac{P_{1,0}}{\omega_1} + \frac{P_{1,1}}{\omega_1 + \omega_2} &= 0 \\
\frac{P_{0,1}}{\omega_2} + \frac{P_{1,1}}{\omega_1 + \omega_2} &= 0
\end{aligned} \tag{3.18}$$

Simple transformations result in the power gain from each power input to the output, equation 3.19.

$$\begin{aligned} -\frac{P_{1,1}}{P_{1,0}} &= \frac{\omega_1 + \omega_2}{\omega_1} \\ -\frac{P_{1,1}}{P_{0,1}} &= \frac{\omega_1 + \omega_2}{\omega_2} \end{aligned} \tag{3.19}$$

Notice how the power gain says nothing about the capacitance type. In fact, one could use a linear capacitance and the power gain would be the same. This is strange because, if the capacitance is linear, there should be no power input to the system nor generation of new frequencies. What happens is that, in this case, the power gain is obtained at the cost of a $\frac{0}{0}$ indetermination (both $P_{1,1}$ and $P_{1,0}$ are zero).

The conclusion one can draw from this is that the Manley-Rowe relations is an important tool to estimate the optimal gain of an amplifier but it fails to describe several important characteristics: transducer gain, input power, sensitivity to non-linearity, etc.. To estimate these the system must be analysed at a deeper level.

Chapter 4

Parametric Amplifier

4.1 Definition

A Parametric Amplifier (ParAmp) is one in which the characteristics of some component vary over time periodically. This variation is usually attained through excitation of a non-linear reactance with a strong periodic signal, this strong signal is called the pump. Amplification is achieved by perturbing the pump's excitation with some other signal, which is the input. Because both signals vary over time, the output of a ParAmp occurs at some other frequency, usually at the sum or difference of the fundamentals of each signal. Figure 4.1 shows the concept of a ParAmp. In a real ParAmp the gain is not only a function of the pump excitation, but also of the input.

The pumping can be done either in current or in voltage, the ParAmp is said current pumped or voltage pumped, respectively. The choice for pumping is dependent on the characteristics of the used devices, benefits and losses should be well pondered when choosing the pumping excitation.

Another important characteristic of ParAmps is whether or not the input and the pump have commensurate frequencies. When they do, the ParAmp is said to be degenerate and it has some special properties because the pump's and input's energies can be converted into each other without interacting with the output. This process does require that the frequencies are commensurate which does not make much sense if the input is a modulated signal, because it would mean that the pump would also need to be modulated inducing a logic loop (amplification of a modulated signal would need an amplified modulated signal from which to extract energy). In this Thesis degenerate ParAmps will be mentioned when some energy considerations are derived but are not the main focus.

Finally a non-degenerate ParAmp can either be inverting or non-inverting (this nomenclature relates to gain considerations), inverting ParAmps can be proved to be always unstable, while the non-inverting have stable operating points. Because of this, the non-inverting case is more thoroughly explored.

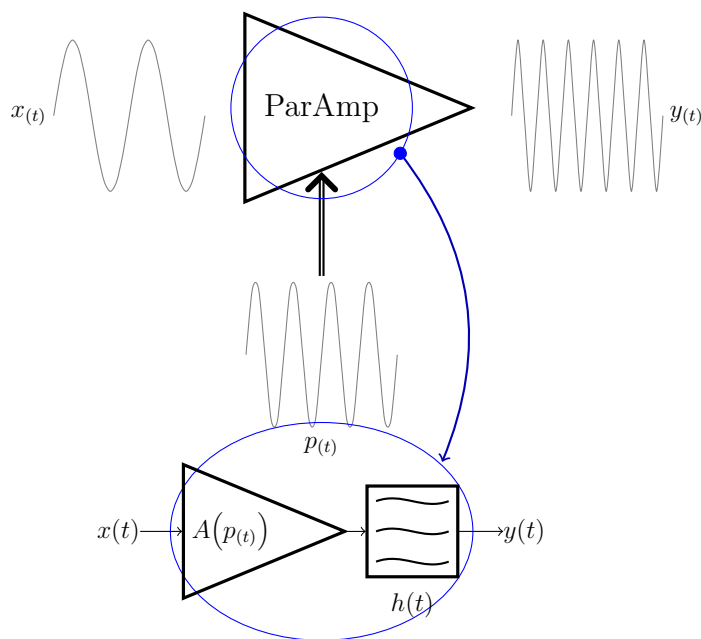


Figure 4.1: Conceptual Parametric Amplifier

4.2 Energy Considerations

Before setting out to discover more about ParAmps, it is useful to look more deeply into the energy relations of non-linear components. As it was explained before, Manley and Rowe deduced in [10] the energy conversion relations that can be achieved using a non-linear reactance, this deduction was restricted to incommensurate frequencies and two sources but very relaxed in terms of the reactance function form.

It would be interesting to restrict the reactance's form more and obtain more insight into the energy conversion process under these restrictions, as far as the author knows, such demonstration has never been done before. To do this, one can begin by assuming that the reactance is a capacitance and that it must be possible to describe as a polynomial, such as the one shown in equation 4.1.

$$c_{(v)} = \sum_{k=0}^{+\infty} C_k v^k \quad (4.1)$$

Even though this restricts the analysis, at least in some operating point the capacitance should be able to be described as a polynomial, if nothing more this will allow for analysis of linearly varying capacitances.

If we assume that the capacitance can be described as the polynomial (shown in equation 4.1) then it is possible to calculate the charge using equation 4.2 and thus the current. More important than that, however, is that the form of the energy can also be extracted using equation 4.3 (noting that $dq = cdv$).

$$q = \int_0^v c(v)dv = \int_0^v \sum_{k=0}^{+\infty} C_k v^k dv = \sum_{k=0}^{+\infty} C_k \int_0^v v^k dv = \sum_{k=0}^{+\infty} \frac{C_k}{k+1} v^{k+1} \quad (4.2)$$

$$e = \int_0^q v(q)dq = \int_0^v vc(v)dv = \int_0^v \sum_{k=0}^{+\infty} C_k v^{k+1} dv = \sum_{k=0}^{+\infty} C_k \int_0^v v^{k+1} dv = \sum_{k=0}^{+\infty} \frac{C_k}{k+2} v^{k+2} \quad (4.3)$$

Equation 4.3 gives the energy that is stored in the capacitance in terms of the voltage, this should be averaged to obtain the general trend. When more energy is stored in the capacitance it means that the charge and voltage waves are in-phase and the capacitance behaves as such. When less energy is stored, it means that the charge has begun to spin out of phase with the voltage and thus actual power is given and taken from the capacitance. This behaviour can be plotted in the trigonometric circle for a better understanding as shown in figure 4.2.

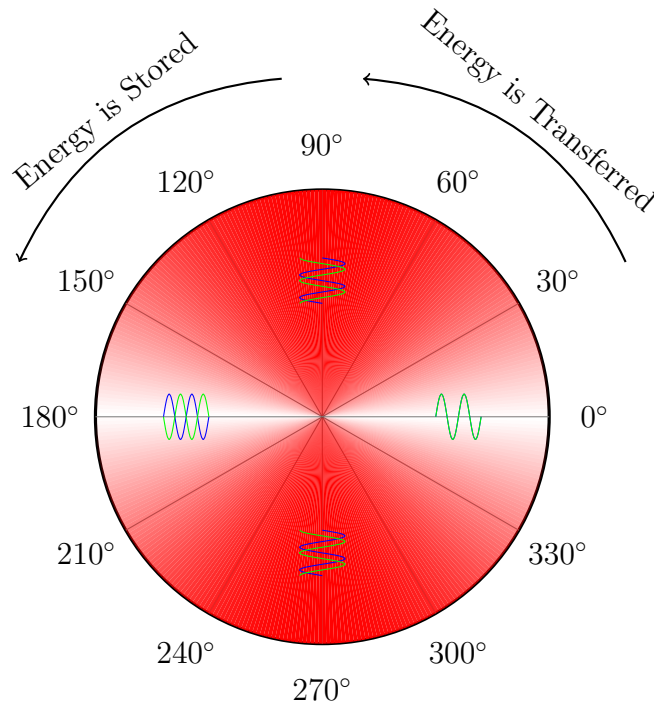


Figure 4.2: Trigonometric Circle of Energy

To keep the analysis simple we will advance up until a linearly varying capacitance. Note that, because the energy is also described as a polynomial of the voltage the energy terms can be analysed for each of the voltage powers. Therefore, we can begin with a constant capacitance for $k = 0$ and follow with the analysis of a linearly varying capacitance with $k=1$, this method could be followed up to any order, but each term is more complex to analyse because more frequency components arise.

First let's define the voltage waveform. If we define the voltage waveform as a sum of cosines of the form shown in equation 4.4, we maintain some generality and a relatively simple analysis, it's also assumed that, if $x > y$ then $\omega_x > \omega_y$.

$$v_{x(t)} = V_x \cos(\omega_x t + \phi_x) \quad (4.4)$$

Let's begin with the analysis of a constant capacitance, in this case the energy is reduced to one term, $e(t) = C_0 \frac{v(t)^2}{2}$, if the developments thus far have been correct then it is expected that it would be impossible to transfer energy for this capacitance type, it should only be possible to store it. To analyse the energy we need to develop the square, this is done in equation 4.5.

$$v_{(t)}^2 = \left(\sum_{n=1}^{n=N} V_n \cos(\omega_n t + \phi_n) \right)^2 = \quad (4.5)$$

$$\frac{1}{2} \sum_{n=1}^{n=N} V_n^2 + \frac{1}{2} \sum_{n=1}^{n=N} V_n^2 \cos(2\omega_n t + 2\phi_n) + \sum_{n=1}^{n=N} \sum_{m=1, m \neq n}^{m=N} v_{n(t)} v_{m(t)}$$

Looking at equation 4.5 it's possible to observe that the only DC term will be the first of the expansion, all the other terms will be at some frequency because all frequencies are different for each voltage index. If we take the average of the energy we quickly see that the average energy stored in the capacitor will be $\frac{1}{2} \sum_{n=1}^{n=N} V_n^2$, which is provided by each source. There is no way to reduce the stored energy, and therefore raise the transferred energy. We conclude that with a constant capacitance there is no possible energy transference between sources.

Now we look at the linearly varying capacitance, in this case the energy has two terms, the first is similar to the linear capacitance and so the result is the same, the second is related to the linear variation, $C_1 \frac{v(t)^3}{3}$. Again, we need to expand the power to obtain a treatable expression because it is difficult to know what the average power will be in this case, this is shown in equation 4.6.

$$v(t)^3 = \left(\sum_{n=1}^{n=N} V_n \cos(\omega_n t + \phi_n) \right)^3 = \quad (4.6)$$

$$\sum_{n=1}^{n=N} v_{n(t)}^3 + 3 \sum_{n=1}^{n=N} \sum_{m=1, m \neq n}^{m=N} v_n(t)^2 v_m(t) + \sum_{n=1}^{n=N} \sum_{m=1, m \neq n}^{m=N} \sum_{k=1, k \neq n, k \neq m}^{k=N} v_n(t) v_m(t) v_k(t)$$

Now we analyse each term of equation 4.6, the first term cannot generate an average value, the second and third terms however can, equation 4.7 shows the DC components that can be generated by these.

$$\begin{aligned}
& \frac{3}{4} \sum_{n=1}^{n=N} \sum_{m=1, \omega_m=2\omega_n}^{m=N} V_n^2 V_m \cos(2\phi_n - \phi_m) \\
& \frac{3}{2} \sum_{n=1}^{n=N} \sum_{m=n+1, \omega_m \neq 2\omega_n}^{m=N} \sum_{k=1, \omega_k = \omega_n \pm \omega_m}^{k=N} V_n V_m V_k \cos(\phi_n \pm \phi_m \mp \phi_k)
\end{aligned} \tag{4.7}$$

The interesting part is that the average energy stored is controlled by the phase of the input frequencies in relation to one another. If we control the phase, we can diminish the stored energy, thus augmenting the energy transference between sources, if we look at figure 4.2 we can conclude that, if the energy stored in the capacitor is described by equation 4.7, the transferred energy should be described by equations in quadrature with these, shown in 4.8.

$$\begin{aligned}
& \frac{3}{4} \sum_{n=1}^{n=N} \sum_{m=1, \omega_m=2\omega_n}^{m=N} V_n^2 V_m \sin(2\phi_n - \phi_m) \\
& \frac{3}{2} \sum_{n=1}^{n=N} \sum_{m=1, m \neq n}^{m=N} \sum_{k=1, \omega_k = \omega_n \pm \omega_m}^{k=N} V_n V_m V_k \sin(\phi_n \pm \phi_m \mp \phi_k)
\end{aligned} \tag{4.8}$$

As a more practical example let's assume that the voltage has three sources, the input, the pump and the output, v_{in} , v_p and v_{out} , respectively. Its frequencies are defined as follows, ω_{in} for the input, ω_p for the pump and $\omega_{out} = \omega_{in} + \omega_p$ for the output.

The input, pump and output would transfer energy according to equation 4.8, this equation describes the amount the energy that is transferred through the capacitance. The conservation of energy requires that the sum of the energies consumed and provided be zero, because equation 4.8 only describes the energy that is transferred this does not happen here, however when we look from the side of the sources some are taking energy while others are giving it, or even doing both at the same time. The sources work at different frequencies and so balancing the energies is more complex than balancing the power, because the energy transference occurs at different time rates. Equation 4.9 shows the total energy transferred through the capacitance considering the pump as the phase reference, the first term is only valid for degenerate ParAmps.

$$E_{transfer} = \left[\frac{C_1}{4} V_{in}^2 V_p \sin(2\phi_{in}) \right]_{\omega_p=2\omega_{in}} + \frac{C_1}{2} V_{in} V_p V_{out} \sin(\phi_{in} - \phi_{out}) \tag{4.9}$$

Using the charge equation we can see the flow of energy for each source, knowing this it is then possible to evaluate how the energy shifts between them. In equation 4.10 the charge formula is expanded for better examination, the charge due to the linear component has been suppressed and the terms important at each frequency have been isolated.

$$\begin{aligned}
q &= \frac{C_1}{2} \left(v_{in}^2 + v_p^2 + v_{out}^2 + 2v_{in}v_p + 2v_{in}v_{out} + 2v_pv_{out} \right) \\
\omega_{in} &\rightarrow C_1 (v_{in}v_p + v_pv_{out}) \\
\omega_p &\rightarrow \frac{C_1}{2} (v_{in}^2 + 2v_{in}v_{out}) \\
\omega_{out} &\rightarrow C_1 v_{in}v_p
\end{aligned} \tag{4.10}$$

The terms are then multiplied by each of the corresponding voltages taking into account a 90° shift in the charge for power to be transferred, and we obtain equation 4.11 that indicates the flow of energy and also that the pump and input provide the same energy amount when they have incommensurate frequencies, the output is the source working opposite. When the pump and input are commensurate there are other two important terms shown in equation 4.12.

$$\begin{aligned}
\omega_{in} &\rightarrow \frac{C_1}{4} V_{in} V_p V_{out} \sin(\phi_{out} - \phi_{in}) \\
\omega_p &\rightarrow \frac{C_1}{4} V_{in} V_p V_{out} \sin(\phi_{out} - \phi_{in}) \\
\omega_{out} &\rightarrow -\frac{C_1}{4} V_{in} V_p V_{out} \sin(\phi_{out} - \phi_{in})
\end{aligned} \tag{4.11}$$

$$\begin{aligned}
\omega_{in} &\rightarrow -\frac{C_1}{4} V_{in}^2 V_p \sin(2\phi_{in}) \\
\omega_p &\rightarrow \frac{C_1}{8} V_{in}^2 V_p \sin(2\phi_{in})
\end{aligned} \tag{4.12}$$

Notice that the energies do not balance, this happens because the energy is transferred in different amounts of time. To avoid this issue the quantity to be analysed should be the power. The power measures the amount of energy per unit of time, each of the sources transfers the described amount of energy per wave period, this means that the power will be described by equations 4.13 and 4.14

$$\begin{aligned}
\omega_{in} &\rightarrow f_{in} \frac{C_1}{4} V_{in} V_p V_{out} \sin(\phi_{out} - \phi_{in}) \\
\omega_p &\rightarrow f_p \frac{C_1}{4} V_{in} V_p V_{out} \sin(\phi_{out} - \phi_{in}) \\
\omega_{out} &\rightarrow -f_{out} \frac{C_1}{4} V_{in} V_p V_{out} \sin(\phi_{out} - \phi_{in})
\end{aligned} \tag{4.13}$$

$$\begin{aligned}
\omega_{in} &\rightarrow -f_{in} \frac{C_1}{4} V_{in}^2 V_p \sin(2\phi_{in}) \\
\omega_p &\rightarrow f_p \frac{C_1}{8} V_{in}^2 V_p \sin(2\phi_{in})
\end{aligned} \tag{4.14}$$

As we can see the power balance is verified. Analysing the expressions we can observe that they meet the Manley-Rowe power relations. They also provide some more information such as the importance of the phase for power transference.

4.3 Searching for the Active Element

As seen before, in a normal PA the transistor is used as the active component, that is able to modulate the power source according to the input. Through energy considerations it can be proved that a transreactance cannot present itself has an infinite impedance in any of the ports. This happens because a variation of a reactance implies the variation of the stored energy, while a variation of a conductance only implies the variation of energy consumption.

The energy stored in a reactance is intimately connected to the value of the reactance. Let's take a capacitance for example. The energy stored in a capacitance can be calculated using the formula deduced in equation 4.15.

$$E = \int_0^V qdv = \int_0^V Cvdv = \frac{1}{2}CV^2 = \frac{1}{2}\frac{Q^2}{C} \tag{4.15}$$

Now imagine that some charge has been accumulated in the capacitance, this means that there is some amount of energy stored and, furthermore, if the value of the capacitance changes then the energy changes. If the capacitance can be controlled by some signal then the amount of energy stored in the capacitance is also controlled by that same signal. What this means is that to control the capacitance some amount of energy must also be provided.

Using non-linear reactances it is known, through the Manley-Rowe Relations[10], that gain can be achieved. Knowing this there is a device that comes to mind to be used as the active element of the developed amplifiers, this device is the diode. A problem occurs

when using two-terminal devices: the excitation is applied at the same terminal for all signals; this problem can be bypassed due to the nature of the parametric amplifiers: all excitations occur at different frequencies and can be filtered out to avoid power exchange between sources. Another way to accomplish this is to use balanced topologies to create virtual short-circuits at the other sources' excitation points. The diode is the typical active element in RF ParAmps and was the one investigated in this Thesis.

In more recent years, the Metal-Oxide-Semiconductor Varactor (MOSVar) as also been used as an active element in ParAmps both for RF and other applications, such is the case of the studies made in [12, 13]. The MOSVar has a different variation characteristic than the common diode but the design theory suffers only small variations. There is a very interesting device that is also a MOSVar but possesses three terminals, this means that the pump and the input can be separated without recurring to filtering, a look at this device is included in this Thesis.

4.3.1 The Diode

The diode is a thoroughly studied device and is thus well modelled, when a reverse voltage is applied, the diode is known to exhibit a voltage dependent capacitance. The capacitance is usually modelled by equation 4.16, the capacitance curves with varying grading coefficients are shown in figure 4.3. As it can be seen, the capacitance depends on few parameters, v is the reverse voltage applied to the device, V_j is the built in junction voltage, C_{j0} is the junction capacitance at zero bias and m is the grading coefficient.

$$C(v) = \frac{C_{j0}}{\left(1 + \frac{v}{V_j}\right)^m} \quad (4.16)$$

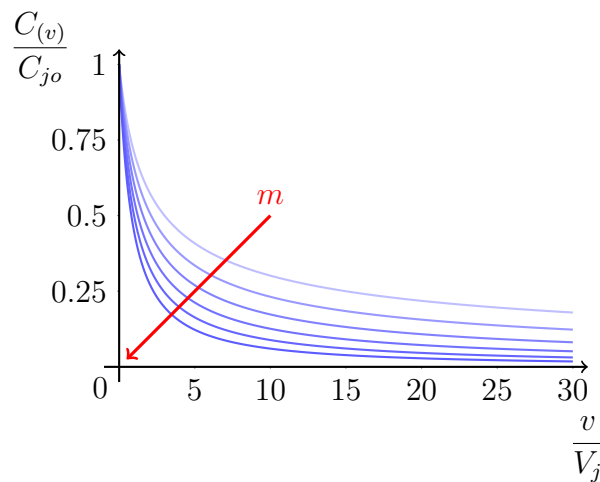


Figure 4.3: Variation of the Diode Capacitance with the Applied Voltage

An interesting fact about the diode is that its elastance can vary linearly with both the current or the voltage, depending on the grading coefficient m but its capacitance can

never exhibit this behaviour. The elastance is the inverse of the capacitance, while the capacitance is defined as the derivative of the charge over the voltage, the elastance is defined as the derivative of the voltage over the charge.

By analysing equation 4.16 it can be noticed that for a linear variation with the voltage the grading coefficient would need to be negative, which is impossible. However, if we invert the function, a unitary grading coefficient would yield a linear expression. The same analysis can be made in terms of the charge (and the current, therefore). To do this, first lets write the elastance in terms of the charge, this is done in equation 4.17.

$$\begin{aligned}
 c(v) &= \frac{C_{jo}}{\left(1 + \frac{v}{V_j}\right)^m} \\
 q(v) &= \frac{V_j C_{jo}}{1-m} \left(1 + \frac{v}{V_j}\right)^{1-m} + Q_0 \\
 v(q) &= V_j \left(\frac{1-m}{V_j C_{jo}} (q - Q_0)\right)^{\frac{1}{1-m}} - V_j \\
 s(q) &= \frac{V_j}{1-m} \left(\frac{1-m}{V_j C_{jo}}\right)^{\frac{1}{1-m}} (q - Q_0)^{\frac{m}{1-m}}
 \end{aligned} \tag{4.17}$$

Looking at expression 4.17 if we make $m = 0.5$ the elastance varies linearly with the charge, however, if we invert the expression notice that there is no grading coefficient that makes the capacitance vary linearly with the charge, figure 4.4 shows the elastance variation with the charge, in this case the expression was redesigned into new parameters, the plotted expression is shown in equation 4.18, S_m is the maximum elastance and Q_m the maximum charge. This characteristic of the elastance is used in [14].

$$s(q) = S_m \left(\frac{q}{Q_m}\right)^{\frac{m}{1-m}} \tag{4.18}$$

In reality the capacitance does not tend to zero but to some residual value which can be modelled as a parasitic linear capacitance in parallel with the non-linear capacitance. In fact, a reverse biased diode should be modelled using more parasitic components, of major importance amongst these is the Equivalent Series Resistor (ESR). The ESR of the diode will determine the efficiency of the parametric amplifier. A more detailed model for the diode is shown in figure 4.5 on the left, usually the parasitic parallel resistor can be ignored or included in the ESR, when an elastance based ParAmp is to be designed the parallel capacitance can be turned into a series capacitance, this is the model shown on figure 4.5 on the right.

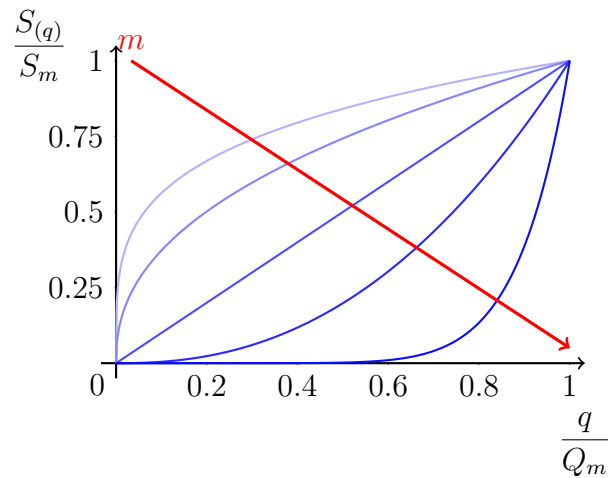


Figure 4.4: Variation of the Diode Elastance with the Stored Charge (Normalized)

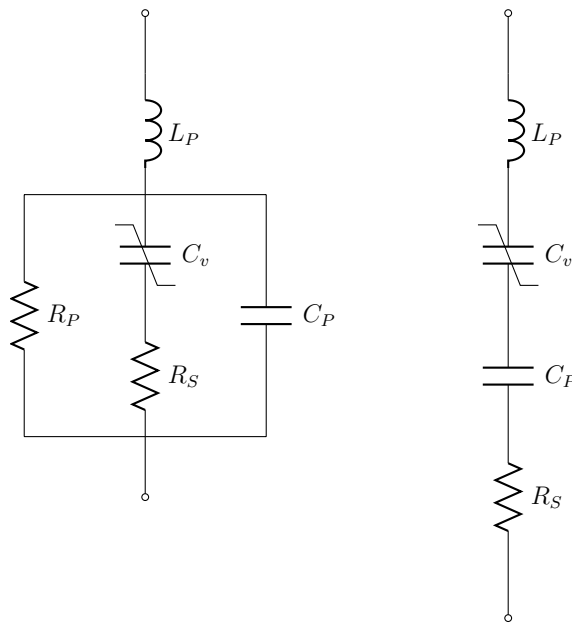


Figure 4.5: Diode Varactor Model

4.3.2 The 3-Terminal MOSVar

Even though the focus of this Thesis is not the MOSVar based ParAmp, the concept behind this device is very interesting and also enables a controlled reactance. The fact that the MOSVar possess one input port and one control port is a big improvement over the diode. The MOSVar effectively implements a transreactance, controlled electronically. Because of this, a small section explaining how the device works as been included.

This type of MOSVar can be seen as a Metal-Oxide-Semiconductor Field-Effect Transistor (MOSFET) in which the source and drain have been shunted, for further purposes

this terminal (source+drain) will be called source, figure 4.6.

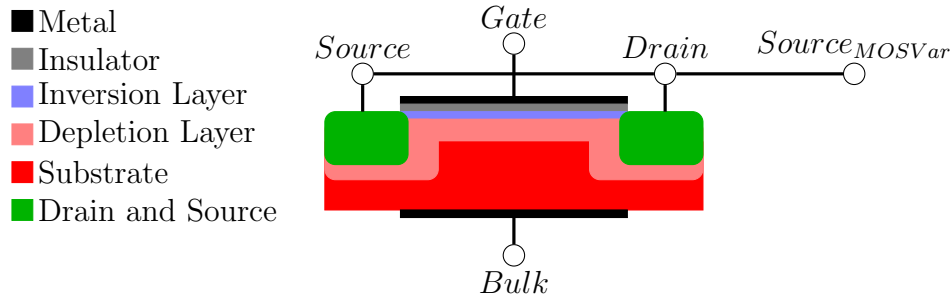
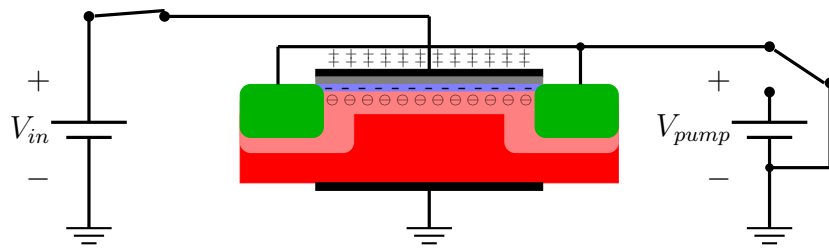


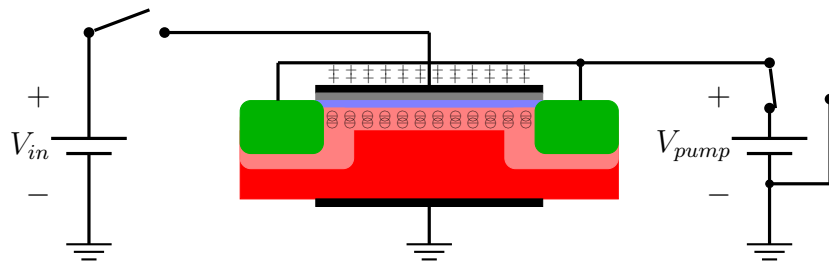
Figure 4.6: The 3-Terminal MOSVar

The MOSVar is therefore a three terminal component: the gate, the source and the bulk. Between the gate and the bulk there is a thin film of isolating material therefore creating a parallel plate capacitor. When a positive voltage is applied from gate to drain, the holes from the bulk are forced back from the gate and a depletion layer is formed in the semiconductor. If the voltage is high enough an inversion layer will form, in a MOSFET this would allow current to circulate from source to drain. When an inversion layer forms in the semiconductor, the source can be used to control the charges there, thus creating a varactor, figure 4.7 exemplifies the behaviour of the MOSVar using an N-channel Metal-Oxide-Semiconductor (NMOS) in discrete time for a better understanding. Note that, contrary to the behaviour of the MOSFET the inversion layer will be uniform, because the source and drain have the same voltage, there exists no pinch-off. The capacitance variation is due to the augmentation of the dielectric thickness when the charges are removed from the inversion layer.

Notice that, even though the example is based on a discrete time operation, this is only because the concept is easier to understand this way. This MOSVar should be able to be operated in continuous time, in this case, the input would modulate the depth of the inversion layer, and the pump would modulate the amount of charge in it. Note that this is not the common MOSVar, which has only two-terminals.



The capacitance is charged by V_{in}



The electrons are drained from the inversion layer, creating a change in the capacitance

Figure 4.7: MOSVar Behaviour, adapted from [13]

4.4 Small-Signal Analysis

In the case of the parametric amplifier, small signal excitation is such that the input does not significantly influence the behaviour of the pump. Frequency-wise the spectrum would be something like the one shown in figure 4.8, of course, the output would be chosen from one of the mixed frequencies.

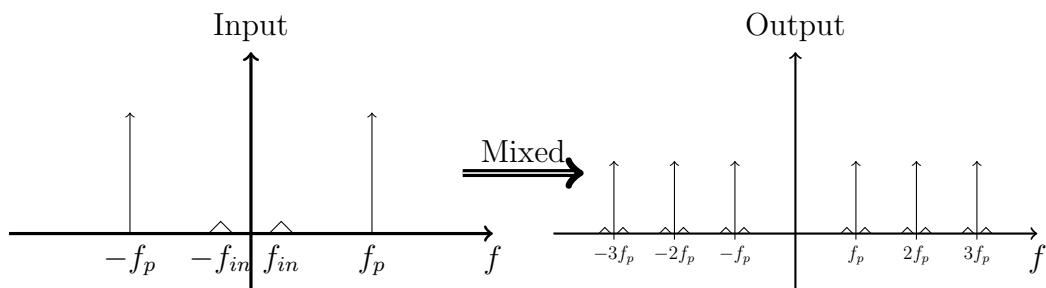


Figure 4.8: Small Signal Input and Output Frequencies

In [15] Rowe determines and describes some of the characteristics for capacitance based

ParAmps. Even though extremely restrictive, small signal operation can give interesting insight into the behaviour of diode based parametric amplifiers.

One of the important specifications that the small-signal analysis can contribute to is which frequency mix to extract at the output. This determines the type of the ParAmp that will be designed. For the sake of reducing the analysis, the considered possible output frequency mixes were the sum and difference of the input frequency around the pump frequency. In fact sub-harmonic pumping is used sometimes, to more easily isolate the pump from the output, in this case, the output is extracted around some higher harmonic of the pump's fundamental frequency (usually the second), [12], but this case was not studied in this Thesis.

This next analysis has been adapted from [15, 11], while, in [15], Rowe does not describe the capacitance dependence on the voltage, assuming the capacitance description is known frequency-wise, in [11], Collin derives the frequency terms using the series diode model shown in figure 4.5. Let's begin by taking Rowe's approach.

4.4.1 General Considerations

Let's assume that some non-linear component possesses a charge that, at any given time can be calculated from the voltage across it through a function, $q = f(v)$, this component is surrounded by linear networks and is excited by two signals one of which can be considered very small in relation to the other. The large signal will be henceforth called the pump signal, and the small signal the input; this is illustrated on figure 4.9, where M_x represents the linear networks.

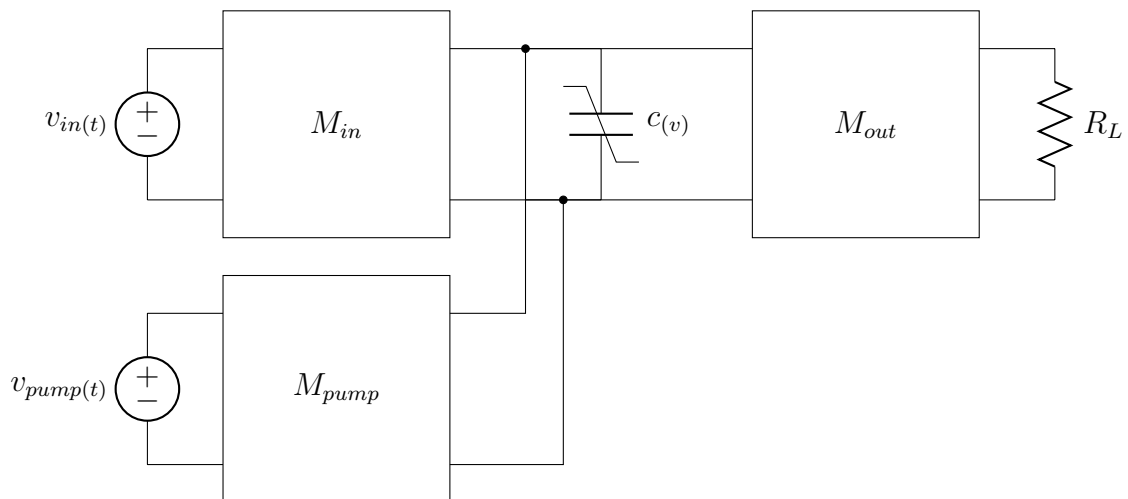


Figure 4.9: Non-Linear Capacitance Concept ParAmp

Because the signal at v_{in} is very small, for the non-linear analysis we can assume that the only frequencies that exist are the pump's fundamental and its harmonics. This means that the method of the conversion matrix can be applied, non-linear analysis is used to

determine the conversion matrix and N-port network theory can be used to analyse the rest of the behaviour.

To calculate the conversion matrix, first we differentiate the non-linear component's characteristic equation (in relation to the independent variable), this yields $\frac{dq}{dv} = f'(v)$, which is the capacitance, this is then converted to the frequency domain, shown in equation 4.19.

$$\begin{aligned} \frac{dq}{dv} = c(v) &= \sum_{n=-\infty}^{+\infty} C_n e^{j\omega_p t} \\ C_n &= \frac{1}{T} \int_{-\frac{T}{2}}^{\frac{T}{2}} c(t) e^{-jn\omega_p t} dt \end{aligned} \quad (4.19)$$

With the series terms we then construct the conversion matrix that relate the small signal voltage Fourier series terms to the small signal charge Fourier series terms, this is the usual capacitance law but in the matrix form shown in equation 4.20.

$$Q = CV$$

$$\begin{bmatrix} Q_{-K}^* \\ \dots \\ Q_0 \\ \dots \\ Q_{+K} \end{bmatrix} = \begin{bmatrix} C_0 & \dots & C_{-K} & \dots & C_{-2K} \\ \dots & \dots & \dots & \dots & \dots \\ C_{+K} & \dots & C_0 & \dots & C_{-K} \\ \dots & \dots & \dots & \dots & \dots \\ C_{+2K} & \dots & C_K & \dots & C_0 \end{bmatrix} \begin{bmatrix} V_{-K}^* \\ \dots \\ V_0 \\ \dots \\ V_{+K} \end{bmatrix} \quad (4.20)$$

Of course the series needs to be truncated for some K , it's assumed that the circuit must ultimately be low pass for some frequency. This condition is necessary and true for every circuit even if only to accommodate the second law of thermodynamics.

To determine K we assume that the linear networks only allow energy to propagate at the fundamental of each source and that the output is extracted at either the sum or difference of the fundamentals. If this is the case, the conversion matrix can be simplified to a two-port for each case, the sum and difference. First we can simplify it to a form that fits both cases, shown in equation 4.21.

$$\begin{bmatrix} Q_{p-in}^* \\ Q_{in} \\ Q_{p+in} \end{bmatrix} = \begin{bmatrix} C_0 & C_{-1} & C_{-2} \\ C_1 & C_0 & C_{-1} \\ C_2 & C_1 & C_0 \end{bmatrix} \begin{bmatrix} V_{p-in}^* \\ V_{in} \\ V_{p+in} \end{bmatrix} \quad (4.21)$$

Because the charge, the voltage and the capacitance are real values in time, the condition $X_{-k} = X_k^*$ must also be fulfilled which can further simplify the conversion matrix.

4.4.2 Inverting ParAmp

The ParAmp is said to be inverting if the frequency difference is chosen as the output. This comes from the fact that the gain will be negative which can be directly extracted from the Manley-Rowe power relations as shown in equation 4.22, where the first index of the power series is the small-signal's frequency index and the second is the pump's frequency index.

$$\begin{aligned} \frac{P_{1,0}}{\omega_{in}} + \frac{P_{1,-1}}{\omega_{in} - \omega_p} = 0 &\Rightarrow -\frac{P_{1,-1}}{P_{1,0}} = -\frac{\omega_p - \omega_{in}}{\omega_{in}} \\ \frac{P_{0,1}}{\omega_p} + \frac{P_{-1,1}}{\omega_p - \omega_{in}} = 0 &\Rightarrow -\frac{P_{-1,1}}{P_{0,1}} = \frac{\omega_p - \omega_{in}}{\omega_p} \end{aligned} \quad (4.22)$$

Looking at the equations there is an interesting notion that arises, if there is power input at the small-signal's fundamental then there's power input at the output's fundamental and vice-versa. To better analyse this result let's turn to the conversion matrix. In the inverting case the conversion matrix can be simplified in the way shown in equation 4.23, if the linear networks suppress the voltage at the frequency sum.

$$\begin{bmatrix} Q_-^* \\ Q_{in} \\ Q_+ \end{bmatrix} = \begin{bmatrix} C_0 & C_{-1} & C_{-2} \\ C_1 & C_0 & C_{-1} \\ C_2 & C_1 & C_0 \end{bmatrix} \begin{bmatrix} V_-^* \\ V_{in} \\ V_+ \end{bmatrix} \Rightarrow \begin{bmatrix} Q_{out}^* \\ Q_{in} \end{bmatrix} = \begin{bmatrix} C_0 & C_{-1} \\ C_1 & C_0 \end{bmatrix} \begin{bmatrix} V_{out}^* \\ V_{in} \end{bmatrix} \quad (4.23)$$

If we take the phase reference at the non-linearity, the value C_1 would be purely real, which would mean that $C_{-1} = C_1$. It's more interesting to have the conversion matrix described in terms of currents and voltages to extract the input and output impedances and the transducer gain, to do this we simply differentiate (in order to time) the conversion matrix in the frequency domain to obtain equation 4.24.

$$\begin{bmatrix} I_{out}^* \\ I_{in} \end{bmatrix} = \begin{bmatrix} -j\omega_{out}C_0 & -j\omega_{out}C_1 \\ j\omega_{in}C_1 & j\omega_{in}C_0 \end{bmatrix} \begin{bmatrix} V_{out}^* \\ V_{in} \end{bmatrix} \quad (4.24)$$

With this conversion matrix we have a two-port description in terms of Y-Parameters. Note however that this description hides the behaviour of the circuit towards the pump, this must be analysed separately. The circuit is now the one shown in figure 4.10, the complete circuit will have the linear networks, the source and the load connected.

The circuit can now be analysed through classical linear analysis. If we calculate the input impedance of this circuit we quickly conclude that the circuit is unstable because the input conductance is negative, as shown in equation 4.25.

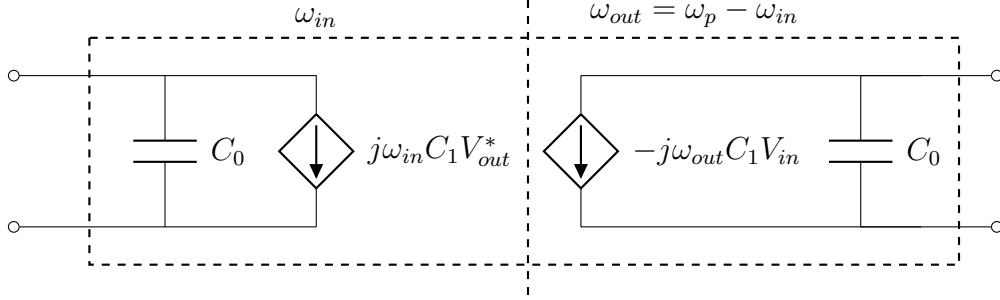


Figure 4.10: Equivalent Small-Signal Circuit, Inverting ParAmp

$$Y_{in} = Y_{11} - \frac{Y_{12}Y_{21}}{Y_L + Y_{22}} \quad (4.25)$$

$$Y_{in} = j\omega_{in}C_0 - \frac{\omega_{in}\omega_{out}C_1^2}{Y_L + j\omega_{out}C_0} = -\omega_{in}\omega_{out}C_1^2 \frac{G_L}{|Y_L + Y_{22}|^2} + jB_{in}$$

In [15], Rowe suggests the use of a circulator to deliver power to loads both at the frequency difference and at the input's fundamental. This approach was not chosen for this Thesis however, the preferred design was the non-inverting ParAmp described next.

4.4.3 Non-inverting ParAmp

The non-inverting case has the frequency sum at the output. In this case the gain is positive, which can again be extracted from the Manley-Rowe power relations, as shown in equation 4.26.

$$\begin{aligned} \frac{P_{1,0}}{\omega_{in}} + \frac{P_{1,1}}{\omega_{in} + \omega_p} = 0 &\Rightarrow -\frac{P_{1,1}}{P_{1,0}} = \frac{\omega_p + \omega_{in}}{\omega_{in}} \\ \frac{P_{0,1}}{\omega_p} + \frac{P_{1,1}}{\omega_p - \omega_{in}} = 0 &\Rightarrow -\frac{P_{1,1}}{P_{0,1}} = \frac{\omega_p + \omega_{in}}{\omega_p} \end{aligned} \quad (4.26)$$

The same train of thought can be applied as in the inverting ParAmp, however, because the frequency is the sum the conversion matrix variables will now be on the positive side of the spectrum. This means that, on differentiation, there will be no negative coefficients on the Y-parameter matrix. In turn this will yield a positive input conductance, contrary to the previous case scenario. The final form of the conversion matrix is shown in equation 4.27, again, the assumption that the voltage at other frequencies is suppressed was made.

$$\begin{bmatrix} I_{in} \\ I_{out} \end{bmatrix} = \begin{bmatrix} j\omega_{in}C_0 & j\omega_{in}C_1 \\ j\omega_{out}C_1 & j\omega_{out}C_0 \end{bmatrix} \begin{bmatrix} V_{in} \\ V_{out} \end{bmatrix} \quad (4.27)$$

Note that now, re-using equation 4.25 it is possible to see that the result will be the same but the conductance will be positive. We can analyse the resulting four-pole to find some interesting characteristics of the ParAmp such as transducer gain, sensitivity to non-linearity, bandwidth, etc..

The equivalent two-port network of the non-linear capacitance is similar to the previous case. However, the current gain in the output frequency is positive, the equivalent circuit is shown in figure 4.11.

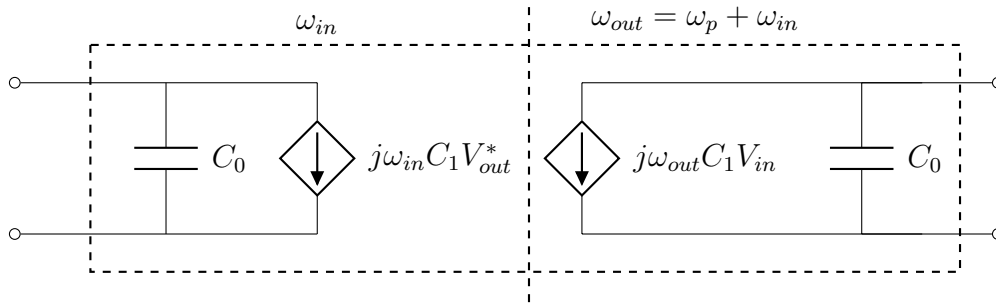


Figure 4.11: Equivalent Small-Signal Circuit, Non-Inverting ParAmp

Transducer Gain

The transducer gain is usually the chosen FoM for evaluation of the gain. This is because the transducer gain measures the gain in relation to the power one could extract by applying the input source directly to the load, unlike the power gain that measures the gain in relation to the power inserted in the system.

The transducer gain is, therefore, one of the main characteristics of an amplifier and is defined by equation 4.28.

$$G_t = \frac{P_{out}}{P_{av}} \quad (4.28)$$

If we take the conversion matrix representation and lump the linear input and output networks into one conductance we would have the equivalent circuit shown in figure 4.12.

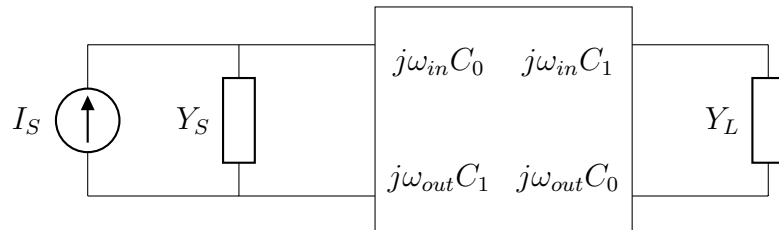


Figure 4.12: Equivalent Small-Signal Circuit, with Admittance Terminations

From classical two-port network analysis, after defining the terminations, the transducer gain can be calculated according to equation 4.29 where G_p is the power gain. Notice that, when $Y_S = Y_{in}^*$ maximum gain is achieved, which is exactly the power gain.

$$G_t = 4G_p \frac{\operatorname{Re}(Y_S) \operatorname{Re}(Y_{in})}{|Y_S + Y_{in}|^2} \quad (4.29)$$

The power gain can be extracted from the Manley-Rowe relations, the input admittance can be calculated using equation 4.30.

$$Y_{in} = Y_{11} - \frac{Y_{12}Y_{21}}{Y_L + Y_{22}} = j\omega_{in}C_0 + \frac{\omega_{in}\omega_{out}C_1^2}{j\omega_{out}C_0 + Y_L} = \quad (4.30)$$

$$Y_{in} = \frac{\omega_{in}\omega_{out}C_1^2g_L}{g_L^2 + (\omega_{out}C_0 + b_L)^2} + j \left(\omega_{in}C_0 - \frac{\omega_{in}\omega_{out}C_1^2(\omega_{out}C_0 + b_L)}{g_L^2 + (\omega_{out}C_0 + b_L)^2} \right)$$

Putting everything together we obtain the transducer gain expression (equation 4.31), which is quite complex for general loads.

$$G_t = 4 \frac{\omega_{out}}{\omega_{in}} \frac{g_S \frac{\omega_{in}\omega_{out}C_1^2g_L}{g_L^2 + (\omega_{out}C_0 + b_L)^2}}{\left(g_S + \frac{\omega_{in}\omega_{out}C_1^2g_L}{g_L^2 + (\omega_{out}C_0 + b_L)^2} \right)^2 + \left(\omega_{in}C_0 + b_S - \frac{\omega_{in}\omega_{out}C_1^2(\omega_{out}C_0 + b_L)}{g_L^2 + (\omega_{out}C_0 + b_L)^2} \right)^2} \quad (4.31)$$

To simplify this equation a helpful assumption is that the output load is always tuned. This assumption is valid because the output frequency is the sum of the input frequency with the pump frequency, if the pump frequency is high enough the percentage variation at the output is small. In the case the output is tuned we would have $\omega_{out}C_0 + b_L = 0$, and the transducer gain would simplify to equation 4.32 a much more treatable expression.

$$G_t = \frac{4\omega_{out}^2 C_1^2 \frac{g_S}{g_L}}{\left(g_S + \frac{\omega_{in}\omega_{out}C_1^2}{g_L} \right)^2 + (\omega_{in}C_0 + b_S)^2} \quad (4.32)$$

The maximum of this expression happens for tuned conditions, $\omega_{in}C_0 + b_S = 0$, and $g_S g_L = \omega_{in}\omega_{out}C_1^2$.

Bandwidth

There are several effects that limit the bandwidth. The first effect is the variation of the power gain given by the Manley-Rowe Relations. This gain is always reduced because the percentage change in ω_{in} is always greater than the one in ω_{out} . The second effect is the detuning of the harmonically tuned filters at the input and the output, this effect is more severe for lower conductances, since the Q factor of the filter is higher. The third and final effect is the change of the input impedance of the amplifier due to the change of the Y-parameters Y_{12} and Y_{21} which cannot be included in the source and load conductances.

The bandwidth can be evaluated by considering the system tuned at a certain frequency and then observe the change that happens for small variations around that frequency. If we consider the narrowband approximation then this middle frequency will be much higher than the perturbation, this is the frequency equivalent of the small signal analysis and the course taken in [15], it ends up limiting the analysis to the bandwidth of the harmonic filters. In this work the analysis was broadened a little to include the variations due to the changes in the transconductances and the power gain, as well as the harmonic filters.

To analyse the bandwidth it is convenient to start with equation 4.29 for the transducer gain and then note the influence on each admittance and the power gain individually, it is also convenient to include the Y_{11} and Y_{22} parameters in the Y_S and Y_L admittances respectively.

Let's begin with the evaluation of the power gain fluctuation, this is shown in equation 4.33, as usual, if the variation is sufficiently small then the power gain is linearly varying with the frequency shift.

$$G_p = 1 + \frac{\omega_p}{\omega_{in, mid} \left(1 + \frac{\Delta\omega}{\omega_{in, mid}}\right)} \approx G_{p, mid} \left(1 - \frac{\Delta\omega}{2\omega_{in, mid}}\right) \quad (4.33)$$

Another influence to the bandwidth is the variation of the source admittance, if we include the Y_{11} parameter in this admittance it presents itself as a tank circuit which is tuned at the center frequency. The bandwidth of such a filter is determined by the Q factor, which is in turn dependent on the source conductance. This same effect happens at the output, but the effect on the input is that of a series RLC , this can be seen through equation 4.30. Equations 4.34 to 4.36 describe some of the properties of parallel resonators, including the variation of the impedance for small enough $\Delta\omega$.

$$Y = g + j\omega C - j\frac{1}{\omega L} = g \left(1 + jQ \left(\frac{\omega}{\omega_{mid}} - \frac{\omega_{mid}}{\omega}\right)\right) \approx g \left(1 + jQ \frac{\Delta\omega}{2\omega_{mid}}\right) \quad (4.34)$$

$$Q = \frac{\omega_{mid}}{2\pi B_w} = \frac{\omega_{mid} C}{g} = \frac{1}{g} \sqrt{\frac{C}{L}} \quad (4.35)$$

$$B_w = \frac{g}{2\pi C} \quad (4.36)$$

Mixing the equations shows that some variation of the input impedance does not depend on the center frequency in contrast with the power gain.

The last effect is the variation of the transconductance parameters, Y_{12} and Y_{21} . This variation is felt in the input impedance of the two-port network but cannot be translated into an equivalent filter as the variation of the load admittance can. In equation 4.30 the variation of Y_L including Y_{22} was explained before, the parameter Y_{11} was included in Y_S leaving only the numerator of the second term which is given by $Y_{12}Y_{21} = -\omega_{in}\omega_{out}C_p^2$, the variation is due to both input and output. Equation 4.37 shows the variation for small $\Delta\omega$.

$$-\omega_{in}\omega_{out}C_1^2 \approx -\omega_{in_{mid}}\omega_{out_{mid}}C_p^2 \left(1 + \frac{\Delta\omega}{\omega_{in_{mid}}} + \frac{\Delta\omega}{\omega_{out_{mid}}}\right) \quad (4.37)$$

To end this analysis we only need to put everything together, using equation 4.31. The dependence of the gain with the frequency shift can be expressed through the use of functions describing each of the effects above as shown in equation 4.38.

$$\begin{aligned} A_{(\Delta\omega)} &= 4G_{p(\Delta\omega)} \\ S_{(\Delta\omega)} &= Y_{S(\Delta\omega)} \\ L_{(\Delta\omega)} &= Y_{L(\Delta\omega)} \\ T_{(\Delta\omega)} &= -Y_{12(\Delta\omega)}Y_{21(\Delta\omega)} \end{aligned} \quad (4.38)$$

$$G_{(\Delta\omega)} = A_{(\Delta\omega)} \frac{\operatorname{Re}\left(S_{(\Delta\omega)}\right) \operatorname{Re}\left(\frac{T_{(\Delta\omega)}}{L_{(\Delta\omega)}}\right)}{\left|S_{(\Delta\omega)} + \frac{T_{(\Delta\omega)}}{L_{(\Delta\omega)}}\right|^2} = \frac{g_S g_L A_{(\Delta\omega)} T_{(\Delta\omega)}}{\left|S_{(\Delta\omega)} L_{(\Delta\omega)} + T_{(\Delta\omega)}\right|^2}$$

If we take the previous descriptions of the effects and substitute them on the expression, taking into account that, for maximum gain, $\omega_{in_{mid}}\omega_{out_{mid}}C_p^2 = g_S g_L$ we can obtain equation 4.39.

$$G_{(\Delta\omega)} \approx \frac{4G_{p_{mid}} \left(1 - \frac{\Delta\omega}{2\omega_{in_{mid}}}\right) \left(1 + \frac{\Delta\omega}{\omega_{in_{mid}}} + \frac{\Delta\omega}{\omega_{out_{mid}}}\right)}{\left|\left(1 + jQ_S \frac{\Delta\omega}{2\omega_{in_{mid}}}\right) \left(1 + jQ_L \frac{\Delta\omega}{2\omega_{out_{mid}}}\right) + \left(1 + \frac{\Delta\omega}{\omega_{in_{mid}}} + \frac{\Delta\omega}{\omega_{out_{mid}}}\right)\right|^2} \quad (4.39)$$

Equation 4.39 as all the effects well separated which is useful from a qualitative point of view, however, to obtain quantitative information the model needs to be further expanded to obtain the joint result of all these effects. To simplify the analysis of this case let's consider that $g_S = g_L = g$, $T_{(\Delta\omega)} = 1$ in the denominator (where it is a sum term and not a multiplicative term) and $T_{(\Delta\omega)} = 1 + \frac{\Delta\omega}{\omega_{in_{mid}}}$ in the numerator. Taking these restrictions, developing equation 4.39 results in equation 4.40.

$$G_{(\Delta\omega)} \approx G_{p_{mid}} \frac{\left(1 - \frac{\Delta\omega}{2\omega_{in_{mid}}}\right)}{1 + \left(\frac{1}{\sqrt{2}} \frac{C_0}{C_1} \frac{\Delta\omega}{2\sqrt{\omega_{in_{mid}}\omega_{out_{mid}}}}\right)^4} \quad (4.40)$$

It's possible to see that three parameters dominate the gain, frequency-wise. First the percentage variation in relation to the input's middle frequency, second the geometric distance between the input's and output's frequency and finally the percentage variation of the capacitance in relation to it's middle value. To aid in the evaluation of each parameter

figures 4.13 and 4.14 show the variation of the gain with each one, unless otherwise specified $\frac{C_0}{C_1} = 200$, $\omega_{in_{mid}} = 100\text{MHz}$ and $\omega_{out_{mid}} = 1\text{GHz}$.

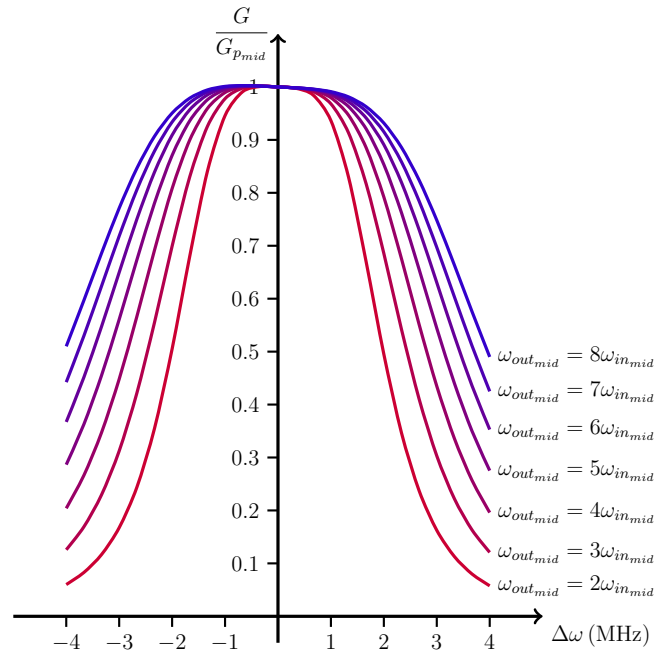


Figure 4.13: Gain Variation with the Output's Frequency

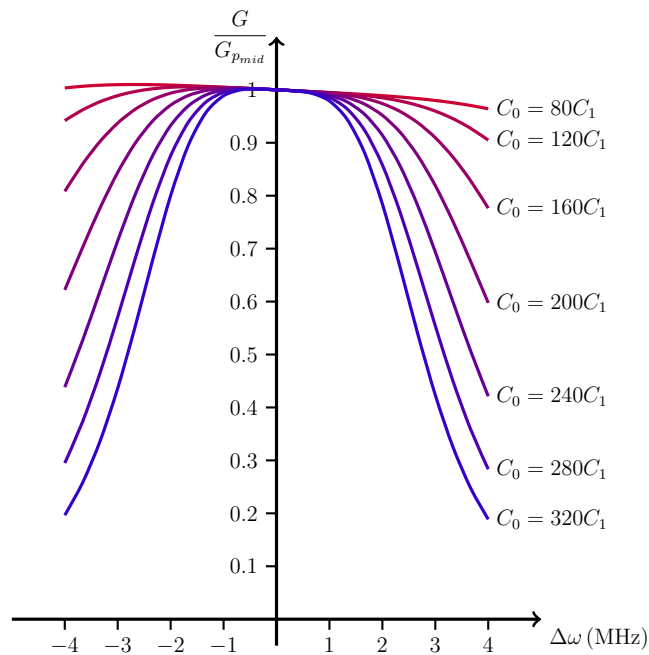


Figure 4.14: Gain Variation with the Capacitance

Notice how the passage band is not flat but has a slight slope, this is due to the numerator but, as expected, is not very significant. The output frequency is a system specification, however, the capacitance variation rate is not which means that it can be used as a FoM for the bandwidth of the system.

Non-Linearity Sensitivity

The sensitivity to non-linearity describes the gain variation in relation to the component's non-linearity. Through this analysis it is possible to understand whether a highly non-linear device is needed for higher gain or if some small non-linearity suffices. The sensitivity can be describe mathematically as the relative change in some quantity due to the relative change in some parameter, equation 4.41.

$$S_f = \frac{df(x)/f(x)}{dx/x} = \frac{df(x)}{dx} \frac{x}{f(x)} \quad (4.41)$$

In this case we have seen before that, when the device is matched, the transducer gain is simply the power gain. The power gain does not depend on the non-linearity, as proved by Manley and Rowe which means that the device is insensitive to the non-linearity, when matched. When the device is not matched, it was seen before that, the non-linearity influences the bandwidth, the device is, therefore, sensitive to it.

The sensitivity to the non-linearity can only have one source, the variation of the transconductances of the two-port. As it can be seen in equation 4.38, the transconductances have influence in the numerator and the denominator of the fraction, as seen in equation 4.42.

$$G_t(C_1) = 4G_p \frac{\frac{\omega_{in}\omega_{out}C_1^2}{gSgL}}{\left(1 + \frac{\omega_{in}\omega_{out}C_1^2}{gSgL}\right)^2} \quad (4.42)$$

The sensitivity is of the same form as the sensitivity of $f(x) = \frac{kx^2}{(1+kx^2)^2}$ to x , which is shown in equation 4.43.

$$S_f = 2 \frac{1 - kx^2}{1 + kx^2} \quad (4.43)$$

For optimum gain kx^2 is close to 1 and so the sensitivity is rather low, as shown in figure 4.15. Notice that for small variations of the non-linearity the sensitivity changes at double the rate of the non-linearity, this means that small perturbations of the pump bias may influence the gain greatly.

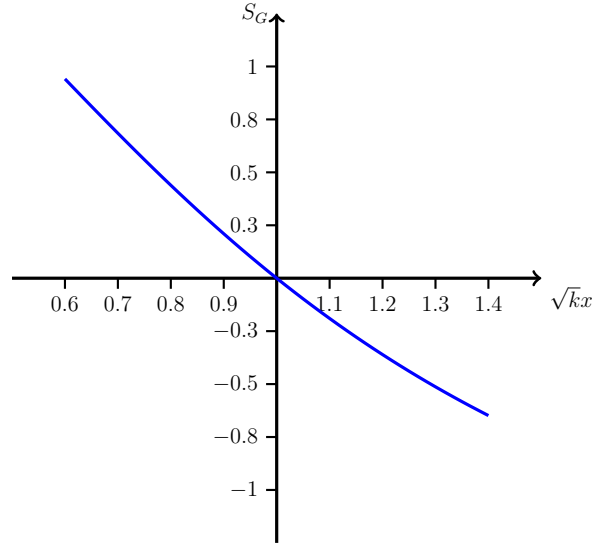


Figure 4.15: Sensitivity of the Gain to the Non-Linearity

4.4.4 Extracting the Parameters

Up to this point the conversion matrix has been used without regard as to how the parameters relate to the capacitance variation. Here, the capacitance function of a diode is used to obtain the parameters needed for the conversion matrix, this as been adapted from [11]. To do this we begin by keeping the small-signal approximation and consider that the diode can only see the pump's voltage and the DC bias. The capacitance of a reverse biased diode is described by equation 4.16, when only the pump and the DC bias influence the capacitance it capacitance can be described as seen in equation 4.44.

$$C_{(v(t))} = \frac{C_{jo}}{\left(1 + \frac{V_B + v_p(t)}{V_j}\right)^m} \quad (4.44)$$

If we assume that the perturbation imposed by the pump is also small compared to the DC bias, then we can use a Taylor expansion around V_B to obtain a linear variation and build equation 4.45.

$$C(t) \approx \frac{C_{jo}}{\left(1 + \frac{V_B}{V_j}\right)^m} - \frac{C_{jo}}{\left(1 + \frac{V_B}{V_j}\right)^m} \frac{\frac{m}{V_j}}{1 + \frac{V_B}{V_j}} v_p(t) \quad (4.45)$$

Now that the equation is linearised C_0 is the first term and C_1 the second, including the pump's amplitude. If we define a parameter $M = \frac{\frac{m}{V_j}}{1 + \frac{V_B}{V_j}} V_P$ then we can write $C_1 = C_0 M$ and associate the bandwidth's FoM with this parameter.

4.4.5 Limitations

Note that with the small-signal approximation no attempts were made to extract the maximum possible power from the pump, it is simply said that the available power needs to be high enough. The first problem with this is that the power that is made available at the pump is not used in the amplification, even though it is not consumed. The second problem is that it is difficult to know how much available power is enough and this power can also be impossible to reach due to bias limitations, since the pump must be small in relation to the bias.

Another limitation that comes from the small-signal approximation is that the pump is assumed to maintain a constant voltage for every input as if it is a perfect voltage source. In real systems, when more power is extracted the pump's voltage will decrease which implies a variation of the C_1 coefficient changing the system's characteristics.

To have more insight into the system a large signal theory is necessary, this is addressed in the next section.

4.5 Large-Signal Analysis

To the author's knowledge there is no large signal model developed for application in parametric amplification. This model was fully developed and studied by the author of this Thesis.

When the system is under large signal excitation, both the input and the pump drive the non-linearity. This increases the difficulty of analysis because the frequency conversions now happen for both sources, which means that the conversion matrix technique cannot be used.

Before going into the large signal analysis, there is a point that needs clarification. In the small signal analysis the voltages across the diode are assumed to be suppressed for every frequency except the input's, pump's and output's. However, the excitations are inserted in parallel with each other, this means that no simple harmonic tuning can be used to suppress the voltages or it would suppress the voltages from the other sources as well. If the sources are inserted in parallel it is easier to eliminate the undesired currents, in this case the capacitance would be current-pumped and the description of the non-linearity must change to a current dependent formula. To do the same using the voltage, the excitations need to be inserted in series with each other.

Rowe did not consider this when developing the small-signal analysis on [15]. However, the characteristics of each form of pumping and the description of the non-linearity should not change the analysis greatly.

4.5.1 General Considerations

An important consideration for the large signal analysis is the chosen description for the non-linearity. In this case there are four suitable descriptions: a voltage controlled capacitance, a voltage controlled elastance, a current controlled capacitance and a current

controlled elastance. As explained before, to minimize the linear networks, there are two circuits worth analysing, one in current and the other in voltage. For each one there should be a chosen non-linearity description. Figure 4.16 can help in this decision, to minimize the feedback loops, the description should be in capacitance when the excitation is in voltage and in elastance when the excitation is in current.

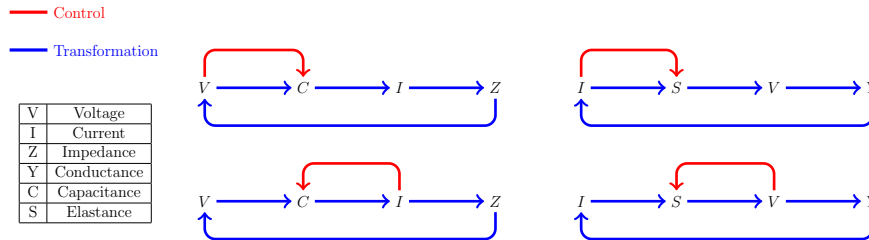


Figure 4.16: Dependence and Transformations in the Non-Linear System

The circuits studied for the large signal analysis are shown in figures 4.17 and 4.20 in the next sections. The LC filters are considered to have a sufficiently high quality factor that all frequency components are cancelled except for the tuned frequency, the filters need to be calculated taking the parasitics of the non-linear component into account. The frequency at the output will be the sum of the pump's and source's frequencies.

The large signal analysis performed on this part of the Thesis is restricted to linearly varying components. This restriction is necessary to resolve the dependence loop as will be seen in the next sections.

4.5.2 Voltage Pumped Capacitance

In voltage pumped ParAmps the excitations are inserted in series with each other and the non-linearity. The tuning filters should be parallel, high Q factor, LC filters to cancel all unwanted voltage frequencies. However, the current at the non-linearity is uncontrolled because the filters tend to short circuits outside the passage band. Figure 4.20 shows the circuit to be analysed, inconveniently the bias requires the use of a Direct Current Choke (DCC) to separate it from the load. The current pumped ParAmp incorporates this function in the bandpass filters.

Modelling

The first step is to replace the diode with its equivalent model, shown in 4.5. The linear part of the model can be copied to each branch (source, load and pump), using the additivity rule, because only one frequency exists in each of the branches. The Thévenin equivalent of each branch at the corresponding frequency is then calculated, at all other frequencies the branches are short circuits.

There are three voltages across the non-linearity, one due to the source, one due to the pump and one due to the load. These three voltages interact with the non-linearity

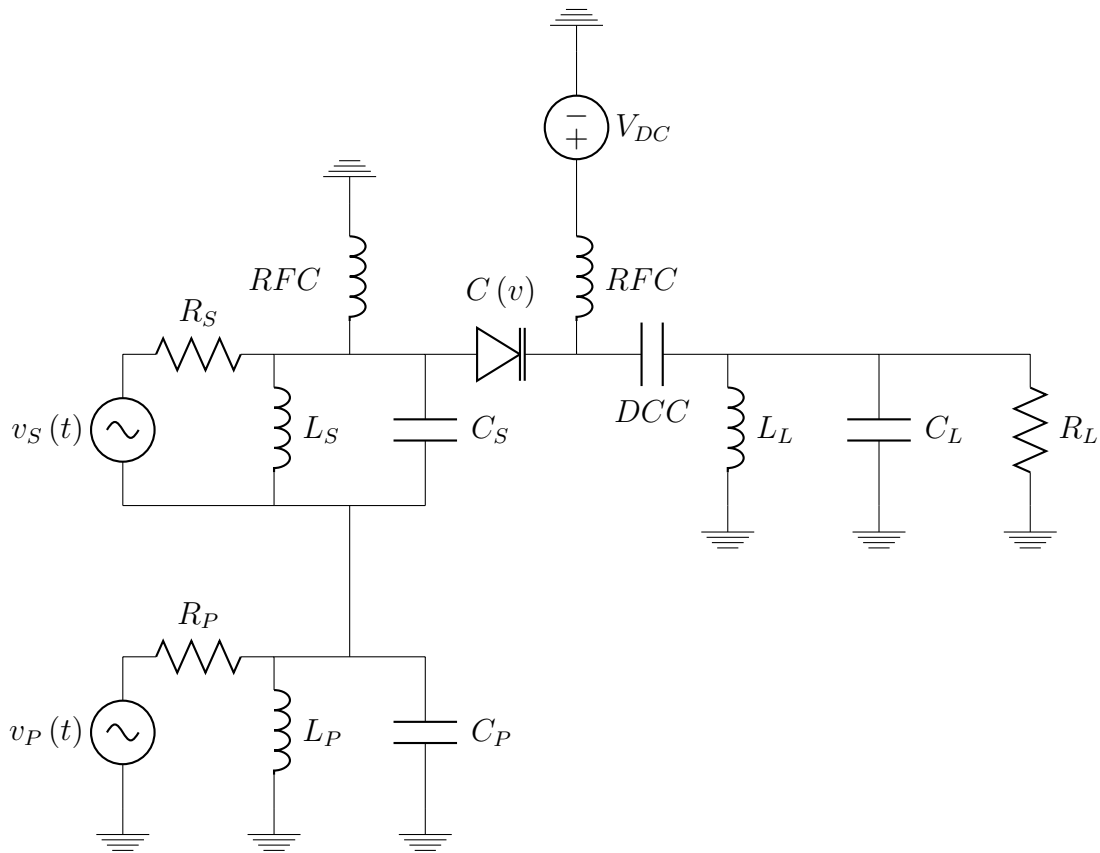


Figure 4.17: Voltage Pumped, Voltage Controlled Capacitance

allowing power to be transferred from one frequency to the others. This process can be described in the time and frequency domain as shown in equation 4.46, where c is the capacitance.

$$i(t) = c(t) \frac{dv(t)}{dt} \quad (4.46)$$

$$I(\omega) = C(\omega) * j\omega V(\omega)$$

The capacitance, $c(t)$, can be written as a double Fourier series because it is dependent on two stimulus of incommensurate frequencies. Because of this, the current across it and the voltage through it are also double Fourier series and can be written as shown in equation 4.47.

$$\begin{aligned}
c(t) &= \sum_{n=-\infty}^{+\infty} \sum_{m=-\infty}^{+\infty} C_{n,m} e^{j(n\omega_s + m\omega_p)t} \\
v(t) &= \sum_{n=-\infty}^{+\infty} \sum_{m=-\infty}^{+\infty} V_{n,m} e^{j(n\omega_s + m\omega_p)t} \\
i(t) &= \sum_{n=-\infty}^{+\infty} \sum_{m=-\infty}^{+\infty} I_{n,m} e^{j(n\omega_s + m\omega_p)t}
\end{aligned} \tag{4.47}$$

Considering that the employed filters eliminate every voltage component except at the tuned frequencies. The voltage double series is reduced to three terms. These will be in $\omega_s \rightarrow V_{0,1}$, $\omega_p \rightarrow V_{1,0}$ and $\omega_s + \omega_p \rightarrow V_{1,1}$. The voltages through the capacitance generate currents across it. The currents generated at the same frequency components interact with the Thévenin equivalents, the other voltage terms may exist but cannot carry power. According to equation 4.46 the important voltage components can be calculated as shown in equation 4.48.

$$\begin{aligned}
I_{1,1} &= j\omega_{1,0}C_{0,1}V_{1,0} + j\omega_{0,1}C_{1,0}V_{0,1} \\
I_{1,0} &= -j\omega_{0,1}C_{1,1}V_{0,1}^* + j\omega_{1,1}C_{0,1}^*V_{1,1} \\
I_{0,1} &= -j\omega_{1,0}C_{1,1}V_{1,0}^* + j\omega_{1,1}C_{1,0}^*V_{1,1}
\end{aligned} \tag{4.48}$$

Remember that the term $C_{0,0}$ has been incorporated into the linear admittance of the Thévenin equivalent at each frequency. Now that we have the voltage at each frequency, the current flowing into the capacitance can be calculated from the Thévenin equivalent, equation 4.49.

$$\begin{aligned}
V_{1,1} &= V_{1,1}^T + Z_{1,1}I_{1,1} = Z_{1,1}I_{1,1} \\
V_{1,0} &= V_{1,0}^T - Z_{1,0}I_{1,0} \\
V_{0,1} &= V_{0,1}^T - Z_{0,1}I_{0,1}
\end{aligned} \tag{4.49}$$

If we assume that the capacitance varies linearly with the charge then both equations can be simplified, as shown in equation 4.50

$$\begin{aligned}
C(\omega) &= c_1 V_{0,1} + c_1 V_{1,0} + c_1 V_{1,1} \\
I_{1,1} &= j\omega_{1,1} c_1 V_{0,1} V_{1,0} \\
I_{1,0} &= j\omega_{1,0} C_{1,1} V_{0,1}^* \\
I_{0,1} &= j\omega_{0,1} C_{1,1} V_{1,0}^*
\end{aligned} \tag{4.50}$$

With these simplified relations, we now understand the dependence of each voltage term with the others. Each voltage depends upon the other two. If we combine the equations it is possible to write each voltage term as a function of the Thévenin equivalents and $C_{1,1}$, equation 4.51.

$$\begin{aligned}
V_{0,1} &= V_{0,1}^T + j\omega_{0,1} Z_{0,1} C_{1,1} V_{1,0}^* = \frac{V_{0,1}^T + j\omega_{0,1} Z_{0,1} C_{1,1} V_{1,0}^*}{1 - \omega_{1,0} \omega_{0,1} Z_{0,1} Z_{1,0}^* |C_{1,1}|^2} \\
V_{1,0} &= V_{1,0}^T + j\omega_{1,0} Z_{1,0} C_{1,1} V_{0,1}^* = \frac{V_{1,0}^T + j\omega_{1,0} Z_{1,0} C_{1,1} V_{0,1}^*}{1 - \omega_{1,0} \omega_{0,1} Z_{0,1}^* Z_{1,0} |C_{1,1}|^2}
\end{aligned} \tag{4.51}$$

The solution for the output voltage is the mixture of both the input voltages (source and pump), equation 4.52.

$$V_{1,1} = j\omega_{1,1} Z_{1,1} c_1 V_{0,1} V_{1,0} = j\omega_{1,1} Z_{1,1} c_1 \frac{(V_{0,1}^T + j\omega_{0,1} Z_{0,1} C_{1,1} V_{1,0}^*) (V_{1,0}^T + j\omega_{1,0} Z_{1,0} C_{1,1} V_{0,1}^*)}{|1 - \omega_{1,0} \omega_{0,1} Z_{0,1}^* Z_{1,0} |C_{1,1}|^2|^2} \tag{4.52}$$

Even though the equation 4.52 seems to be a closed form, remember that $C_{1,1}$ is dependent on $V_{1,1}$. Because of this, the closed solution to $V_{1,1}$ is the solution to a fifth order polynomial which lacks an analytical general solution (Abel-Ruffini theorem). Even though the equations are not a closed form, they converge extremely quickly to the result using a recursive method.

Model Confirmation

A confirmation of the provided large signal model would be to check if it follows the Manley-Rowe power relation. This has been proved in equation 4.53.

$$G_p = \frac{|V_{1,1}|^2}{R_L \text{Re}(I_{0,1} V_{0,1}^*)} = \frac{|V_{1,1}|^2}{R_L \text{Re}(j\omega_{0,1} C_{1,1} V_{1,0}^* V_{0,1}^*)} = \frac{|V_{1,1}|^2}{R_L \text{Re}(j\omega_{0,1} c_1 V_{1,1} V_{0,1}^* V_{1,0}^*)} \quad (4.53)$$

$$G_p = \frac{|V_{1,1}|^2}{R_L \text{Re}\left(-\frac{j\omega_{0,1}}{j\omega_{1,1}} V_{1,1} I_{1,1}^*\right)} = -\frac{\omega_{1,1}}{\omega_{0,1}}$$

This first proof is purely theoretical, to observe if the model behaves correctly a circuit level simulation was constructed. The results of the model were obtained using the Newton-Raphson method and compared to the simulation results. The Newton-Raphson method was used on equation 4.54.

$$f_{(C_{1,1})} = C_{1,1} - c_1 V_{1,1(C_{1,1})} =$$

$$f_{(C_{1,1})} = C_{1,1} - j c_1^2 \omega_{1,1} Z_{1,1} \frac{\left(V_{0,1}^T + j\omega_{1,0} Z_{0,1} C_{1,1} V_{1,0}^{T*}\right) \left(V_{1,0}^T + j\omega_{0,1} Z_{1,0} C_{1,1} V_{0,1}^{T*}\right)}{\left|1 - \omega_{1,0} \omega_{0,1} Z_{0,1}^* Z_{1,0} |C_{1,1}|^2\right|^2} \quad (4.54)$$

The simulation parameters are shown in table 4.1.

$f_s = f_{0,1}$	100MHz
$f_p = f_{1,0}$	900MHz
$f_l = f_{1,0} + f_{0,1}$	1GHz
P_s	2mW
P_p	30mW
R_s	50Ω
R_p	50Ω
R_L	50Ω

Table 4.1: Test Circuit, Simulation Parameters

Two tests were performed. First, c_1 was varied to obtain the gain variation with the variation of the non-linearity. Second, the input power was varied at the 100MHz to obtain the characteristic AM/AM of the circuit.

Advanced Design System (ADS) was used as the circuit level simulator and Matrix Laboratory (MatLab) was used as the numerical calculator. The convergence speed of the model was also tested.

The circuit used for testing purposes was the one shown in figure 4.18. The diode has been changed to an equation based capacitor, this is done for simpler testing and circuit control. The tuning filters have an extremely high Q factor and include compensation for the capacitor's average capacitance. The impedance at each frequency is purely real.

The results of the simulations, figure 4.19, show that the model is accurate, the convergence is very quick and the prediction can indeed be extracted in the suggested conditions.

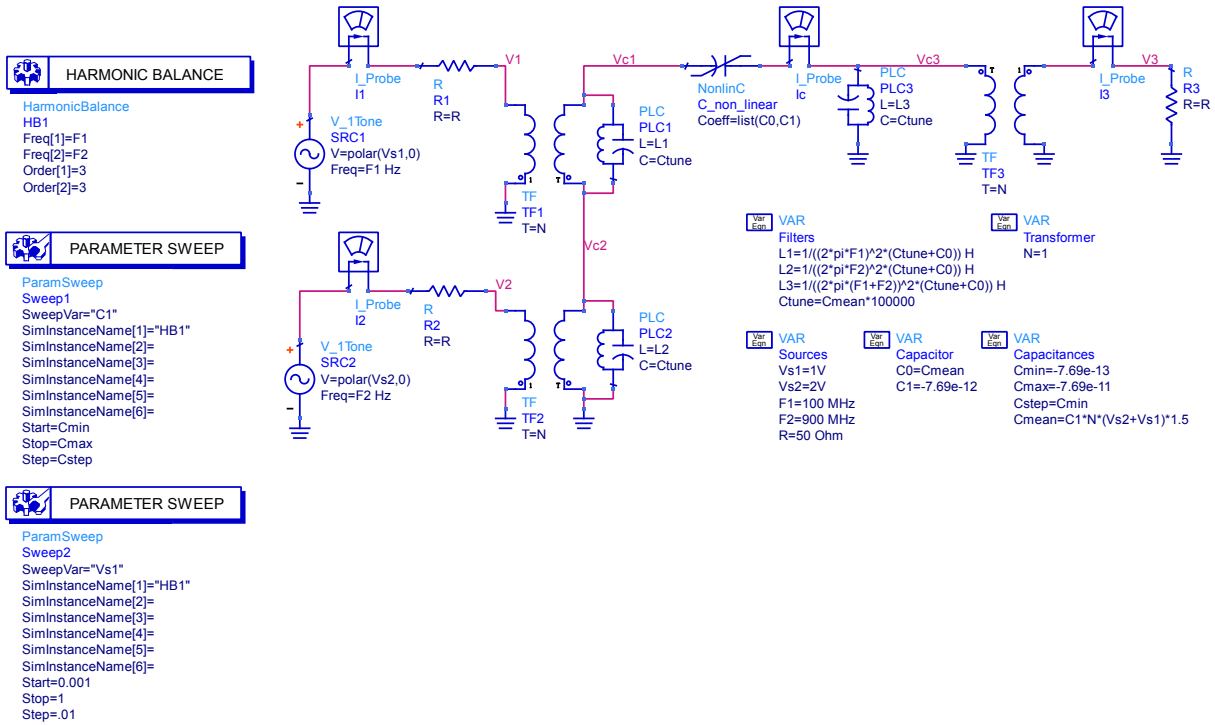


Figure 4.18: Test Circuit, Circuit Level Simulation

Usage in Design

The developed equations provide a good option to analyse a circuit similar to the one presented. However, to use in the design of the amplifier they are too complex and require iteration. This problem can be tackled aside if we consider the following scenario: the maximum output power will occur either for a perfectly tuned input or a perfectly tuned pump. This idea has been proved in the small signal case, the power tends to the maximum for a perfectly tuned input since the pump is not even considered. In the large signal case it is possible to see that, if the pump lacks power capabilities, the limitation in output power can come from the pump.

If we consider that the maximum power happens for tuned input or pump, we can use the equations for $V_{0,1}$ and $V_{1,0}$ to obtain the tuning condition. Each of the equations provides the perfect tuning for the corresponding source. It is unnecessary to provide both equations since the formulas have the same form. Taking $V_{0,1}$ we know that perfect tuning is achieved for $V_{0,1} = \frac{Z_{0,1}^*}{2Re(Z_{0,1})} V_{0,1}^N$. Using this condition we can obtain $C_{1,1}$, equation 4.55.

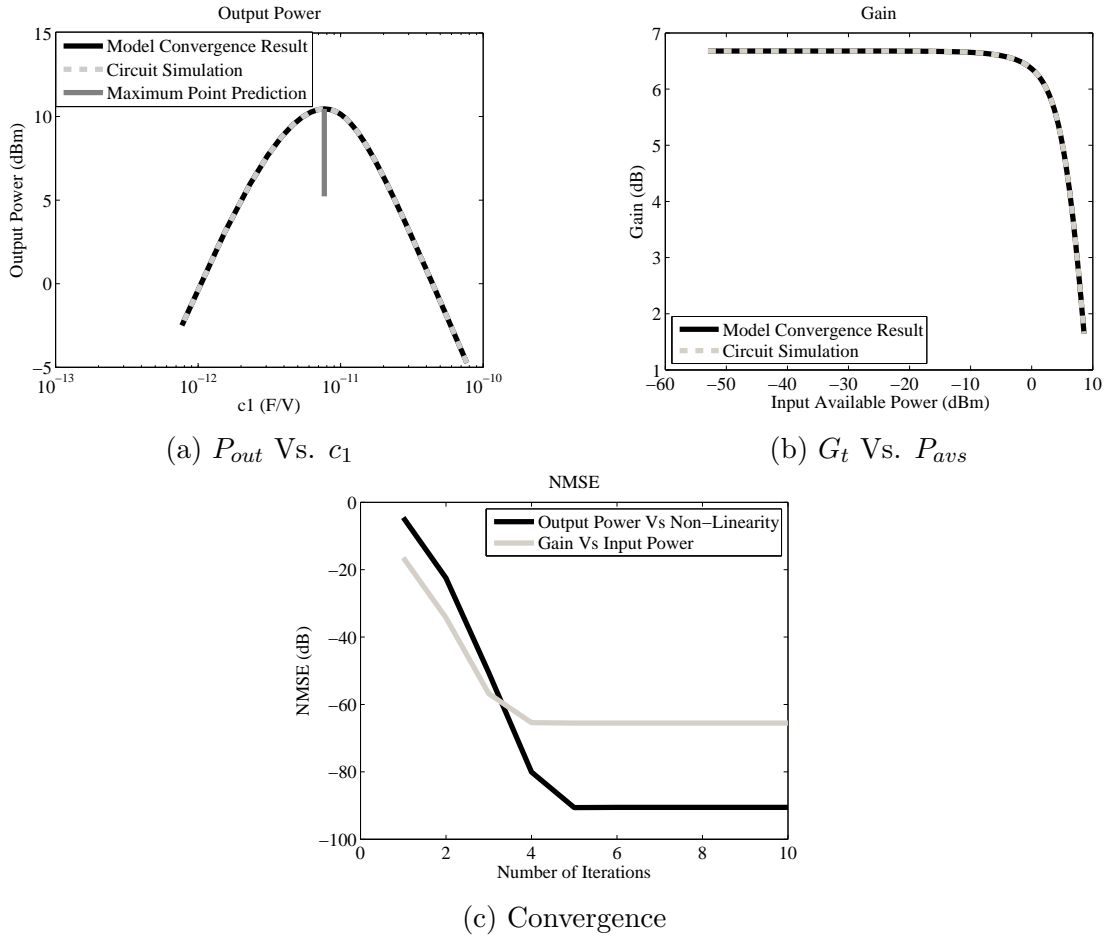


Figure 4.19: Simulation and Model Results for the Test Circuit

$$\frac{Z_{0,1}^*}{2\text{Re}(Z_{0,1})} V_{0,1}^T = \frac{V_{0,1}^T + j\omega_{0,1} Z_{0,1} C_{1,1} V_{1,0}^{T*}}{1 - \omega_{1,0} \omega_{0,1} Z_{0,1} Z_{1,0}^* |C_{1,1}|^2} \quad (4.55)$$

$$C_{1,1} = \frac{-j \frac{V_{1,0}^{T*}}{V_{0,1}^{T*}} \pm \sqrt{\left(j \frac{V_{1,0}^{T*}}{V_{0,1}^{T*}}\right)^2 - \frac{Z_{0,1}^* Z_{1,0}^* \omega_{1,0}}{\text{Re}(Z_{0,1})^2 \omega_{0,1}}}}{\omega_{1,0} \frac{Z_{0,1}^* Z_{1,0}^*}{\text{Re}(Z_{0,1})}}$$

The parameter $C_{1,1}$ must be purely real to guarantee the condition $|C_{1,1}|^2 = C_{1,1}^2$. For real admittances the phases of the currents can be calculated using the relations shown in equation 4.56, for a positive c_1 . For a negative c_1 the first angle must equal $(2k + 1)\pi$ which yields the symmetric result.

$$\begin{aligned}
-\angle V_{0,1} - \angle V_{1,0} - \frac{\pi}{2} &= 2k\pi \\
-2 \left(\angle V_{0,1} + \angle V_{1,0} - \frac{\pi}{2} \right) &= 2k\pi
\end{aligned} \tag{4.56}$$

The result is that for real impedances the phases of the voltages should be $-\frac{\pi}{4}$. One might think that the meaning of this phase is questionable, however, note that it is measured in relation to the output current which is commensurate with both frequencies.

The phase is only possible to obtain for $|V_{1,0}|$ sufficiently high. In case it is not, there is no solution for the equation and the tuning should be performed for the pump input.

To choose between the + or – sign we can use the small-signal limit condition. When the system tends to small-signal operation $V_{1,0} \gg V_{0,1}$ and both $V_{0,1}$ and $V_{1,1}$ do not drive the non-linearity. In this case, $C_{0,1} = C_{1,1} = 0$ and so $I_{1,0}$ tends to zero, making $V_{1,0} = V_{1,0}^T$. This condition is achieved when the – sign is chosen, for a positive c_1 and when the + sign is chosen, for a negative c_1 .

After obtaining $C_{1,1}$, the c_1 parameter can be obtained by combining equation 4.52 with $C_{1,1} = c_1 V_{1,1}$. This results in equation 4.57.

$$c_1 = \pm \sqrt{\frac{C_{1,1}}{j\omega_{1,1} Z_{1,1} V_{0,1} V_{1,0}}} \tag{4.57}$$

Since $C_{1,1}$ and c_1 are real coefficients, $V_{1,1}$ must undoubtedly be purely real and positive.

Interestingly enough, looking at equation 4.55 it is clear that, when there is no real solution for $V_{0,1}$, this solution exists for $V_{1,0}$ which suggests that the maximum indeed occurs for one of these tuning situations.

The expressions derived here for $V_{0,1}$ can be derived for $V_{1,0}$ bearing similar results, this is a must since it is not explicit which of these frequency components is the pump's or the input's, only that $V_{1,1}$ is the output.

4.5.3 Current Pumped Elastance

For current pumped ParAmps the excitations are inserted in parallel with each other and the non-linearity, therefore the currents are summed. If the tuning filters are series, high Q factor, LC filters then all currents outside the filters' tuned frequencies are cancelled. However, the voltage at the non-linearity is uncontrolled because the filters tend to open circuits outside the passage band. Figure 4.20 shows the circuit to be analysed.

The modelling of this case is similar to the voltage pumped capacitor since they are quasi-dual. The only difference is that the elastance is the inverse of the capacitance and not the dual, which generates minor differences.

An implementation based on the elastance was tried due to the possibility of a truly linearly varying non-linearity. The uncontrolled voltage at the diode terminals proved to be a severe problem because breakdown was easily attained when simulating the circuit.

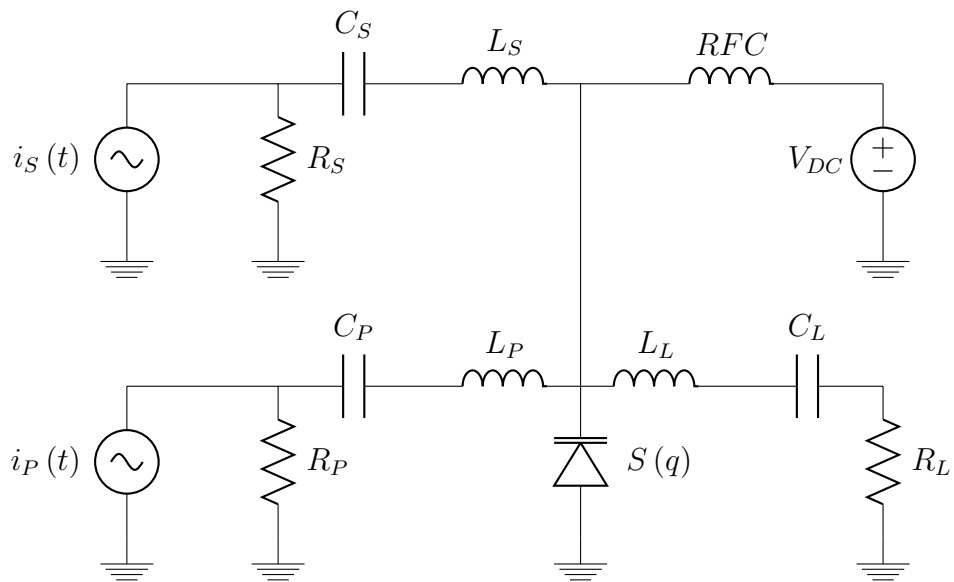


Figure 4.20: Current Pumped, Charge Controlled Elastance

Chapter 5

Designing a Parametric Amplifier

5.1 Specifications

The first step in designing an amplifier is to know the specifications. In the particular case of parametric amplifiers this is even more important because some specifications are directly and unusually linked. For instance, by specifying a gain and an output frequency there is immediately a maximum input frequency established through the Manley-Rowe relations.

It is important to lay out all the wanted specifications initially and verify their possibility with the basic theory before starting to build the amplifier. For the amplifier to be developed in this work two restrictions were made. The input's center frequency is at 100MHz and the output's at 1GHz allowing for a maximum gain of 10dB.

Because the developed device is intended as a proof of concept high powers are not going to be used. The target output power is 100mW, to make use of the large signal theory developed in this work the pump power should be as reduced as possible.

5.2 Pumping Type

Initially the ParAmp was to be pumped in current because of the excellent non-linear elastance characteristic of some diodes. However, after some testing, it was concluded that the uncontrolled voltage across the diode poses too great a risk for the ParAmp. The voltage rises very quickly forcing the device into breakdown which is outside the non-linear mode which it is intended to work on.

After these tests, voltage pumping was chosen for the developed ParAmp.

5.3 Topology

The topology is very important when designing these types of amplifier, mainly if the active component is a bipole as is the case. The problem with using bipoles as the active

components is the leakage between ports. The filtering needs to be extremely potent to eliminate direct power transmission. When the right topology is chosen the leakage can be reduced greatly using the symmetries of the circuit.

Leakage from the pump to the output is the most concerning since their frequencies are very close. As such, the circuit benefits greatly from balanced pumping. If possible, doubly balanced designs provide isolation from the source as well, and remove the need for filters. For this reason, a doubly balanced circuit was used in the design of this particular amplifier.

The doubly balanced topology that works in voltage pumping is the ring.

5.3.1 Ring Topology

The ring topology works by balancing the voltages across four similar components. These components are arranged in such a way that two pairs of virtual grounds are generated. In these virtual grounds it is possible to inject signals that will drive the components but are isolated from each other. If balanced signals are inserted in the virtual grounds, the generated frequency mixes can be extracted by connecting their center taps. Figure 5.1 exemplifies the concept. In the picture, the arrows symbolize the current phases for each branch, the dotted and dashed arrows correspond to the dashed and dotted inputs and the filled arrows to the output.

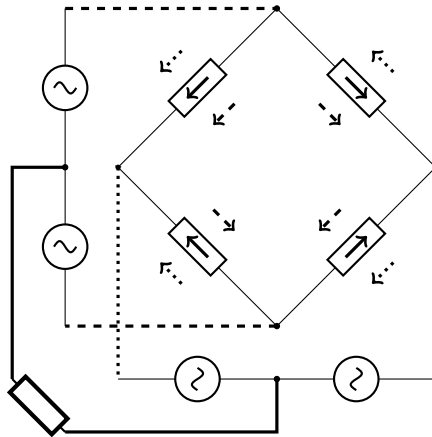


Figure 5.1: Ring Topology Example, Evidencing the Inherent System Symmetry

The components used in the ring will be the varactors. There is also the need to ground one of the center taps, usually the pump is grounded because of its higher power and closer frequency to the output.

To analyse this topology, the power was considered to be split equally amongst all the diodes, this means that each of the diodes find themselves being driven by a quarter power source. Of course, the load is also equally shared which means each diode only sees a quarter load as well. By doing this the ring is now separated into four equal circuits. To design the ParAmp only one of these circuits needs to be designed, the advantage

being that there is no further need for filtering out the other frequencies for each branch. Figure 5.2 shows this circuit. Of course, the generated frequencies across the diode are still a problem, the diode needs to be tuned to only three frequencies.

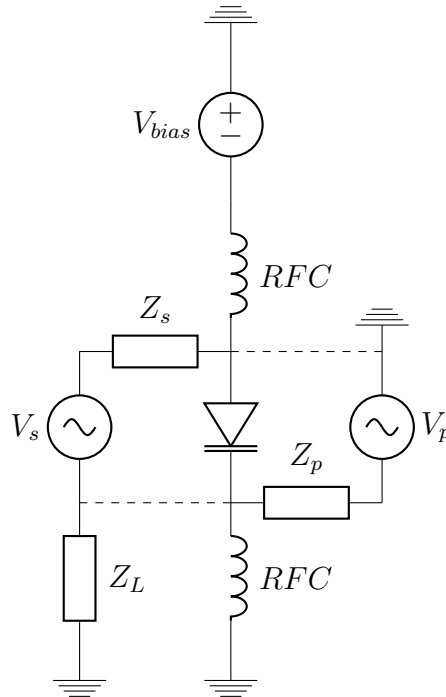


Figure 5.2: Part of the Amplifier to be Designed

From figure 5.2 it is possible to see that the load has a virtual connection to the pump. However, if we look at the ring topology in figure 5.1 we can see that the load also has a virtual connection to the 180° shifted pump input. This means that the generated currents cancel each other out. The same is true for the connection to the other source.

5.4 Non-Linearity and Tuning

To reduce the pump power to as little as possible, the large signal model should be used to calculate the necessary non-linearity. However, we know from the small-signal analysis that the bandwidth is related to the pump's voltage. A suitable trade-off must be attained by careful consideration.

The minimum pump power required would be 90mW if there were no power losses. Considering there are power losses and the high influence the pump voltage has in the bandwidth (in small-signal operation) it was decided that the pump power would be 400mW, about four times the required power, to improve the characteristics of the system. This rise in the pump's power will, however, reduce the efficiency of the system due to the equivalent series resistance in the diodes.

Knowing the pump's power we can calculate the ideal non-linearity. In the case of this amplifier the ideal value is -0.2pF/V . To obtain this value, low grading coefficient diodes were chosen. Low grading coefficient diodes are ideal because they allow for higher voltage swings across their terminals maintaining a relatively linear capacitance curve. Unfortunately, the capacitance variation is also smaller which means a higher junction capacitance is needed to obtain the ideal parameters. This higher junction capacitance raises the linear capacitance, reducing the bandwidth.

There is a way to profit from the situation. Every branch needs to be tuned to its specific frequency, to avoid unwanted frequency mixes leaking power. This is especially true for the output since the mix at the Lower Side Band (LSB) is not cancelled by the topology. Since the junction capacitance is high, the linear capacitance is high enough that, when resonating with coils at each input a high Q filter is generated. This effect is such that no other filtering is needed for the device. The down-side is the effect on the bandwidth due to the same filters.

The coil can be calculated for each input easily. If we consider that the capacitance varies linearly, then the average capacitance depends only on the bias and the parasitics of the used active device. Using the left varactor model from figure 4.5, we can deduce that the resonance at a given frequency will happen for a coil calculated using equation 5.1.

$$L_{tune} = \frac{1}{\omega^2(C_{parasitic} + C_{bias})} - L_{parasitic} \quad (5.1)$$

The capacitance C_{bias} is given by the component's characteristic capacitance curve, equation 4.16, for the bias voltage. The obtained filter is not exactly a parallel tank LC but it serves its purpose. The parasitics will restrict the frequencies because the filter must be as close as possible to a parallel LC. For this condition to be true equation 5.2 should be valid.

$$\frac{1}{\omega(C_{parasitic} + C_{dc})} \gg R_{parasitic} + \omega L_{parasitic} \quad (5.2)$$

This condition will assure that the capacitance will dominate the impedance seen from the tuning coil onward. The parasitics play an important role in restricting the frequency. Note that, the higher the parasitics the lower the frequency can be.

An interesting fact is that, because each input is inserted at the other's virtual ground the tuning can be done using coils only without the fear of shorting the other frequencies to ground.

5.5 Simulations

After the circuit was designed it was simulated in ADS at circuit level and in MatLab to further test the developed model. As expected, as the ADS description approximates the practical amplifier the more the model shows inconsistencies. This is mainly due to the fact that some effects were simply not modelled, such as the behaviour of the

parasitics outside the chosen frequency components. To prove this point an ideal circuit was simulated in ADS where the diode was replaced by a linearly varying capacitance and lumped parasitic components. The parasitics were extracted from [16] and the linear coefficients were extracted using the minimization of the NMSE for the maximum input voltage swing, using the diode's characteristic capacitance curve.

Recall that, when the circuit was simulated without the parasitics, the model converged very faithfully to the results of the harmonic balance simulator, figure 4.19. When a similar circuit is simulated with the parasitic components the model shows some error. Since the test circuit is similar to the previous one, it is only included in the annexes in figure B.2. The capacitor was modified to include the parasitics as shown in figure B.1. The simulation results with and without the parasitics is shown in figure 5.3. Note that the main power deviation happens at the pump frequency. This hints that, due to the pump's higher voltage, current mixing products of the type $2\omega_p$ and $2\omega_p + \omega_s$ will circulate in the parasitic components dissipating power.

In the simulations, the tuning coils were adjusted when the parasitics were removed. Also, the optimum non-linearity was not chosen to show that the model still behaves well outside the optimum values. Even when the parasitics are eliminated, for very small inputs the model diverges from the circuit level simulator. This problem seems to occur because the very small powers at other frequencies that manage to travel across the filters begin to be comparable to the input powers. The results obtained in MatLab offer, nonetheless, good information on the behaviour of the circuit.

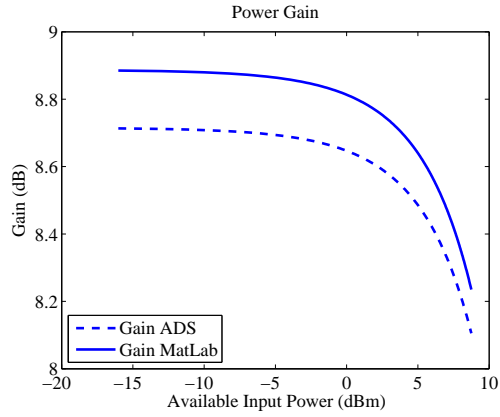
The ParAmp to be implemented uses diodes, of course. This may be yet another source of error in relation to the developed model, since higher order coefficients were not modelled. Figure 5.4 shows the results of the simulations ran in ADS and MatLab. The ADS schematic was included in the annexes, figure B.3.

Looking at the simulation results using the diodes a more severe error can be noted, about 2dB maximum error. The increased error is probably due to the poor approximation to the capacitance curve used by the model, shown in figure 5.5.

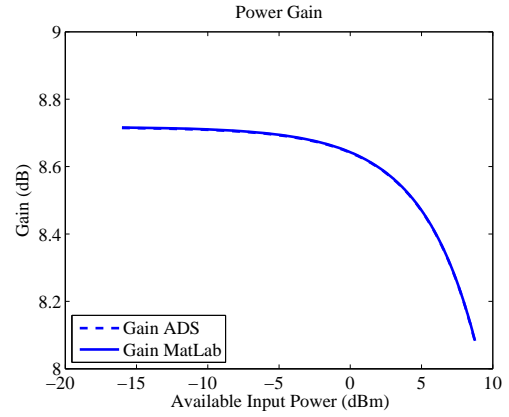
When designing the ParAmp the bandwidth of the device was neglected. However, since it is a parameter of some importance it is important to extract this information, figure 5.6 shows the expected bandwidth according to the large signal model and the circuit level simulation bandwidth.

Note how the bandwidth is decreased almost to half in the simulation. Again this is probably due to the unaccounted effects of the higher order capacitance terms. These terms can have this effect because the even terms will influence the average capacitance thus detuning the filters quicker. This could also account for the frequency shift that is observed in the figure for the circuit level simulation.

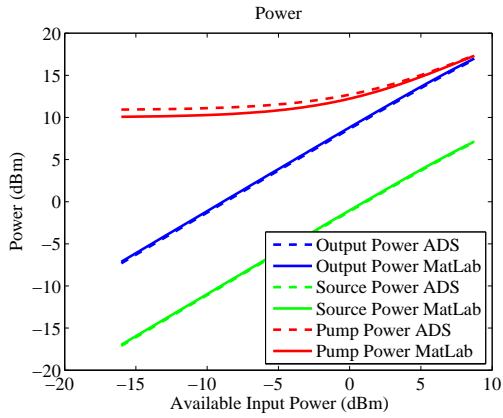
Both the large signal model and the small signal model show that the pump's available power influences the system behaviour. As such, this effect should be analysed to better understand the pump's influence over the amplifier, figure 5.7 shows the influence of the available pump power over the power output.



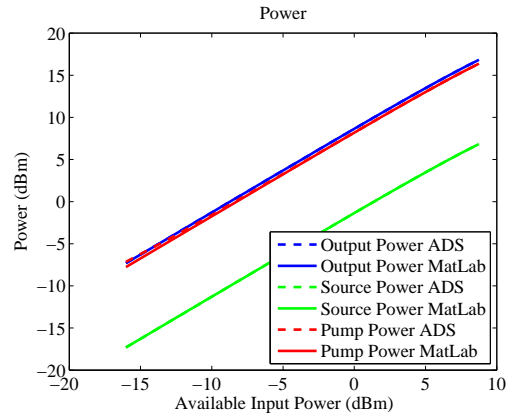
(a) Transducer Gain with Parasitics



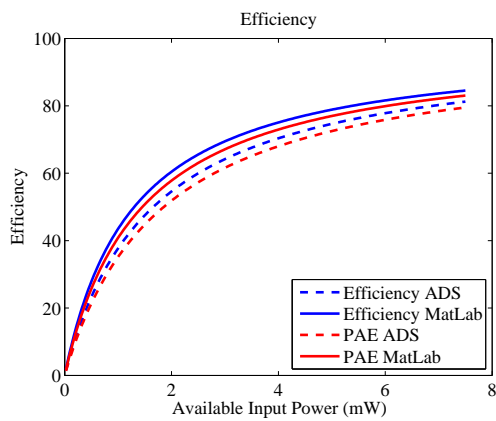
(b) Transducer Gain without Parasitics



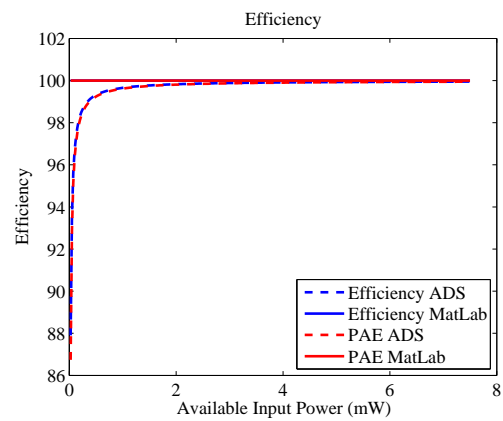
(c) Input and Output Power with Parasitics



(d) Input and Output Power without Parasitics



(e) Efficiency with Parasitics



(f) Efficiency without Parasitics

Figure 5.3: Simulation Results Vs Model Results with (left) and without (right) the Parasitic Components

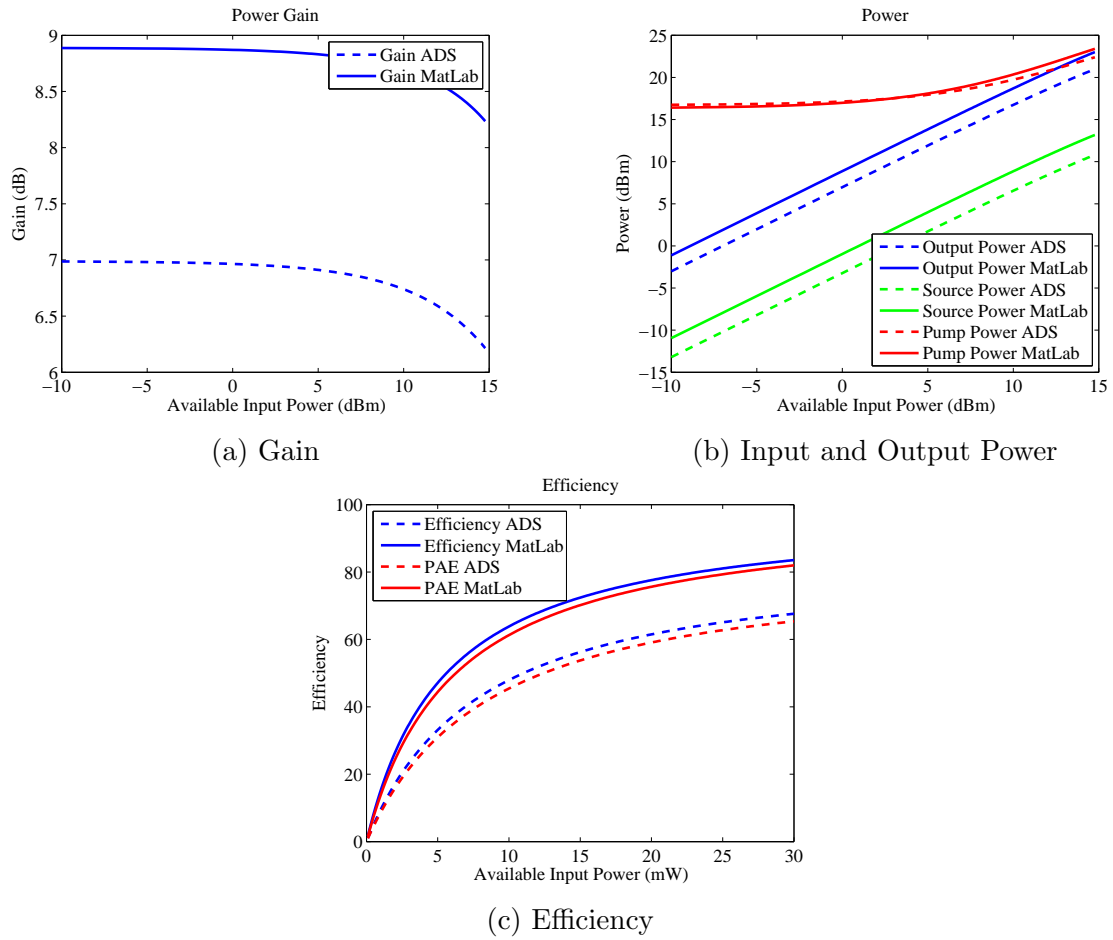


Figure 5.4: Simulation Results Vs Model Results for the ParAmp to be Implemented

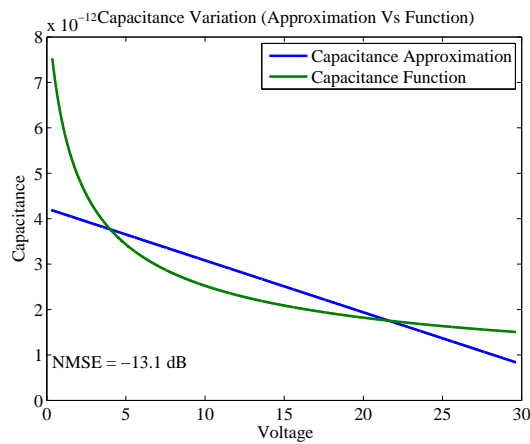
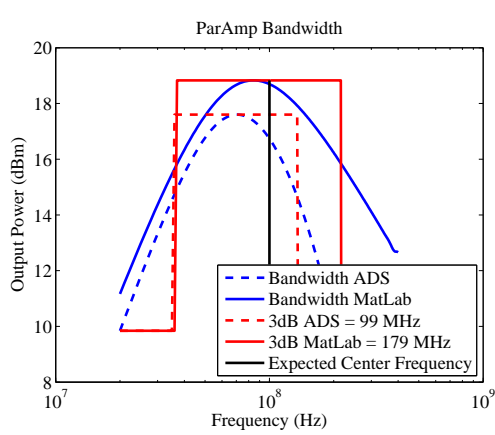
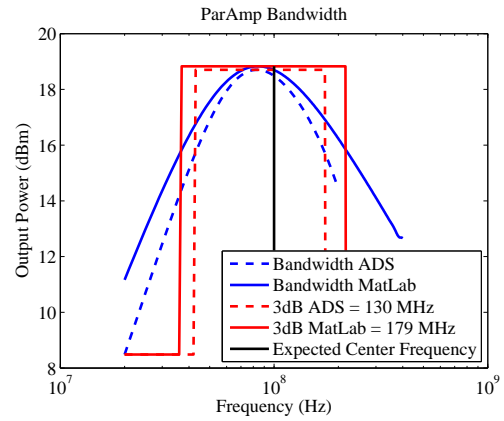


Figure 5.5: Capacitance Curve and Used Approximation

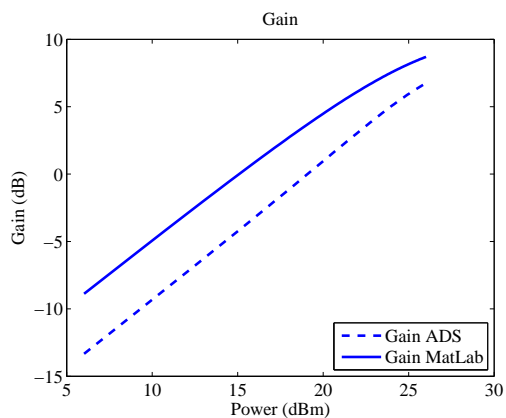


(a) Bandwidth using Diodes

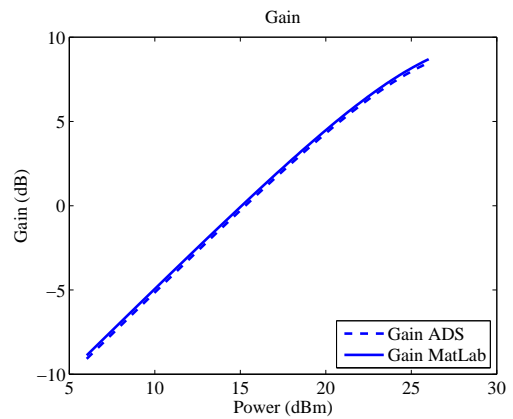


(b) Bandwidth using Linearly Varying Capacitances

Figure 5.6: Simulation and Model Bandwidth for the Designed ParAmp Using Diodes (left) and Using Linearly Varying Capacitances



(a) Gain Vs Pump Power using Diodes

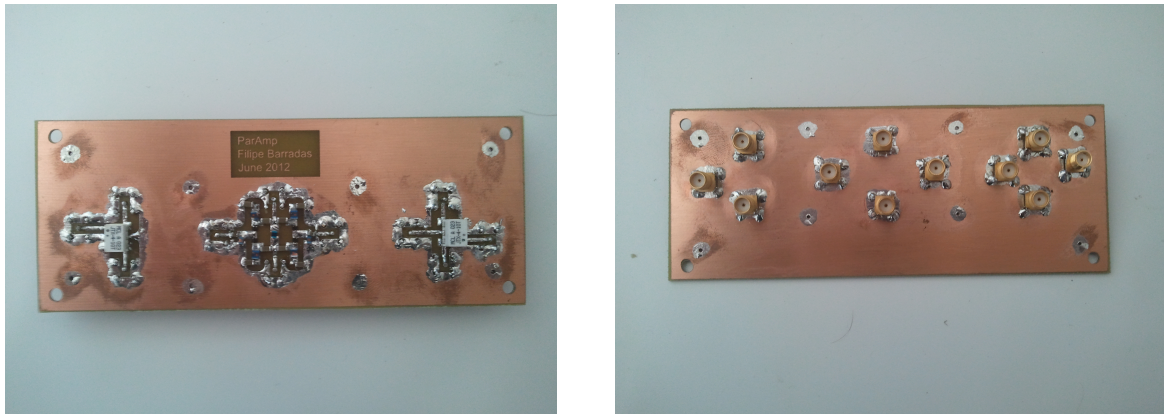


(b) Gain Vs Pump Power using Linearly Varying Capacitances

Figure 5.7: Simulation and Model Pump Influence over the Gain for the Designed ParAmp Using Diodes (left) and Using Linearly Varying Capacitances

5.6 Practical Implementation

The ParAmp is fully designed and can therefore be practically implemented. To do this, ADS was used to create a layout for the ParAmp which was then transferred to Printed Circuit Board (PCB). Figure 5.8 shows the practical implementation of the parametric amplifier.



(a) Top of ParAmp PCB

(b) Bottom of ParAmp PCB

Figure 5.8: ParAmp Practical Implementation

Unfortunately, the practical implementation of the parametric amplifier was not tested due to time constraints.

Chapter 6

Conclusions and Future Work

6.1 General Aspects

The focus of this work was to study and evaluate parametric amplification. Within this broad field, this work started with some general aspects, essentially describing energy transfer between sources through reactive components. These first steps provided solid ground to move on to more specific areas. To do them the requisites of each type of amplification were evaluated. It was decided that the type of amplification that would bring most benefit to study would be non-degenerate, non-inverting parametric amplification. This type of parametric amplifier has two main advantages: the pump does not need to be a commensurate frequency with the input and the input impedance of the amplifier can have a positive resistance (providing stability).

When the type of parametric amplification was chosen, this work moved on to deepen the analysis. A small-signal analysis was performed that allowed the extraction of several important parameters, such as transducer gain, bandwidth and sensitivity to non-linearity. The transducer gain allowed to clear the ambiguity of the obtained power gain, which showed a constant gain independent of the non-linearity. When the exploration of the small-signal model was finished, a disturbing unknown fact remained: how much power the pump needs for the circuit to operate in small-signal? Since this question is impossible to be answered accurately with the small-signal model, the hypothesis to build a large signal model was explored. By observing the feedback of each variable in the system, it was concluded that this was indeed possible. Limiting the non-linearity to the first order, the large signal model became sufficiently simple to solve through a Newton-Raphson iteration process, which showed fast convergence. Furthermore, it was observed that for normal operation conditions of a parametric amplifier, the model can be used to analytically extract optimum design values.

With the proper tools investigated or developed, this work set out to design a parametric amplifier. In this phase it was noted that this type of amplification suffers greatly from leakage between ports, due to the nature of the active device (bipole). Upon noticing this downside, the parametric amplifier was changed into a balanced topology to obtain

good port isolation without resorting to extreme filtering. A doubly balanced topology was chosen to provide isolation in all ports. Due to the large signal model, the parametric amplifiers needed to be separated into two more categories, voltage or current pumped. A current pumped parametric amplifier was the first choice for development, due to the elastance characteristic of the used devices. However, this proved unsound because the nature of this type of parametric amplifier allows uncontrolled voltages. These voltages could rise quickly and easily send the used diodes into breakdown. Due to this, a voltage pumped parametric amplifier was developed and simulated using both the large signal model and a circuit level simulator. For linear capacitance characteristics both the model and the simulator converged to the same values with little error. For other capacitance shapes the model still provides useful design information but shows some error.

The broad objectives of this work were achieved. Parametric amplification was studied and the relationships and transformations that exist in this type of amplification were detailed and explained. Some interesting aspects come to light when these effects are looked upon all together. First, there seems to be no way to parametrically amplify a signal while no energy is asked from it. This means that, the input of a parametric amplifier is never an infinite impedance. That is true for the bipoles but also for the MOSVar tripole. Second, parametric amplification has its gain and frequencies tied together. This is the most basic of rules, imposed by the power balance equations. And third, due to the first aspect, losses in these circuits have a "double" negative effect, since the amplification is only accomplished on the power provided to the reactance.

6.2 Comparison to Previous Work

The focus of this Thesis was in efficient power amplification, using parametric amplifiers. As it was said in the introduction, there has already been work developed in this area, some of it with practical implementations. Recently, there were two works that would be interesting to compare with this one. These works were developed in [17, 18] and reveal some of the same properties intended for the amplifier developed in this work. The common links that unite the amplifiers developed in [17, 18] to this one are, the power gain (10dB) and, in one of the cases, the used frequencies.

The amplifier developed in [18] managed a very high gain, close to maximum, but suffered in efficiency. This amplifier worked at lower frequencies than the one developed here but the ratio $\frac{\omega_{out}}{\omega_{in}}$ was the same. The amplifier developed in [17] worked at approximately the same frequencies as the one developed here. This amplifier did not achieve optimum gain and still suffered from the efficiency problem. In theory, the amplifier developed in this work could achieve both a higher efficiency and a higher gain.

The efficiency problem was attenuated in the developed amplifier by using diodes in parallel, thus reducing the current through each of the diodes. Also, the topology allowed for a great number of diodes to be used and so, even though all are highly driven in voltage, the current through each one is very small (which reduces losses). The gain is also raised with this technique. Note that reducing the losses in the power delivered to the capacitors

allows the system to apply the constant power gain over a higher power.

Note that these comparisons are model based only since the practical implementation of the amplifier is yet to be tested.

6.3 Future Work

An important fact is the drop in efficiency due to the ESR of the diodes. This effect must be studied carefully and evaluated. It would be interesting to find if there is some way to dim the effect without reducing the pumping voltage.

On the device level, it would be interesting to build some work on methods for reducing the ESR of the active elements in parametric amplification.

From a purely theoretical point of view, it would be interesting to develop the study for tripole varactor or transcapacitances; i.e. some kind of device where the control voltage has an independent port from the pump voltage. This study should focus on whether the input must, indeed, deliver energy in the process of amplification.

From a system point of view, an analysis of the effects of the higher order capacitance coefficients could give useful design information. Of some importance in this case is the shift in bias due to the even terms and the higher order frequency conversion.

It would be interesting to study the application of techniques developed for transistor based amplifiers in parametric amplifiers. For instance, modulation of the pump voltage using envelope detection. These techniques might help reducing the consumed power for lower inputs in the same way the ET and EER techniques do for the transistor.

It would also be very interesting to develop the current pumped parametric amplifier mentioned in this work. The objective would be to obtain a more linear amplifier by making use of the linearly varying elastance obtainable with this type of diodes.

6.4 Final Remarks

Parametric amplifications has the potential to change the paradigm of high efficiency amplification. However, it suffers from many deficiencies. Whether these deficiencies can be bypassed or are intrinsic to the amplification method is difficult to say, especially with the lack of tripole varactors. First, there is the problem of having to provide energy to the amplifier, not only from the power source, but also from the signal source. Second, there is significant efficiency drop due to the parasitics and higher order reactance coefficients. Should the conditions change for the devices in which the future systems will be based, and the parametric amplifier may well be a solution for efficiency hungry engineering.

Bibliography

- [1] S. Maas, *Nonlinear microwave and RF circuits*, ser. Microwave Library. Artech House, 2003. [Online]. Available: <http://books.google.pt/books?id=SSw6gWLG-d4C>
- [2] K. Vandermot, W. Van Moer, Y. Rolain, and R. Pintelon, “Extending the best linear approximation for frequency translating systems: The best mixer approximation,” in *Instrumentation and Measurement Technology Conference Proceedings, 2007. IMTC 2007. IEEE*, may 2007, pp. 1 –6.
- [3] W. Chudobiak and D. Page, “Frequency and power limitations of class-d transistor amplifiers,” *Solid-State Circuits, IEEE Journal of*, vol. 4, no. 1, pp. 25 –37, feb. 1969.
- [4] N. Sokal and A. Sokal, “Class e-a new class of high-efficiency tuned single-ended switching power amplifiers,” *Solid-State Circuits, IEEE Journal of*, vol. 10, no. 3, pp. 168 – 176, jun 1975.
- [5] V. J. Tyler, “A new high-efficiency high-power amplifier,” *Marconi Review*, vol. 21, pp. 96 – 109, 1958.
- [6] J. Staudinger, B. Gilsdorf, D. Newman, G. Norris, G. Sadowiczak, R. Sherman, and T. Quach, “High efficiency cdma rf power amplifier using dynamic envelope tracking technique,” in *Microwave Symposium Digest. 2000 IEEE MTT-S International*, vol. 2, 2000, pp. 873 –876 vol.2.
- [7] G. Wimpenny, “Improving multi-carrier PA efficiency using envelope tracking,” 2008. [Online]. Available: <http://www.eetimes.com/design/microwave-rf-design/4018959/Improving-multi-carrier-PA-efficiency-using-envelope-tracking>
- [8] L. Kahn, “Single-sideband transmission by envelope elimination and restoration,” *Proceedings of the IRE*, vol. 40, no. 7, pp. 803 –806, july 1952.
- [9] W. Doherty, “A new high efficiency power amplifier for modulated waves,” *Proceedings of the Institute of Radio Engineers*, vol. 24, no. 9, pp. 1163 – 1182, sept. 1936.
- [10] J. Manley and H. Rowe, “Some General Properties of Nonlinear Elements-Part I. General Energy Relations,” *Proceedings of the IRE*, vol. 44, no. 7, pp. 904 –913, July 1956.

- [11] R. Collin, *Foundations for Microwave Engineering*, ser. IEEE Press Series on Electromagnetic Wave Theory. Ieee Press, 2001.
- [12] S. Magierowski, H. Chan, and T. Zourntos, “Subharmonically pumped rf cmos paramps,” *Electron Devices, IEEE Transactions on*, vol. 55, no. 2, pp. 601 –608, feb. 2008.
- [13] S. Ranganathan and Y. Tsvividis, “Discrete-time parametric amplification based on a three-terminal mos varactor: analysis and experimental results,” *Solid-State Circuits, IEEE Journal of*, vol. 38, no. 12, pp. 2087 – 2093, dec. 2003.
- [14] B. Perlman, “Current-pumped abrupt-junction varactor power-frequency converters,” *Microwave Theory and Techniques, IEEE Transactions on*, vol. 13, no. 2, pp. 150 – 161, mar 1965.
- [15] H. Rowe, “Some General Properties of Nonlinear Elements. II. Small Signal Theory,” *Proceedings of the IRE*, vol. 46, no. 5, pp. 850 –860, May 1958.
- [16] *SMV1405-SMV1430 Series Datasheet*. [Online]. Available: <http://www.skyworksinc.com/uploads/documents/200068M.pdf>
- [17] B. Gray, B. Melville, and J. Kenney, “Analytical modeling of microwave parametric upconverters,” *Microwave Theory and Techniques, IEEE Transactions on*, vol. 58, no. 8, pp. 2118 –2124, aug. 2010.
- [18] B. Gray, J. Kenney, and R. Melville, “Behavioral modeling and simulation of a parametric power amplifier,” in *Microwave Symposium Digest, 2009. MTT '09. IEEE MTT-S International*, june 2009, pp. 1373 –1376.
- [19] D. Pozar, *Microwave Engineering*. John Wiley & Sons, 2011. [Online]. Available: <http://books.google.pt/books?id=Zys5YgEACAAJ>
- [20] B. Gray, F. Ramirez, B. Melville, A. Suarez, and J. Kenney, “A broadband double-balanced phase-coherent degenerate parametric amplifier,” *Microwave and Wireless Components Letters, IEEE*, vol. 21, no. 11, pp. 607 –609, nov. 2011.
- [21] R. L. Boylestad and L. Nashelsky, *Electronic Devices and Circuit Theory*, 7th ed. Upper Saddle River, NJ, USA: Prentice Hall Press, 2008.
- [22] L. C. C. Nunes, “Amplificador em classe f para sistemas de transmissão polar,” Master’s thesis, Universidade de Aveiro, 2010.

Appendix A

Mathematics

A.1 Parametric First Order Linear Differential Equation

Suppose the first order differential equation of time-varying coefficients defined by the functions $f(t)$ and $g(t)$ shown in equation A.1.

$$f(t)y(t) + g(t)\frac{dy(t)}{dt} = x(t) \quad (\text{A.1})$$

A.1.1 Solution

One way to prove this is to solve the differential equation for $y(t)$ and replace $x(t)$ with the sum of its elements in the solution.

The first step to solve the differential equation is trying to solve the associated Homogeneous equation A.2.

$$f(t)y(t) + g(t)\frac{dy(t)}{dt} = 0 \quad (\text{A.2})$$

The equation is solvable as described below.

- Divide all by $f(t)y(t)$ and subtract 1 to obtain equation A.3.

$$\frac{g(t)}{f(t)y(t)}\frac{dy(t)}{dt} = -1 \quad (\text{A.3})$$

- Divide all by $\frac{g(t)}{f(t)}$ to obtain equation A.4.

$$\frac{1}{y(t)}\frac{dy(t)}{dt} = -\frac{f(t)}{g(t)} \quad (\text{A.4})$$

- Integrate in order to t to obtain equation A.5.

$$\int \frac{1}{y(t)} \frac{dy(t)}{dt} dt = \int -\frac{f(t)}{g(t)} dt \quad (\text{A.5})$$

- Replace the integration variable in the first integral from t to $v_{o(t)}$ to obtain the solution A.5.

$$\log y(t) = \int -\frac{f(t)}{g(t)} dt \quad (\text{A.6})$$

- Exponentiate

$$y(t) = e^{\int -\frac{f(t)}{g(t)} dt} \quad (\text{A.7})$$

Now that the homogeneous equation is solved, the complete equation can be examined. The solution can be reached through the following steps.

- Assume the solution is of the form $y(t) = h(t) e^{\int -\frac{f(t)}{g(t)} dt}$

- Replace the solution in the differential equation obtaining equation A.8

$$h(t) e^{\int -\frac{f(t)}{g(t)} dt} + \frac{g(t)}{f(t)} \frac{dh(t)}{dt} e^{\int -\frac{f(t)}{g(t)} dt} - \frac{g(t) f(t)}{f(t) g(t)} h(t) e^{\int -\frac{f(t)}{g(t)} dt} = x(t) \quad (\text{A.8})$$

- Solve equation A.9 and obtain equation A.10

$$\frac{g(t)}{f(t)} \frac{dh(t)}{dt} e^{\int -\frac{f(t)}{g(t)} dt} = x(t) \quad (\text{A.9})$$

$$h(t) = \int \frac{x(t) f(t)}{g(t)} e^{\int \frac{f(t)}{g(t)} dt} dt \quad (\text{A.10})$$

- Replace equation A.10 in the first solution to obtain equation A.11.

$$y(t) = \int_0^t \frac{x(\tau) f(\tau)}{g(\tau)} e^{-\left(\int \frac{f(t)}{g(t)} dt - \int \frac{f(\tau)}{g(\tau)} d\tau\right)} d\tau \quad (\text{A.11})$$

Notice that the integral above degenerates to the convolution integral if the coefficients are static. This falls in-line with the expected linear system response.

A.1.2 Linearity Proof

The differential equation is said linear if the solution for $y(t)$ is the sum of the solution for each element comprising the signal $x(t)$. The simplest way to prove this is to replace $x(t)$ with $\alpha_1 x_1(t) + \alpha_2 x_2(t)$ and observe that the solution is the sum of the solution for y_1 for x_1 times α_1 and y_2 for x_2 times α_2 , this can be seen in equation A.12.

$$\begin{aligned}
 y(t) &= \int_0^t \frac{(\alpha_1 x_1(\tau) + \alpha_2 x_2(\tau)) f(\tau)}{g(\tau)} e^{-\left(\int \frac{f(t)}{g(t)} dt - \int \frac{f(\tau)}{g(\tau)} d\tau\right)} d\tau = \\
 &= \alpha_1 \int_0^t \frac{x_1(\tau) f(\tau)}{g(\tau)} e^{-\left(\int \frac{f(t)}{g(t)} dt - \int \frac{f(\tau)}{g(\tau)} d\tau\right)} d\tau + \alpha_2 \int_0^t \frac{x_2(\tau) f(\tau)}{g(\tau)} e^{-\left(\int \frac{f(t)}{g(t)} dt - \int \frac{f(\tau)}{g(\tau)} d\tau\right)} d\tau = \\
 &= \alpha_1 y_1(t) + \alpha_2 y_2(t)
 \end{aligned} \tag{A.12}$$

Appendix B

Circuits

B.1 Parasitics Test

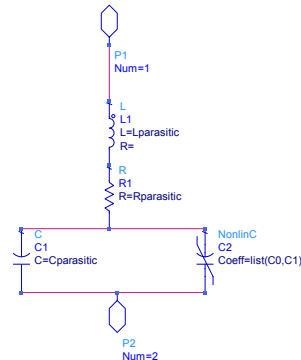


Figure B.1: The used Active Component Including the Parasitics

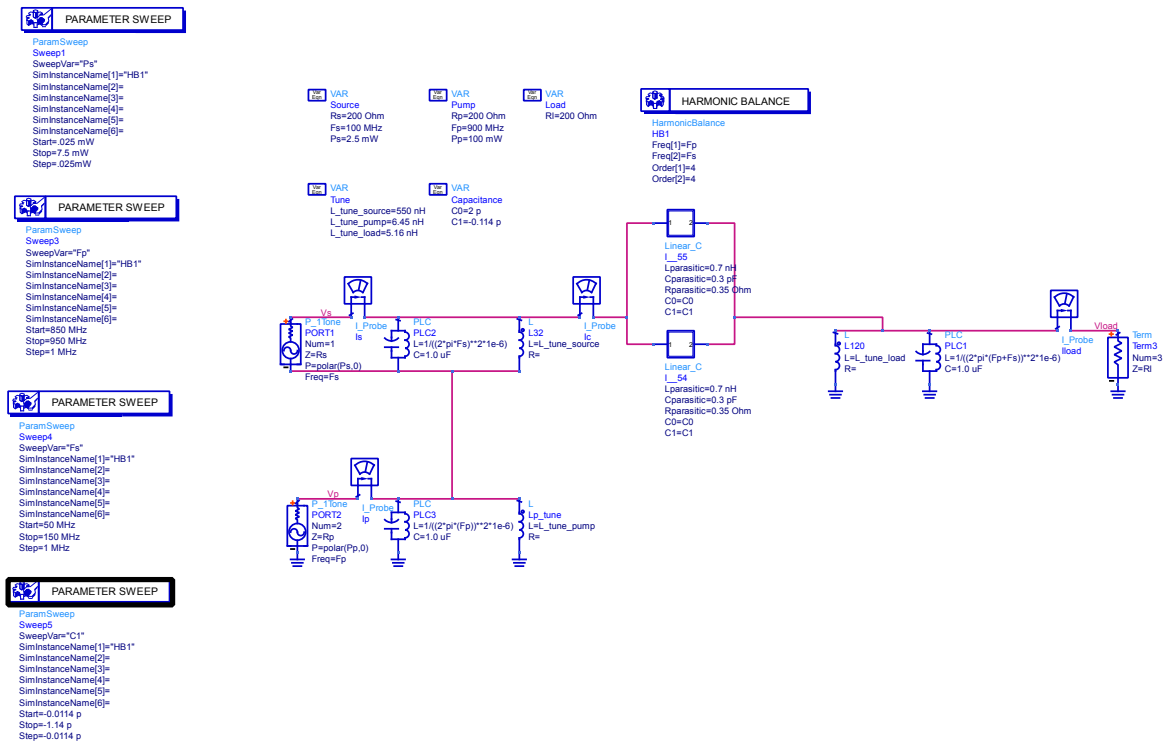


Figure B.2: Test Circuit for the Influence of the Parasitic Components in the Model

B.2 Doubly Balanced Voltage Pumped ParAmp

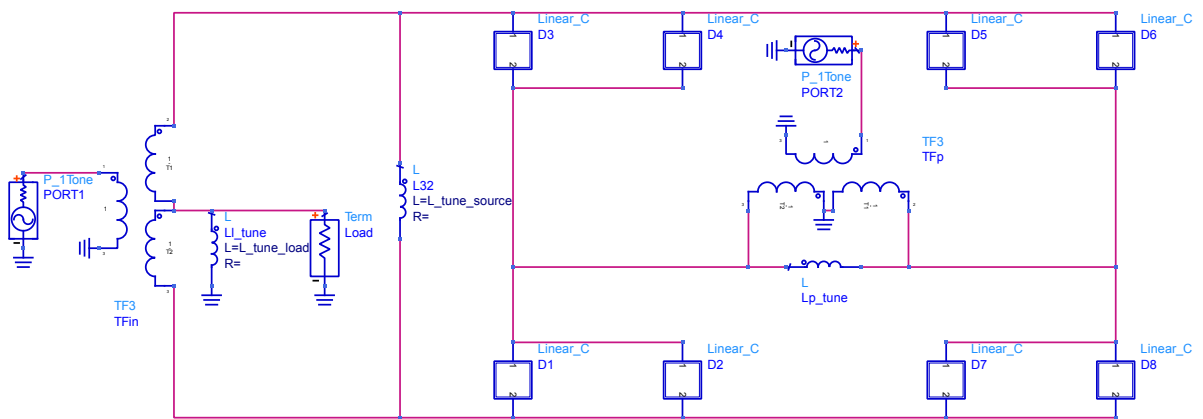


Figure B.3: Doubly Balanced Voltage Pumped ParAmp